Semisolid forging of steel components for automotive industry

JOKIN LOZARES ABASOLO

Mondragon Goi Eskola Politeknikoa
Mechanical and Manufacturing Department

March 15, 2014

MONDRAGON
UNIBERTSITATEA

A dissertation submitted
in fulfilment of the requirements for the degree of
Doctor por Mondragon Unibertsitatea

Semisolid forging of steel components for automotive industry

JOKIN LOZARES ABASOLO

Supervised by Zigor Azpilgain

Mechanical and Manufacturing Department
Mondragon Goi Eskola Politeknikoa
Mondragon Unibertsitatea

Ixeko Arantzari

Laburpena

Gaur egun bizi dugun globalizazio egoerak ekoizpen prozesuen hedapen eta arrakasta azkarra ahalbidetzen du, enpresa Europearren lehiakortasuna oztopatuz garapen bidean dauden herrialdeen aurrean. Lehiakorrak izaten jarraitzeko bide bakarra ekoizpen kostu txikiagoa duten lurraldetara deslokalizatzea edo ekoizpen prozesu berritzaileak ikertzea da. Azken honen bitartez jatorrizko materialen kontsumoa jaitsi eta ekoizpena handituko litzateke, beti ere ekoiztutako elementuen kalitatea mantenduz edo hobetuz.

Ingurune industrial honetan, material eta energien prezioak etengabe gorantz doazela, 'near net shape' ekoizpen prozesuak lehiakortasuna berreskuratzeko funtsezko giltzarri izan daitezke.

Teknika horietako bat da, hain zuzen, solido eta likido artean egindako konformaketa. Bere ezaugarri nagusia, soberakinik gabeko azken geometria lortzeko gaitasuna, dituen abantail guztien baturak ematen dio; eraginkortasun energetikoak, ekoizpen mailak, moldeak betetzeko duen era leunak eta uzkurtze porositate baxuak. Honi esker, azken piezak lortzeko prozesu klasikoek baino pauso gutxiago behar ditu prozesu erdisolidoak.

Guzti hau frogatu eta egiaztatu da Mondragon Unibertsitateko ekoizpen laborategian beren beregi garatu eta ezarri den forja erdisolidorako zelulan. Bertan pauso bakarrean lortutako piezen kalitateak erakusten duen bezala, altzairuen forja erdisolidoa prozesu sendo eta errepikagarria da, xehetasunak zehazki erakusten dituena. Lortutako emaitzek % 20-ko material aurrezpenak erakusten dituzte formaketa indarren gutxitze nabarmen batekin batera. Gainera, piezen ezaugarri mekaniko bikainek azken helburu den prozesuaren industrializazioa gerturatzen dute.

Abstract

Nowadays, globalisation enables a rapid uptake of the classical manufacturing and production technologies, thus making it much harder for European companies to compete with low labour costs of emerging countries. In order to remain competitive, these factories, such as OEM´s and automotive companies, have to either relocate their main production to low labour cost countries or invest in innovative production processes; in so doing they mainly allow lowering raw material consumption and production time while they perform high quality components.

In this industrial framework, with the current trend in prices of raw material and their sources, near net shaping of mechanical components will become a key factor to get the desired competitiveness.

Semisolid metal (SSM) forging is one of those near net shape techniques. It presents several advantages, such as energy efficiency, production rates, smooth die filling and low shrinkage porosity, which together lead to near net shape capability and thus to fewer manufacturing steps than in classical methods.

The foregoing advantages have been tried and tested in the semisolid forging cell developed and implemented at the forming laboratory of Mondragon Unibertsitatea. The high quality components, obtained in a single step, show that thixo-lateral forging of steels is a robust and highly repeatable forming process with a great surface finishing and much more remarked details. Material savings of the 20% have been reported together with a substantial decrease of the forming forces. In addition, great mechanical properties have been achieved which brings the process closer to the desired final industrial application.

Resumen

La globalización ha facilitado la rápida difusión y aceptación de los clásicos procesos de fabricación, lastrando la competitividad de las compañías Europeas frente a la de los países emergentes. Para seguir siendo competitivas, dichas empresas, deben deslocalizarse a países con menores costes de fabricación o investigar en procesos y productos innovadores que permitan disminuir el consumo de materias primas y el tiempo de fabricación, manteniendo, o incluso incrementando, la calidad de los componentes finales.

En este entorno industrial, con la imparable tendencia al alza del precio de las materias primas y la energía, la fabricación 'near net shape' puede resultar un factor clave en la recuperación de la deseada competitividad.

El conformado semisólido es precisamente una de ésas técnicas 'near net shape'. En conjunto, su eficiencia energética, productividad, llenado de las huellas y baja porosidad le confieren la capacidad para obtener componentes con geometria final lo que significa reducir pasos de fabricación respecto a los procesos tradicionales.

Esto es precisamente lo que se ha probado y demostrado en la célula de forja semisólida diseñada e implementada en el laboratorio de conformado de Mondragon Unibertsitatea. La calidad de los componentes obtenidos en un solo paso demuestra que la forja semisólida de acero es un proceso robusto y repetible con un excelente acabado superficial y detalles mucho más definidos. Ha permitido un ahorro de material del 20% junto con una disminución considerable de los esfuerzos de conformado. Además, las excelentes propiedades mecanicas obtenidas permiten acercar aún más el proceso al objetivo final, su industrialización.

Eskertzak

Denbora azkar pasatu da; badira bost urte doktoretzarekin katramilatu nintzela eta egia esan ez naiz damutzen. Gauza asko gertatu dira bidean baina azkenik iritsi da etapa hau ixten joateko garaia, eskertzak idaztekoa, tesia bukatu den seinale. Lerro hauen bitartez zuzenean edo zeharka hainbeste lagundu ditaten pertsonei nire eskerrik beroena adierazi nahiko nieke.

Mila esker zuri Oihana, beti ondoan egoteagatik, Intzak ekarri digun pozagatik eta ideia zoro hauek aurrera eramaten laguntzeagatik, guzti hau ezinezkoa izango litzateke zure babesik gabe.

Nola ahaztu etxekoak, eskerrik asko ama sukaldatutako tupper guztiengatik eta urte luzeetan (oraindik ere) edozertarako euskarri izateagatik. Munduko bekario onenari, proiektu honen arte eta parte izateagatik, bere aholku, laguntza eta jakituria pixkat (asko du eta) elkarbanatzeagatik, mundiala haiz viejo!

Hospital kaleko beste gurasoei beti hor egoteagatik, beti ulerkor. Naiara eta Mikeli, Iruña zaharra eta Auzperri bisitatu eta gozatzeko aukera emateagatik, beraien alaitasunagatik, Txokotoko bokatengatik eta Onako kalimotxoengatik, gora Manzanillo!

Ezin aipatu gabe utzi Garaiako alma materra, Rafa, berarekin pasatako denbora eta erakutsitako guztia, agertu zaigun arazo bakoitzeko soluzio egokia emateagatik, oporretan ere ondoan egoteagatik, beti adi, beti prest. Zu gabe lan hau ez litzatekeelako posible izango.

Maider eta Xabierri, beraien zuzenketa zehatzengatik baina batez ere Joanes eta Maleni, gurasoen denbora lapurtzen uzteagatik. Gainontzeko

familiari ere nire eskerrik kutunena, pasa ditugun eta pasako ditugun momentu paregabeengatik.

Bost urte hauetan lankide baino gehiago lagun bihurtu zareten guztiei, Euskal Herriko txokoak gehiago maitatzeko arrazoiak emateagatik, biba zuek! Nola ahaztu Getariko arratoia eta Zarautzeko kodilo festa, Deustun gure txinatarra euskaldundu genuenekoa, Elorrixoko oilaskoak eta San Pankraziotako makarroiak, Hernaniko sagarra eta Izalgo sagardoa, Zeztoako patana edota Arrasateko Santamasak. Dudarik gabe zuek izan zarete urte hauetako aurkikuntzarik onena. Mila esker Jabitxu zure paseoengatik eta fabri biko gelan elektroiak aurkitzeagatik. Nagoreri Alemanian inoiz pasatu eta pasatuko dudan asterik onena elkarbanatzeagatik, scooter patinen sekretuak erakusteagatik eta Oihanari ezer ez ezateagatik. Alaitzi, egindako barre eta momentu on guztiengatik, zehaztasunak duen garrantzia erakusteagatik. Sarriegiri, gauzak egiteko beste modu bat dagoela sinestarazteagatik eta nola ez gure 'hall of fame'-ean sartu den kurrikulumeko argazkiagatik. Ioneri bere komentario fin eta zorrotzengatik. Monsieur Martini bere kontakizun eta umoreagatik. Larrañaga komandanteari, bere gastronomiaren tenplua partekatzeagatik, errugbiaren esentzia gerturatzeagatik eta berriz uger egitea zer den gogoraraztea- gatik. Manexi bere jakinegon eta aholkuengatik. Elenari Teruel existitzen dela ziurtatzeagatik. Nuria eta Kintanari, beti laguntzeko prest egoteagatik eta alkarrik bidea egin duten pertsonen oinatzak inoiz ezabatzen ez direla gogo- rarazteagatik. Ziur nago gertuko norbait aipatu gabe uzten dudala baina... ez zara zu izango flako! Mila mila esker Joanes zure laguntza eta pazientziagatik.

Eskerrak baita Fabri2-ko gelatxoan etxeko lez hartu ninduten Ibai, Andrea, Jon Ander, Eneko eta Gurutzeri eta baita David, Iñigo, Ireneo eta Ainaritari ere.

Azkenik, eskerrak eman Mondragon Unibertsitateari, doktoradutza egiteko aukera emateagatik, bereziki Iñaki eta Zigorri beraien burutazioa izan baitzen altzairuaren thixoformaketaren gaiari heltzea.

Contents

Introduction

1.1 Motivation and background

Nowadays, globalisation enables a rapid uptake of the classical manufacturing and production technologies, thus making it much harder for European companies to compete with low labour costs of emerging countries. In order to remain competitive, these factories, such as OEM´s and automotive companies, have to either relocate their main production to low labour cost countries or invest in innovative production processes; in so doing they mainly allow lowering raw material consumption and production time while they perform high quality components.

According to Euroforge data [1], Europe´s production of steel closed die forgings in 2012 was 21% of the world wide overall, distributed mainly between Germany, Italy, France and Spain (Figure 1.1). These data show that Europe´s leading role in the market is weakening dragged by the increasing maturity of the process and the alloy surcharge for steel. The latter could be so high that it actually has a huge impact on the price of the final component. Therefore, raw material consumption must be monitored and lowered to a minimum without influencing the final part´s mechanical properties.
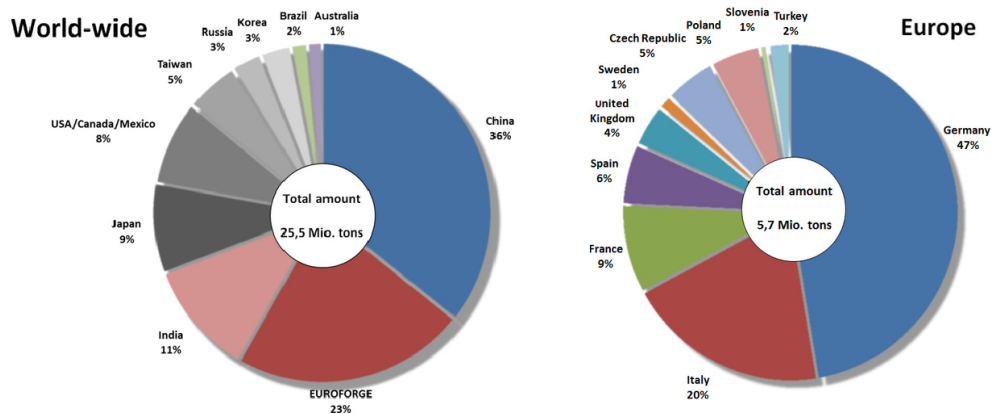
Figure 1.1 Production of forgings in 2012 [1].

In order to remain competitive, European manufacturing companies have to face a cost-effective production lines keeping the quality and reliability of the components high. To do this, a company´s research and development must go further than obtaining high mechanical properties; it should include a complete optimisation of the production process, taking into account also raw material and energy consumption.

In this industrial framework, with the current trend in prices of raw material and their sources, near net shaping of mechanical components will become a key factor to get the desired competitiveness.

Semisolid metal (SSM) forming is one of those near net shape forming techniques. This family of innovative manufacturing methods based on the thixotropic behaviour has been developed and has gained interest for the past 40 years. These processes present several advantages, such as energy efficiency, production rates, smooth die filling and low shrinkage porosity, which together lead to near net shape capability and thus to fewer manufacturing steps than in classical methods. SSM processes have already proved to be efficient in several application fields, such as military, aerospace and, most notably, automotive industries. Thixoforming of aluminium and magnesium alloys is state of the art and a growing number of serial production lines are already operating

all over the world. However, so far, there are no industrial applications of semisolid processing of higher melting point alloys such as steel. This can be partly attributed to the high temperature range involved in the process and the tendency for oxidation and scale formation. Furthermore, the complex microstructure evolution during reheating of some alloys creates problems difficult to solve. Despite this, the semisolid forming of steels reveals a high potential to reduce material as well as energy consumption compared to conventional process technologies. Thus, the aim of this research work is to demonstrate the above by designing and setting up a semi automated thixoforging cell. A commercial automotive part will be manufactured as a demonstrator and its microstructure and mechanical properties as well as the process itself will be deeply analysed.

1.2 Scope of the present thesis

As I have mentioned, the main goal of this research dissertation is to develop a laboratory scale steel thixoforging cell whereby high quality components, reduction of energy and labour production will be reported. Additionally, the cell will be the key element and definitive touchstone to know how the process can be transferred to industry fulfilling its requirements and border conditions.

To achieve this, this dissertation has been divided into four different sections as shown in Figure 1.2:

1. SSM forming. Background information and general aspects of the semisolid processing will be given in this section. The ground covered by the semisolid processing to the present will be reviewed and the current situation in relation to industrialisation and commercial application assessed. I will devote chapter 2, 3 and 5 to this.

2. Material characterisation. A complete characterisation of the used steel grades will be presented in this section, from microstructural properties to

thermophysical ones. An approach combining experimental results from Differential Scanning Calorimetry (DSC) and thermodynamic prediction will be also presented. This is the object matter of chapter 4.

3. The thixoforging cell. In this section I will fully describe the implemented thixoforging cell and its operation as well as the special tool designed to use all the press capacity during the forming stage. This will be discussed in chapter 6.

4. Forming. In this section, I will describe all the steps of the forming process in depth. Some components will be produced in order to define the optimised working parameters and to find out possible shortcomings that must be taken under control to obtain successful components. The microstructure and mechanical properties of the designed components will be analysed in chapter 7.
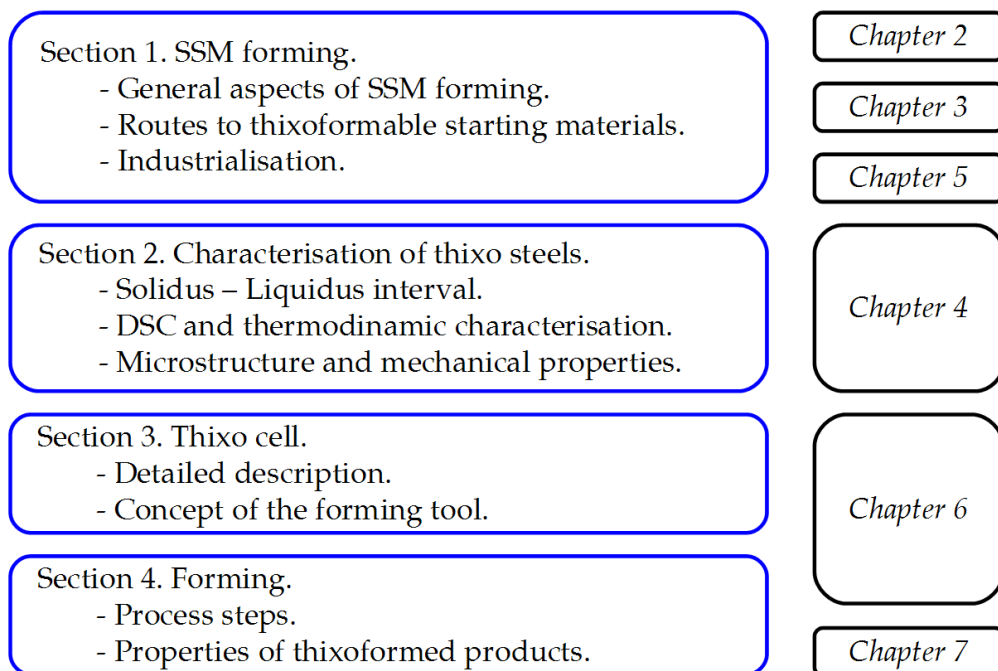
Section 1. SSM forming.
- General aspects of SSM forming.
- Routes to thixoformable starting materials.
- Industrialisation.

Chapter 2

Chapter 3

Chapter 5

Section 2. Characterisation of thixo steels.
- Solidus – Liquidus interval.
- DSC and thermodinamic characterisation.
- Microstructure and mechanical properties.

Chapter 4

Section 3. Thixo cell.
- Detailed description.
- Concept of the forming tool.

Chapter 6

Section 4. Forming.
- Process steps.
- Properties of thixoformed products.

Chapter 7

Figure 1.2 Summarised structure of this dissertation.

As it is described in Figure 1.2 the first section - chapters 2, 3 and 5 - covers the state of the art of the semisolid technology. Chapters 2 and 3 give a general overview of the semisolid forming describing material aspects and routes to obtain proper starting material. Due to this, I have considered convenient to dedicate chapter 4 to material characterisation. In order to maintain the continuity of the dissertation industrialisation issues, which are more related to the production cell, are reviewed in chapter 5 despite being part of the first section. Chapter 6 covers completely the section dedicated to the implemented thixoforging cell and the first part of the forming section. The reason to do this is the direct relation existing between each process step with each particular device of the thixoforging cell. Finally, microstructural characteristics and mechanical properties of the manufactured components are analysed in chapter 7. Chapter 8 is devoted to sum up the research conclusions and future work.

Semisolid Forming

The aim of this chapter is to present the background information and general aspects of the semisolid processing. I will review the ground covered by the semisolid processing to the present and describe the material aspects for thixoforming.

2.1 Introduction

We do not know exactly who discovered the iron, but the truth is that its history and the one from its offspring, the steel, go hand in hand with human culture and civilisation.

Our ancestors felt drawn by the metal´s brightness and shaping properties that made it possible to manufacture tools and weapons, so necessary for their survival. Thus, metal forming became a major concern for human beings. Since then, lots of metal forming techniques have been developed and most of them can be classified in two main categories: casting and forging.

> **Casting:** The alloy is heated up to complete melting and then poured into a die, which contains a hollow cavity of the desired shape. It is allowed to solidify and then the part is ejected or broken out of the die. The

major energy consumption concerns melting and holding molten alloy in preparation for casting. This kind of process is used to produce complex shapes, most notably thin wall components that would be difficult or uneconomical to obtain otherwise. However, during solidification, the material tends to shrink, and this can lead to porosities that weaken the mechanical properties of the final product.

Forging: The alloy in solid state is transformed into a useful shape by hammering or pressing. In cold forging, the energy consumption is mainly due to the load necessary to produce the prescribed deformation. On the contrary, in hot forging as well as in casting, most of the energy is consumed during material´s heating. This kind of process makes it possible to obtain components with very good mechanical properties but is limited to simpler designs than casting.

The **Semisolid metal (SSM) forming** is a novel metal forming technique located halfway between casting and forging. It relies on a particular behaviour exhibited by semisolid materials; *thixotropy*. This means that the material exhibits a reduction in structural strength during the shear load phase and the more or less rapid structural regeneration during the subsequent rest phase. Depending on the liquid fraction and the process used to shape the material it is closer to casting or forging.

Compared to conventional casting, the high viscosity of semisolid metal avoids the turbulent filling of the dies and consequently reduces part defects coming from air entrapment. In the same way, the high solid fraction of the semisolid material (more than 70% in our case) reduces the loss of volume during solidification, leading to less shrinkage porosity.

Compared to conventional forging, thixoforming offers reduced forming loads and the opportunity to produce geometrically complex components which cannot be obtained by conventional forging in a single-step. Besides, the near net shape capabilities of thixoforming reduces final machining to a

minimum. However, the superior mechanical properties of forged parts cannot be achieved for the moment.

2.2   Historical Background

In the early 1970s Spencer, Mehrabian and Flemings studied the flow behaviour of metals in semisolid state [2] establishing the origin of this fabrication process. As described by Kirkwood *et al.* [3], after an unsuccessful attempt to exploit this technology, patents were licensed to International Telephone and Telegraph corporation (ITT Corp.) in the late 1970s. Soon after, ITT Corp. and Alumax Inc., who acquired the technology from ITT around 1985, started to industrialise parts for automotive applications but the secrecy and the reluctance to licensing requests or joint ventures that both companies had hindered the development during that time.

However, around 1985 ITT-Teves, a subsidiary of ITT Corporation established a semisolid manufacturing facility in Northern Germany, which aroused the interest of other European manufacturers. As a consequence, some of those manufacturers began to develop their own proposals for obtaining both raw material and manufactured parts. Primary material in different dimensions and quality became available and new heating technologies and pressure casting machines led to various mass production applications. Nevertheless, with an automotive industry extremely exacting on price, and the rapid improving quality of highly cost-effective fully liquid casting, the surcharge for the raw material was too much for the market to support, and billet based producers could no longer compete.

During the first stages of the semisolid forming, only low melting point alloys were studied. Until the mid 1990s steel thixoforming did not become the focus of various research activities [4, 5, 6, 7, 8]. These investigations demonstrated the feasibility of semisolid forming of steels but the major challenges, mainly related to the high temperature range, still need to be

overcome. With temperatures above 1250°C the process requires exact heating technologies that must take into account severe heat loss due to radiation and, also, surface degradation caused by scale formation. At the same time, because of the high temperature difference between the billet and surroundings, well above 1000°C, an extensive effort should be made to reduce the thermal gradient inside the billet aiming at obtaining a good homogeneity.

Another challenge to confront is the thermal and mechanical loading of tools and dies. The surface to interior temperature differentials in steel thixoforming dies are much larger than with aluminium and magnesium, and the cyclic thermal stresses produced require very specific features of tool materials. As a matter of fact, no efficient tool materials that can survive several thousand semisolid forming operations have been developed yet.

2.3   Thixotropic SSM alloys

As mentioned in the previous section, everything started with the very unexpected results of some viscosity measurements during solidification of Sn-15% Pb alloy carried out at Massachusetts Institute of Technology (MIT)[2]. All the alloys have a solidification range where two phases coexist, the liquid and the solid phases. That is exactly the semisolid range. As the solidification moves forward, the viscosity and the solid fraction (f_s) of an alloy increase. The rise in viscosity speeds up at a certain solid fraction where the alloy starts to stiffen, usually close to 0.2. This sudden stiffening depends on solidification conditions. In contrast, stirred metal melts, depending on the shear rate, behave like liquids up to 0.4 or more solid fraction.

Figure 2.1 shows how sensitive the viscosity of a SSM alloy is regarding the shear rate. Viscosity in turn, can be used as a measure of the fluidity for a material and thus, it is demonstrated that at the same solid fraction, the stirred melt flows more easily than the unstirred one.
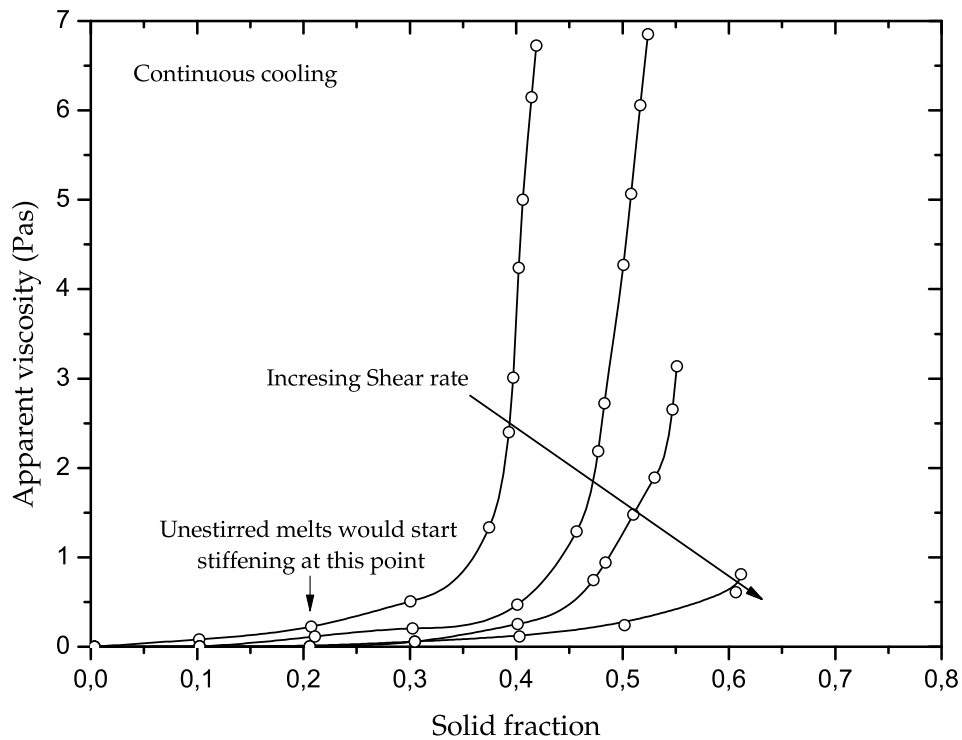
Figure 2.1 Apparent viscosity versus solid fraction for Sn-15% Pb stirred at different shear rates during continuous cooling [2].

Joly and Mehrabian [9] continued the research analysing the viscosity of the same alloy, Sn-15% Pb, and the results showed that the viscosity was also very sensitive to the cooling rate. They noticed that, at the same shear rate, viscosity decreased by decreasing the cooling rate (Figure 2.2).

Flemings and his MIT group attribute this particular behaviour to the microstructural evolution of the molten alloy during cooling. It was well known that a steady solidification led to a dendritic microstructure. They show that a vigorous agitation along with a proper cooling rate leads to a globular microstructure. Even if the first nuclei grow like dendrites, due to grain ripening and particles´ abrasion and wear phenomena, they end up with

a spheroidal shape. In rheological terms, the viscosity decrease due to shearing is represented by the pseudoplastic behaviour.
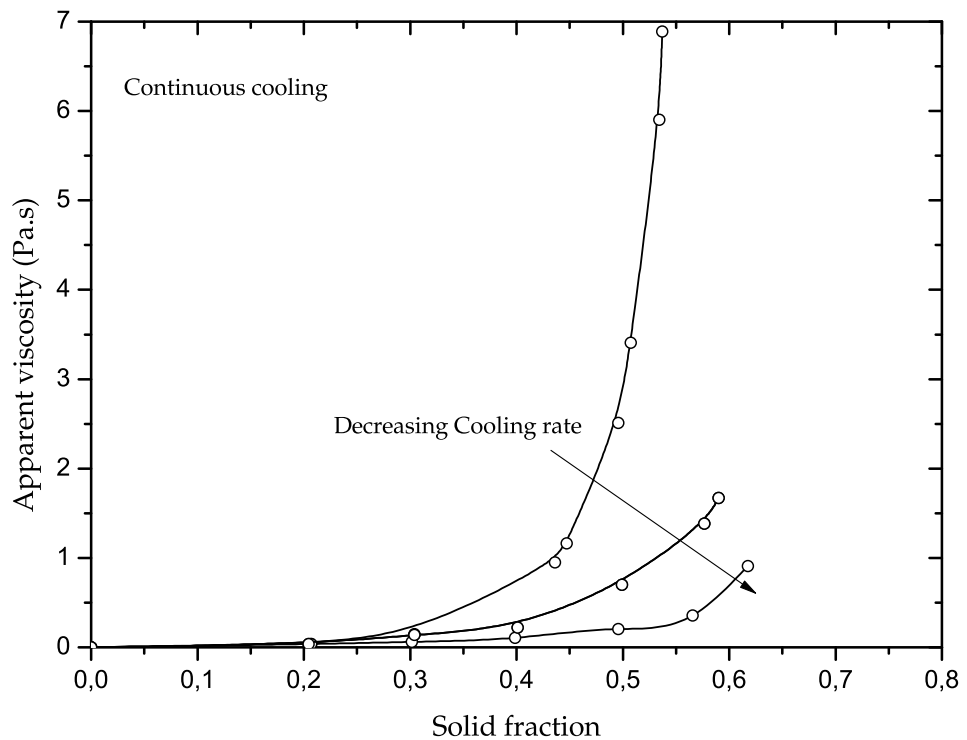
Figure 2.2 Apparent viscosity versus solid fraction for Sn-15% Pb at different cooling rates [9].

In turn, Moon [10] made some shearing experiments with an aluminium alloy. He observed that, after restarting shearing, viscosity was higher than in the steady state, demonstrating that the microstructure had built up during rest time. However, if shearing continued, the viscosity returned to steady state values (Figure 2.3). The rupture of the rigid network is fast while its build up needs more time. This time depending reversible pseudoplastic behaviour is known as thixotropy.
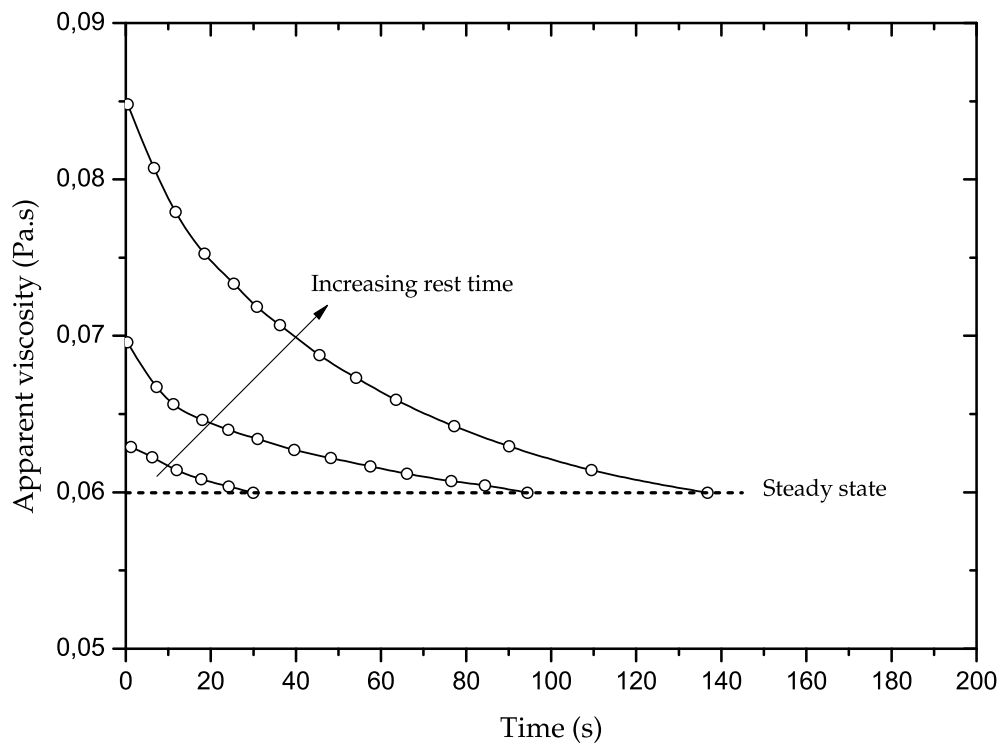
Figure 2.3 Time needed to return to stationary viscosity values after rest time [10].

2.4 The semisolid material

As it has been mentioned in section 2.3, the process of shearing clearly altered the microstructure (Figure 2.4), changing the dendritic morphology of the solid into a more spherical form that brought about a dramatic fall in shear stress and viscosity. These initial findings clearly showed that the viscosity of a semisolid metal alloy is dependent on the solid fraction, shear rate and time history.

2.4.1 Material aspects for SSM forming

For SSM forming, the alloy has to fulfil at least these specific requirements:

- First, the material needs to have a freezing range where liquid and solid phases coexist. A low temperature sensitivity is really important for the correct adjustment of the solid-liquid fraction; this way, a little change in temperature will not suppose a big change on the solid-liquid fraction.

- Second, a particular micro-structural formation is needed in the semisolid state; globular solid particles should be embedded inside a liquid matrix.
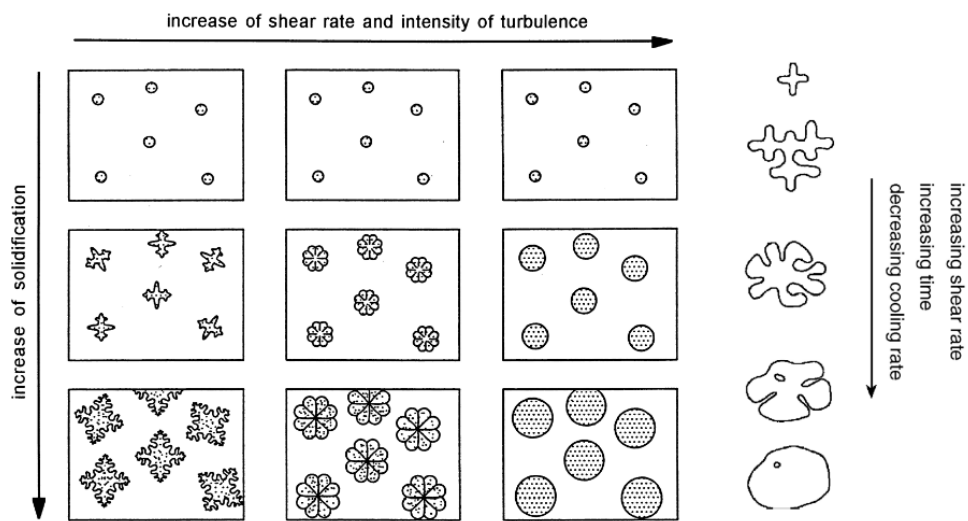

Figure 2.4 Structural changes during the solidification and shearing of metallic suspensions [11].

During processing, a semisolid material is a mixture of rounded, rosette like particles in liquid. In contrast to Newtonian fluids, the semisolid metal alloys exhibit thixotropic behaviour. The viscosity decreases under increasing shear rates and when the shear rate decreases, the viscosity increases again, but much less than it dropped initially (Figure 2.5). It may take seconds or minutes to break down a thixotropic structure but, in many cases, it requires much longer time to fully recover the original status. Ultimately and simplifying to the maximum it is possible to say that semisolid materials become fluid when shear stress increases and return to behave like a solid when allowed

to stand. In fact, they can be handled like solids due to the development of a rigid network in the quiescent state between solid particles. Of course, this is possible whenever shearing forces do not exceed the network resistance. If sufficient shear stress is applied, the framework breaks and the agglomerates are dissolved. A suspension of solid particles within a liquid matrix develops, resulting in a reduction in viscosity, which makes the semisolid alloy fluid and capable to fill the die.
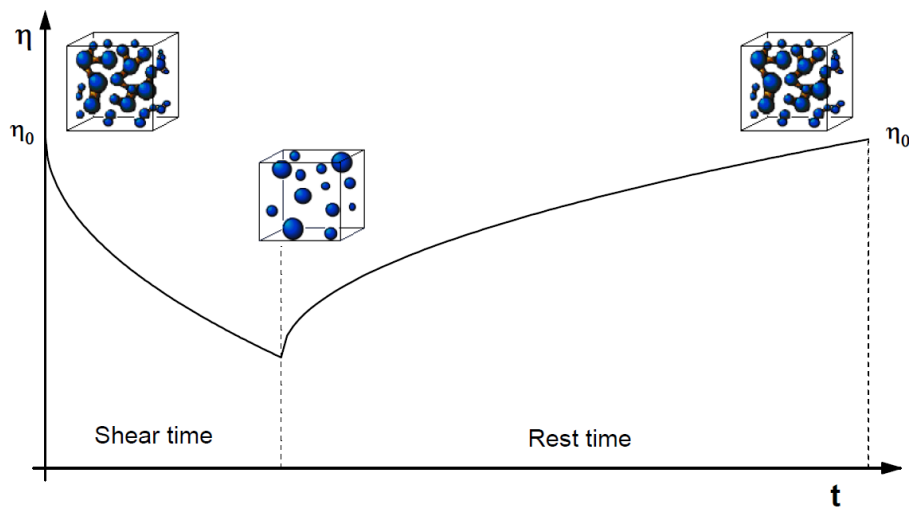

Figure 2.5 Vicosity evolution under shear stress [12].

The most important parameters for semisolid materials are: the solid fraction, the temperature sensitivity, the grain size and shape and the steric arrangements of the solid phase[12].

2.4.1.1 The solid fraction (f_s)

The solid fraction is one of the most important parameters in semisolid forming because it has a crucial influence on the viscosity and therefore on the flow and filling behaviour of the material. Depending on the forming process it varies steeply. In our case, thixo lateral (or transverse) forming, the material

is expected to be able to fill up the die completely avoiding turbulent flow with a solid fraction between 75-85%.

Details about different methods used to determine the volume fraction of solid as a function of temperature are given in a study carried out by Tzimas and Zavaliangos [13].

Another parameter directly related to the solid fraction is the inter-globular liquid phase. Not all the liquid phase is available as inter-globular. There is also an intra-globular liquid phase, which does not contribute to the sliding of globules during forming and therefore the liquid phase volume fraction is lower than the theoretical value. The solid particles adhere more to each other and, as a result, the viscosity raises and the sponge effect[1] is promoted.

2.4.1.2 **Temperature sensitivity**

In a real thixoformig process the temperature will always be subject to some error and as the thixoforming window is not usually too wide for steels, the impact of the temperature variation on the solid fraction can have devastating consequences in the forming step. Because of that, it is important for semisolid alloys to have a low temperature sensitivity, thereby a little change in temperature will not suppose a big change in the solid fraction. The impact of temperature variations on the solid fraction can be expressed by the negative slope of the solid fraction curve.

$$S = -\frac{df_s}{dT} \tag{2.1}$$

---

[1]The sponge effect is called this way because of its similarity to the wringing out of a water filled sponge. If a reheated billet is plastically compressed and no thixotropy occurs, the liquid phase, which is embedded in the spaces between the solid particles, is extruded from the compacted solid phase. The segregation due to this effect should be avoided because of the resulting poor component properties.

2.4.1.3 **The grain size and shape**

From the process´s point of view, the grain size must be large enough to build a three dimensional network and withstand the manipulation of the billet. At the same time, it has to be small enough to flow across the thinnest sections of the part. The grain size also plays a crucial role on the mechanical properties of the final component and, because of that, reheating has to be tightly controlled in order to avoid an excessive growth of solid particles.

The spherical morphology of the particles is essential for the flow behaviour of semisolid metals. When solid particles exist in a globular form within a liquid matrix and a shear stress is applied over them, they are able to translate, rotate or slide past each other. As it has been shown in Figure 2.4, longer holding times, higher temperatures and higher shear rates in the partial liquid state result in rounder grains. One commonly used descriptor, which may be obtained from two-dimensional sections, is the form factor, F , defined by the equation:

$$F = \frac{4.\pi.A}{P^2} \tag{2.2}$$

A is the grain section and P is the perimeter length of a particle present in a section. For ideal round globules, the form factor takes the value 1. A low value for this parameter indicates a complex grain structure, such as dendritic structure. In any case, circular sections may not only arise from spheres, but also from much more complex morphologies in three dimensions, such as sections through cylindrical dendrite arms that are not reflected in this simple shape factor. To overcome this drawback, Loué and Suery have introduced a different dimensionless shape factor [14].

$$F_g = \frac{1}{6.\pi.f_s}.\frac{S_v^2}{N_A} \tag{2.3}$$

f_s is the volumetric fraction of the solid phase, S_v represents the solid-liquid

surface area per unit of volume and N_A is the grain number per unit of surface. For dendritic microstructures F_g has a high value but it moves close to 1 when the solid phase consists on fully spherical grains.

2.4.1.4 Contiguity and continuity

The steric arrangements of the solid phase are really important for the semisolid processing. Solid particles have to form a three dimensional network to absorb the forces derived from the handling of the billet. The cohesion of solid phase particles is characterized by contiguity, a measure of grain boundary contact. Gurland [15] defined it as the average fraction of the surface area of a particle shared with neighboring particles of the same phase.

$$Cf_s = \frac{2S_v^{ss}}{2S_v^{ss} + S_v^{sl}} \tag{2.4}$$

Cf_s is the contiguity of the solid phase, S_v^{ss} is the boundary surface of the solid-phase particles and S_v^{sl} is the boundary surface of the solid and the liquid phase. The contiguity can be determined in metallographical images by measuring the solid-solid and solid-liquid boundary surfaces. It takes values between 0 and 1. If Cf_s is zero, the particles of the solid phase are completely surrounded by liquid.

In addition to this, the probability of forming long chains of connected particles providing a rigid framework is defined as continuity, the average number of contacts that a particle makes with neighboring particles of the same phase.

2.5 Forming operations

The key point of semisolid forming processes is the thixotropy of metallic alloys at the semisolid state. For this, a spheroidal microstructure is required. Thus,

the SSM forming processes take place in several steps:

1. Production of nondendritic microstructures.
2. Reheating to the semisolid state.
3. Forming.

Depending on the type of the process, the reheating step can be avoided as shown in Figure 2.6. The standard terminology is as follows.

Rheoforming: Processes, in which the semisolid slurries produced from the liquid phase are directly used in shaping operations.

Thixoforming: A particular type of solid feedstock is reheated into the semisolid range to form a globular, non-dendritic slurry that is then used in subsequent forming operations.
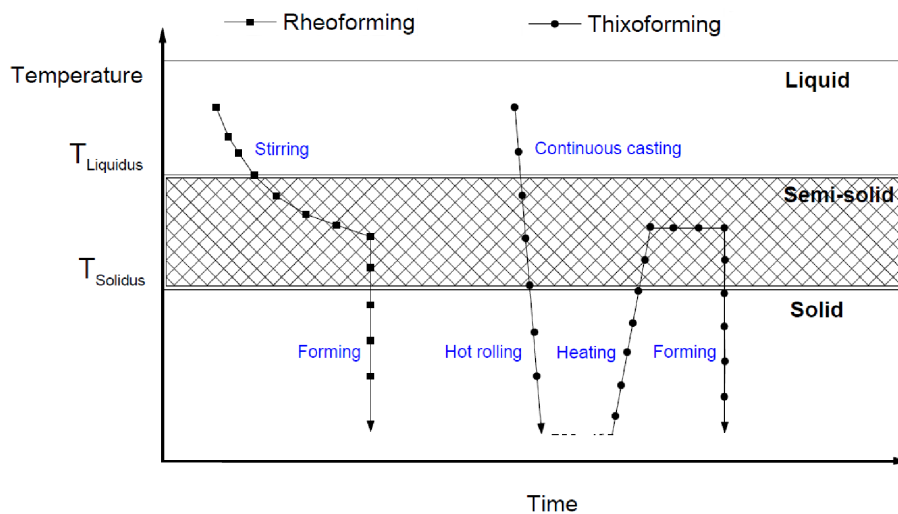
Figure 2.6 Schematic illustration of different routes for SSM processing [16].

Depending on the liquid fraction, the forming stage can be close to casting or to forging. If the liquid fraction is relatively high (i.e., above about 50%) the

process is closer to *casting*. On the other side, a process working with lower liquid fraction is closer to *forging*. The different types of semisolid processes can be categorised as thixocasting, thixoforging, or rheocasting as shown in Figure 2.7.

They are performed using modifications of conventional processes, such as high-pressure die casting, forging, transverse extrusion, bar extrusion and rolling. Of these, only semisolid casting and, to a lesser extent, modifications of semisolid forging have so far been applied to industrial production.
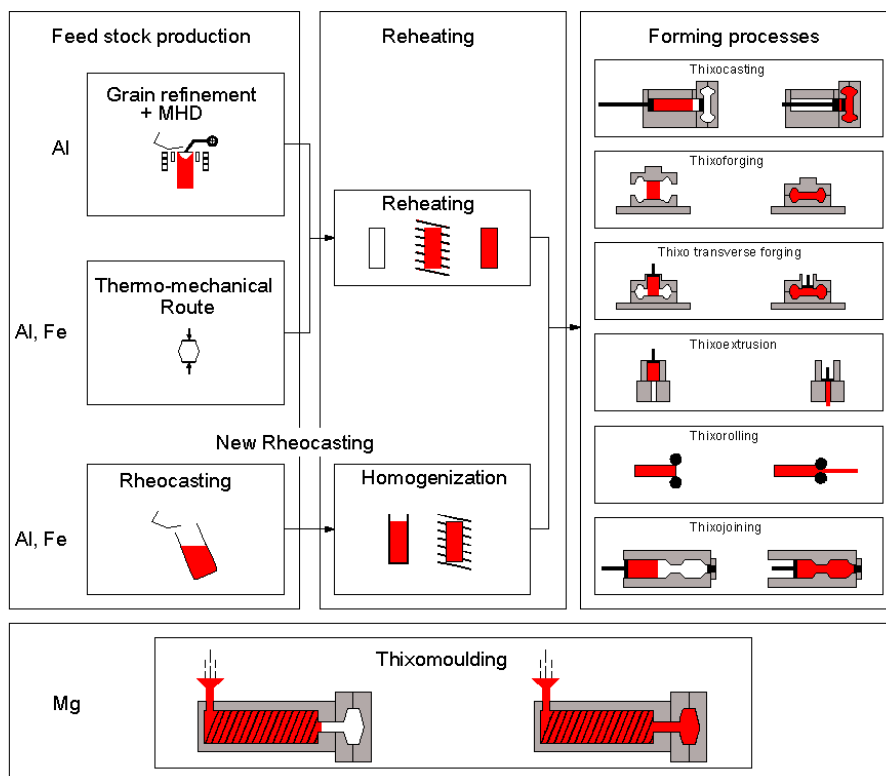
Figure 2.7 SSM process routes [12].

The thixomoulding of magnesium alloys has also found its market niche, but the process is quite different. This process uses magnesium chips and a modified injection moulding machine. Metal pellets are injected into a continuously rotating screw where they are heated to the semisolid condition.

The material is then directly injected into a die, making the process similar to polymer injection moulding.

The term thixoforming includes all forming processes of semisolid alloys into a metallic die. If the forming process is carried out in a nearly conventional die casting machine, it is called *thixocasting*; otherwise, if it is performed using a forming press, it is known as *thixoforging*.

In thixocasting, a billet with solid fraction in the range of 30-50%, is placed in an adapted shot chamber, modified to accept semisolid billets instead of liquid metal, and squeezed into a closed die by a shot piston. The flow during die filling is laminar and the velocity is significantly higher than in thixoforging but lower than in conventional high-pressure die casting. One of its strengths is the possibility to use the highly advanced high-pressure die casting technology that makes possible to manufacture very complex components.

In thixoforging, a semisolid billet of a higher solid fraction, 75-85%, is inserted directly in the lower half of a horizontally sectioned tool, analogous to the conventional drop forging process. The forming operation is performed by closing the die halves. In contrast to thixocasting, the force transmission for the forming and densification step is applied over the whole tool surface, not only on the shot piston area, so that hydrostatic pressure is affected evenly during solidification. However the geometric complexity is limited to geometries which allow forging without flash. Furthermore, oxides on the billet surface must be reduced to a minimum, so as to eliminate the risk of including them into the part during forming.

In this research dissertation, I am focusing on steel thixoforming, using the thixo lateral (or transverse) forging method (Figure 2.7) for components´ manufacturing. First of all, because of the means at our disposal -we have a servo-mechanical forging press at the forming lab- and, secondly, because of its advantages with regard to conventional thixoforging. Although the forming velocity is of the same order of magnitude, thixo lateral forging is

characterised by squeezing the semisolid material into an already closed die, eliminating possible material ejection and allowing an increased degree of geometric freedom.

Routes to Thixoformable Starting Material

Looking closely into the area of alloy development for thixoforming, Kapranos [17] discerns two main strands: that of high strength aluminium alloys and another concerned with steels and other high melting point alloys. Current research in the latter field is concentrating on the development of high melting point alloys. Thus, this chapter will be devoted to review the past and current developments to get thixoformable starting material. Different processes to produce globular microstructure are shown as well as the thermomechanical routes, the best methods to provide appropriate feedstock from various steel grades.

3.1 General overview

Conventional partial solidification or remelting leads to solid dendrites in a liquid matrix, which is precisely what is to be avoided in an efficient semisolid process. Therefore, the stage of production of a globular microstructure is critical and requires the development of innovative processes besides regular

casting or forging. In his book, Suéry classifies the processes into two main categories [18]. The first category contains processes where the main microstructure modifications occur during *solidification*; it does not matter then whether the semisolid thixotropic material is formed right away (rheo) or cooled back down to the solid state and reheated before the forming step (thixo). The other category includes processes where *remelting* plays the major role in structure modification.

Microstructure modification during solidification The goal of this kind of processes is to act on the solidification stage in order to avoid the development of dendrites. According to Suéry [18], this can be done in three ways:

- **Mechanical methods** impose shearing to the structure under solidification. The shearing can be produced by different kinds of stirring, mechanical, passive, or electromagnetic stirring, by ultrasound or by electric shock. The shear generated prevents the formation of large dendrites and create nuclei of crystals by dendrite fragments.
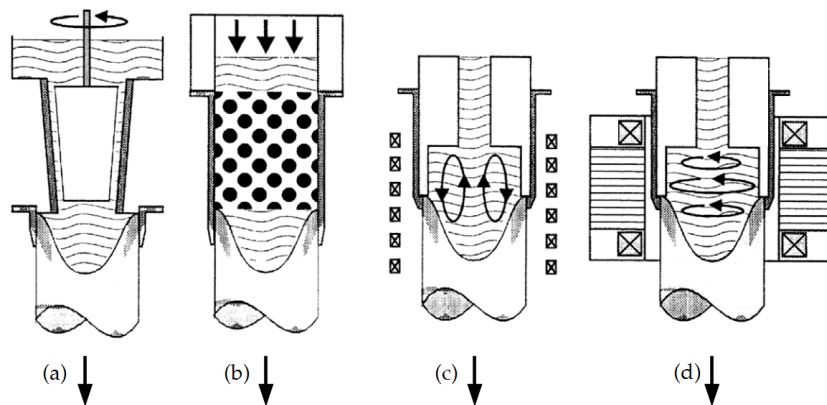
Figure 3.1 Stirring modes: (a) mechanical stirring; (b) passive stirring; (c) and (d) electromagnetic stirring.

- **Chemical methods** modify the composition of the alloy by addition of different particles. The goal is to produce a fine grained and homogeneous

microstructure and, for this purpose, various methods of chemical grain refinement that provide a large number of nuclei have been developed.

- **Thermal methods** use some appropriate cooling conditions to get globular microstructures. To avoid the higher costs of producing primary billets with globular microstructures and reheating them to the semisolid condition, cheaper and shorter routes to achieve the slurry have been developed in recent years. They create the slurry during cooling from the melt: cooling slope, low superheat casting, single slug production method, continuous rheoconversion process, SEED process, etc.

  Most of these processes make use of the high nucleation rate associated with low temperature casting and chill cooling, but chemical reactions and other principles can also be used.

Microstructure modification during remelting   The non-dendritic microstructure is achieved during the remelting stage, although the structure of the alloy at the initial solid state is also very important. These processes can be sorted into three kinds [18].

- **Powder metallurgy:** The partial remelting of a fine powder made of several alloys with different solidus temperatures can lead to a globular microstructure under proper heating conditions.

- **Deformation processes:** In addition to solidification processes, there also exist solid working routes to produce feedstock for semisolid forming. This routes typically consist of plastic deformation followed by recrystallisation during the reheating stage. When reheating gets the semi-solid range, the fine grains start to melt at their boundaries, resulting in globular particles surrounded by liquid. Depending on the temperature at which the plastic deformation has been performed there are two different processes. A route called *(SIMA) Strain Induced Melt*

Activated involves hot working, above the recrystallisation temperature, while *(RAP) Recrystallisation And Partial remelting* process involves warm working, below recrystallisation temperature.

- **Thixomolding**: As mentioned in section 2.5 this is an exception to the terminology 'thixo'. Thixomolding is a licensed process highly effective for magnesium alloys and applied mainly for electronic products.

3.2 Starting material for steel thixoforming

The level of success in semisolid processing depends mostly on using an adequate starting material. To produce suitable thixoforming feedstock, different routes have been developed so far [19, 16, 3, 12], including: simple mechanical stirring, rheocasting, magneto hidrodynamic stirring (MHD), recrystallisation and partial melting (RAP), strain induced melt activated (SIMA) and low superheat casting.

Regarding thixoforming of steels, the thermomechanical route has been the most suitable method to provide appropriate feedstock from various steel grades [12].

3.2.1 Thermomechanical routes

As mentioned in section 3.1, the semisolid metal processes can be divided in two main categories, depending on whether the microstructure is modified during solidification or during remelting. From the microstructural point of view, there is a significant difference between *thixo-* and *rheo-* materials. Spheroidization of thixo material occurs during reheating and final holding at the semisolid temperature. During this process, entrapped liquid arises within the globules that will not contribute to the flowing in the forming step. In rheo processes, this phenomenon never occurs.

However, this shortcoming is counterbalanced by the superior sphericity of the solid particles in extruded or rolled materials which contribute to have a better fluidity [12].

3.2.1.1 **Material spheroidisation**

Even if it is not completely clear yet, spheroidisation in *rheo-* materials starts up with dendrite´s fragmentation. Different fragmentation mechanisms are listed by Flemings [11], which may be reduced to three main groupings:

1. Dendrite arms break off at the root due to shear forces. It is difficult to estimate the magnitude for these forces which originate from the velocity gradient along an arm belonging to a free floating dendrite. It must be born in mind that these dendrites, due to their dimensions and growth conditions, are likely to be initially near perfect crystals without dislocations or notches and, therefore, simple fracture could be difficult.

2. Dendrite arms melt off at their root. This occurs as a result of the normal ripening process in which the surface area is reduced and may be assisted by fluid flow: (a) accelerating diffusion in the liquid, (b) causing thermal fluctuations, or (c) generating stresses at the root which aid melting. Higher solute content in the solid at the roots will also lower the melting point and encourage local melting there.

3. An entirely different mechanism has been proposed by Vogel et al. [20] and discussed by Doherty *et al.* [21]. They suggest that dendrite arms bend under the flow stresses and the plastic strain is accommodated by dislocation generation. At the melting temperature, the dislocations can climb and coalesce to form grain boundaries. When the misorientation between grains across a boundary exceeds about 20$^{\text{o}}$, the grain boundary energy exceeds twice the solid-liquid interface energy: the liquid will now

wet the grain boundary and rapidly penetrate along it, separating the arm from its stalk, figure 3.2.
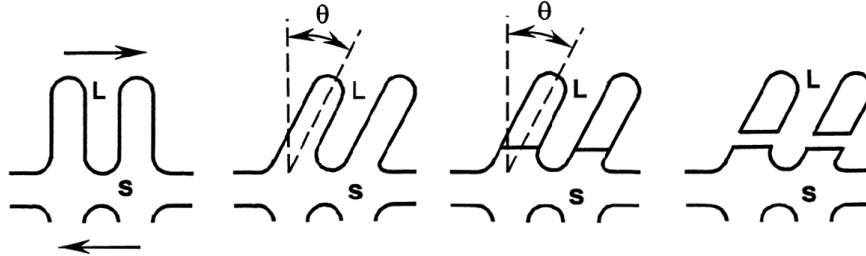

Figure 3.2 Schematic picture of dendrite arm fragmentation mechanism [22].

It may well be that all the above mechanisms operate under different conditions. However, grain boundary penetration by liquid has been observed to occur in solid alloys which have been heated just above the solidus to cause incipient melting and then quenched. This forms the basis of SIMA and RAP processes. Two thermomechanical ways for producing suitable feedstock for semisolid forming and what has been outlined by Kirkwood [23] in a patent. Both processes are shown schematically in figure 3.3 below.

3.2.1.2 Description of SIMA and RAP processes

I have explained in the previous section that, during the formation of the liquid phase, high angle boundaries between solid grains will, in general, be penetrated causing fragmentation. If the material has been sufficiently deformed to generate a fine grained microstructure, partial melting will then cause it to fragment into an ideal slurry composed of well rounded solid particles within a liquid matrix [19].

The initial deformation may be carried out above the recrystallisation temperature (hot working, SIMA) followed or not by cold work, or alternatively, below the recrystallisation temperature (warm working, RAP) to ensure that the maximum strain hardening is introduced in the material. Recrystallisation
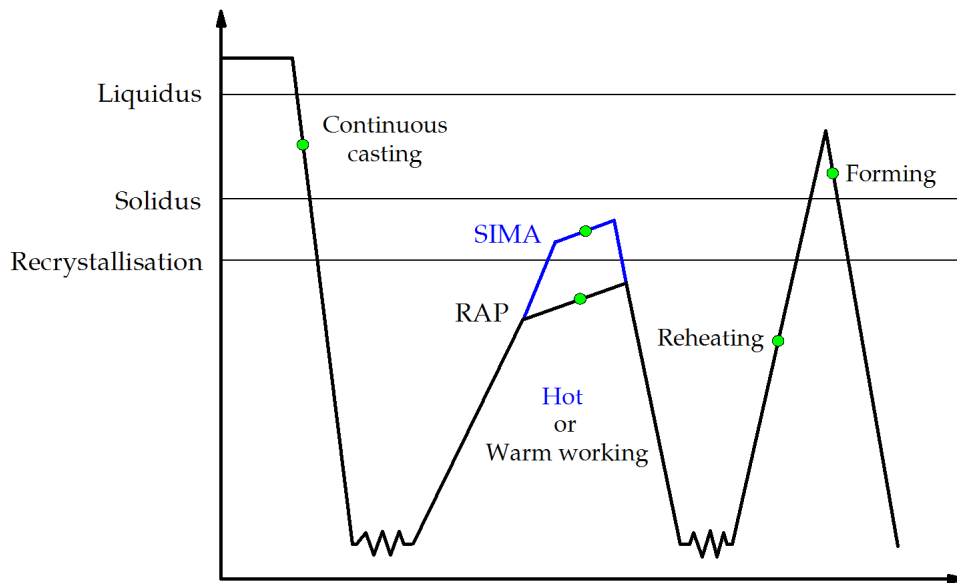
Figure 3.3 Schematic illustration of SIMA and RAP processes [23].

occurs in the work hardened alloy during reheating: if this can be induced just before remelting occurs, little time for grain growth is allowed before fragmentation begins and a finer particulate structure of the slurry is obtained. According to Fan [22], the particle can be as small as 30 μm, depending on the degree of cold work and the rate of heating. A minimum of 10% cold work would seem to be required for effective fragmentation, which sets a limit on the maximum practical billet achievable by extrusion at around 50 mm; however, it has been shown that heavy forging processes may also be used with success and this may allow larger billet diameters to be achievable for thixoforming.

3.2.1.3 Hot rolled, the standard state

There has also been interest in whether steel can be thixoformed as cast or in the standard state. In this research work the standard state or as-supplied state means that the steel bars have been directly received from the steel supplier hot rolled above the recrystallisation temperature. Despite being a similar thermomechanical route, it does not fit with the 'classical' RAP and SIMA

routes. Different experiments carried out at Sheffield established that austenitic ductile iron and high chromium ductile iron offer the possibility of processing in the semisolid state straight from the as-cast condition [24]. Bulte and Bleck [25] compared the microstructure of a 100Cr6 rolled bar, after quenching from the semisolid state, with a laboratory cast billet and a laboratory cast billet with liquid core reduction. They found no significant difference and therefore suggested that primary as-cast billet can be used. Omar and co-workers [26] demonstrated that HP9/4/30 a high performance steel manufactured by vacuum arc remelting (VAR), which is very difficult to form by other routes, can be successfully thixoformed. Casted ingots were subjected to hot rolling at 1250-1310°C in order to achieve homogenisation and then given a commercial heat treatment according to the AMS 6526C standard.

Hot rolled bars present excellent geometrical characteristics as cylindricity, close tolerance on the diameter for the same batch and between various batches, low surface roughness and no scale. This set of properties play an important role during the induction reheating, in terms of reproducibility, temperature homogeneity and surface quality of the thixoformed part.

3.2.2 Other routes for thixoformable steel

Atkinson and Rassili quote [8] some other authors that have studied routes where molten steel has been treated. A group based in Seoul has produced stainless steel billets by Magneto Hydrodynamic (MHD) stirring and shown excellent microstructures [27]. The University of Science and Technology in Beijing has also electromagnetically stirred steels (in this case spring steels and stainless steel) and then rheorolled the semisolid slurry [28]; that is, they reduce the liquid macrosegregation trough grooved rolling. CRM in Liege, Belgium, has developed a specially designed hollow jet nozzle for continuous casting which allows powder injection and a low superheat to be combine to obtain a globular structure in the core of a continuously cast steel billet [29].

Other groups [30, 31, 32, 33] are investigating the use of a cooling slope (similar to the New Rheocasting -NRC- process or the work made by Haga and co-workers [34]) with some success. Vibratory casting has also been used [35].

Up to now a complete review of the background information and general aspects of the semisolid processing has been provided (thixotrophy, material aspects for SSM forming, forming operations, routes to obtain thixoformable starting material, etc.), focused especially in steel alloys. I have exposed past and current developments and insights into the possibilities of thixoformable steels. Because of that, in order to give the proper continuity to the work, I will fully characterise the tested thixoforming steels in the next chapter.

Material Characterisation: Thixoformable Steels Used

A complete characterisation of the steel grades used is presented in this chapter, from metallurgical to thermophysical characterisation, with the aim of determining the proper heating strategy. For that purpose, I compare results from Differential Scanning Calorimetry (DSC), thermodynamic prediction software and quantitative metallography.

4.1 Introduction: identifying suitable steels

There is a range of special carbon and low alloyed steels between 0.1% and 2% of carbon content, with or without alloying elements, which improve forming or application properties. Rassili, Robelet and Lecomte-Beckers classify these steels into three categories [17]:

1. *Low carbon steels - with between 0.1% and 0.3% carbon*. These steels are generally steels with 'electric', 'magnetic' properties or steels for cold forming. Nowadays, this category has evolved towards steels with

high mechanical characteristics, 'low alloy' steels, mainly bainitics, and classically hot forged steels for mechanical parts of large series.

2. *Steels with carbon content between 0.3% and 1%*, which are carbon or low alloyed steels mainly used in the car industry and for sophisticated parts of the mechanical industries. These steels are mainly formed by hot forging and offer mechanical characteristics adapted to the application properties. The metallurgical structure and the mechanical characteristics of the parts are obtained either after a controlled cooling directly at the end of the hot forming operation or with an adequate heat treatment operation made subsequently to the forming and cooling operations.

   This class of steel grades is mainly well adapted to the semisolid forming.

3. *Steels with more than 1% carbon or high alloy content*. These steels are classically intended for cold forming tools. Their solidus temperature is low and the gap between solidus and liquidus is large. Due to this, these kind of steel grades are useful for studying the behaviour of the semisolid steel during thixoforming operations. High speed steels can also be included in this category. The carbon content can be lower than 1% but the concentration in alloying elements is high and the solidus temperature consequently low.

One of the major challenges for steel thixoforming is the identification and development of suitable steels that can be successfully thixoformed. The first approach to that involves examining the phase diagram to get an idea of the solidus-liquidus range, without considering the effects of alloying elements. Two main conditions must be ensured: lowering the solidus temperature and enlarging the solidus-liquidus range and thus, the thixoforming window.

The phase diagram (Figure 4.1) shows that low carbon steels have narrow solidus - liquidus ranges and, therefore, process control is likely to be difficult.
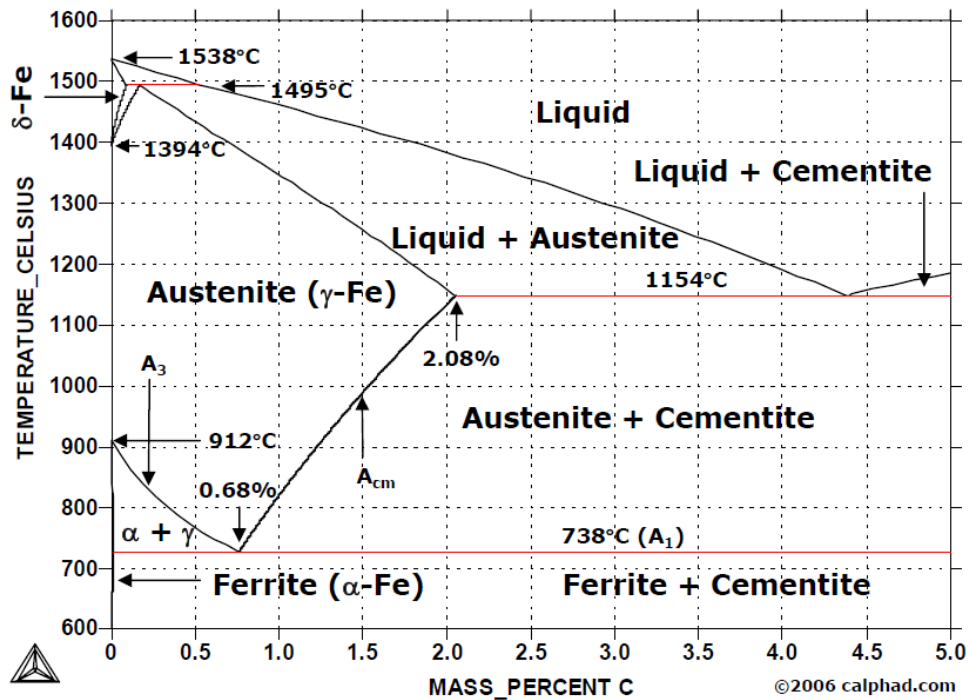
Figure 4.1 Fe-C metastable phase diagram.

The present work focuses on two low alloyed steels and a high carbon steel, which tends to be the most difficult composition to work with by conventional means.

As mentioned in chapter 3, the starting steel grades can be supplied mainly in two states: **a)** already presenting a globular structure in the as-cast state due to the usage of special techniques for cooling and nucleation or **b)** hot rolled, where the globular structure is achieved during the reheating stage.

Some attempts to obtain the globular structure directly on steel cast with electromagnetic stirring have demonstrated the difficulty of this route. The major obstacles are the power needed for the electromagnetic agitation of the liquid metal and the low productivity of the continuous casting set up.

In the present research work, I have used different hot rolled steel grades in the as-supplied state. This means that the material is already recrystallised

due to the hot rolling step and, in the case of LTT 100Cr6, it has also received a globularisation annealing.

The steel supplier is Ascometal, a special steel manufacturer who designs commercial thixoforming steels, modified to have a wider solidification range and lower solidus temperature. The selected steels are, in principle, the best suited to fulfil final mechanical requirements and are designated as Low Thixoforming Temperature (LTT) steels: LTT C45, LTT 100Cr6 and LTT C38.

4.2 Metallurgical characterisation of steels

In this section, I present the metallurgical characterisation of the steels by analysing their chemical composition, hardness and microstructure in the as-supplied state. It is important to keep in mind that both LTT C45 and LTT C38 were hot rolled from continuous casted square blooms of 240 mm x 240 mm. In contrast, LTT 100Cr6 steel grade was hot rolled from a square ingot of 540 mm x 540 mm. Thus, the hot working rate for LTT C45 and LTT C38 is around 15 and for LTT 100Cr6 around 78.

4.2.1 Chemical composition

The chemical composition has been analysed and compared to the one sent by Ascometal in two different laboratories, Gerdau I+D Europe and Azterlan, a metallurgy research centre from IK4 Research Alliance.

The contents of the different alloying elements for all steel grades are in the range established by Ascometal in its thixoforming patent EP 1 426 460 A1 [36].

4.2.1.1 LTT C45

In accordance with the results of Table 4.1, it is possible to classify LTT C45 as a spring steel with high contents of silicon, molybdenum and nickel, elements that widen the semisolid range.

Table 4.1 Chemical composition of LTT C45.

LTT C45 Composition						
	C	**Mn**	**Si**	**P**	**S**	**Cr**	**Ni**
Ascometal	0.473	0.721	1.397	0.01	0.009	0.661	0.211
Gerdau	0.5	0.7	1.35	0.008	0.008	0.64	0.21
Azterlan	0.5	0.72	1.45	0.008	0.007	0.67	0.25
	Mo	**V**	**Cu**	**Al**	**Sn**	**Ti**	
Ascometal	0.209	0.007	0.203	0.019	0.013	0.004	
Gerdau	0.2	0.004	0.2	0.017	0.012	0.004	
Azterlan	0.22		0.2	0.016		0.005	

4.2.1.2 **LTT C38**

As Table 4.2 shows, LTT C38 presents vanadium and titanium below the 10% in its composition along with higher amounts of manganese, molybdenum and nickel. Because of that we can consider LTT C38 a microalloyed steel with a carbon content around 0.4% where the most remarkable parameter is the high phosphorus and sulphur content. These two elements, together with carbon, widen the solidus-liquidus range.

The phosphorus quantity is specially high and that is why it could be specifically designed for thixoforming processes.

Table 4.2 Chemical composition of LTT C38.

LTT C38 Composition						
	C	**Mn**	**Si**	**P**	**S**	**Cr**	**Ni**
Ascometal	0.388	1.375	0.582	0.078	0.089	0.147	0.082
Gerdau	0.41	1.38	0.57	0.085	0.087	0.14	0.08
Azterlan	0.39	1.39	0.61	0.092	0.081	0.15	0.1
	Mo	**V**	**Cu**	**Al**	**Sn**	**Ti**	
Ascometal	0.021	0.096	0.153				
Gerdau	0.02	0.09	0.15	0.002	0.012	0.013	
Azterlan	0.02		0.14	<0.003		0.015	

4.2.1.3 **LTT 100Cr6**

The chemical composition of LTT 100Cr6 is displayed in Table 4.3. Due to its high carbon, silicon and manganese content this steel grade has been widely used for thixoforming trials. In this case, the high silicon and manganese content widens the thixofomring window a little bit more.

Table 4.3 Chemical composition of LTT 100Cr6.

LTT 100Cr6 Composition						
	C	**Mn**	**Si**	**P**	**S**	**Cr**	**Ni**
Ascometal	0.979	0.992	1.272	0.011	0.007	1.365	0.113
Gerdau	0.96	1.01	1.26	0.01	0.007	1.37	0.11
Azterlan	0.94	1.02	1.24	0.009	0.007	1.43	0.14
	Mo	**V**	**Cu**	**Al**	**Sn**	**Ti**	
Ascometal	0.025		0.138	0.045			
Gerdau	0.02	0.004	0.13	0.046	0.009	0.003	
Azterlan	0.03		0.13	0.042		<0.005	

4.2.2 **Hardness**

A hardness scan has been made from the surface to the centre of each rounded bar. The hardness profile obtained is shown in Figure 4.2.

On comparing the hardness profiles of the three steel grades, it is worth pointing out that the LTT C38, the steel with the lowest carbon content, has the highest hardness followed by LTT C45. The latter presents a lower hardness than expected according to its carbon content due to a softening annealing. Finally, the LTT 100Cr6, the steel grade with the highest carbon content and, because of that, the one that should have the highest hardness profile, is the softest one, as a result of a globulisation annealing process.
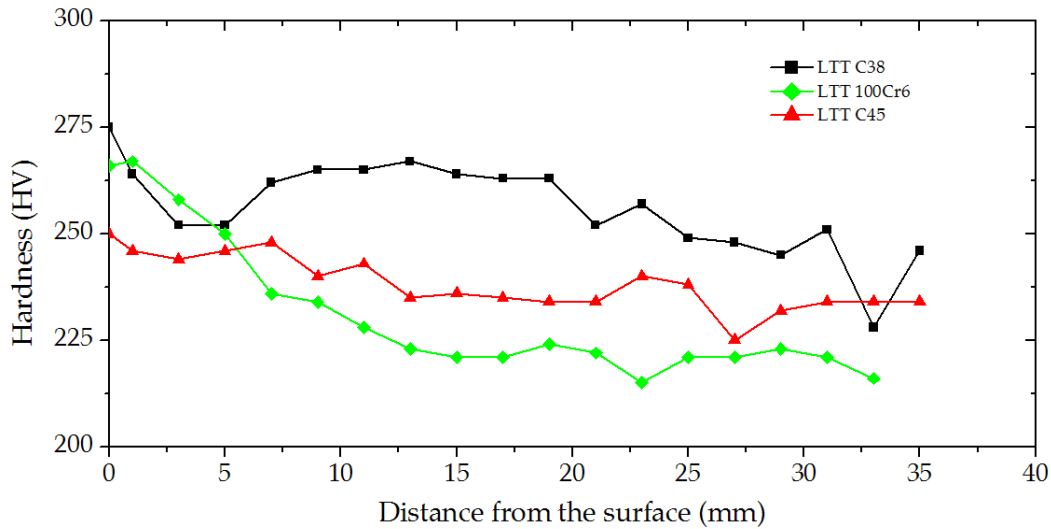
Figure 4.2 Hardness profile of different LTT steel grades.

4.2.3 **Microstructural analysis**

The steel grades were supplied in hot rolled state, but in addition, LTT C45 and LTT 100Cr6 were subjected to an annealing and a globulisation treatment respectively. The microstructural analysis was carried out in different areas of the rounded bar, the surface, the medium radius and the centre using an Olympus optical microscope.

4.2.3.1 **LTT C45**

The micrographs for LTT C45 show that its microstructure basically consists of 100% bainite with some ferrite and isolated martensite segregations as can be seen in Figure 4.5.

As mentioned in the previous section 4.2.2 and shown in Figure 4.2, the LTT C45 steel has a low hardness for the presenting structure and its carbon content as a consequence of an annealing process to soften the material.
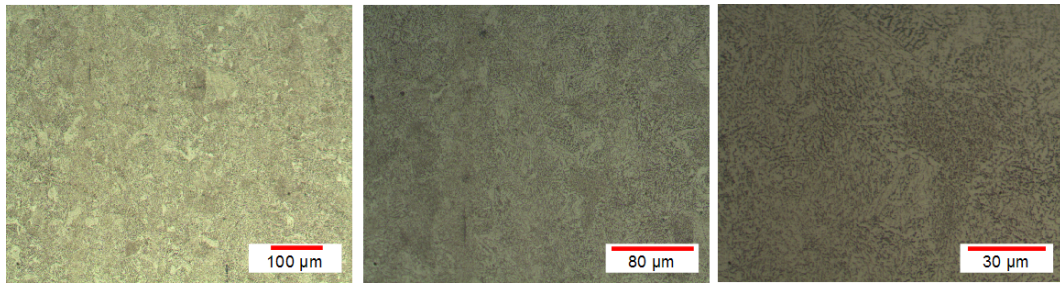
Figure 4.3 Surface microstructure of the LTT C45 (x100, x200, x500).
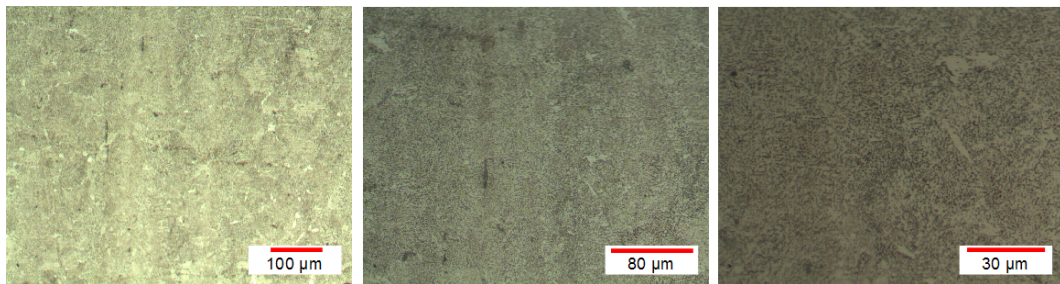
Figure 4.4 Middle radius microstructure of the LTT C45 (x100, x200, x500).
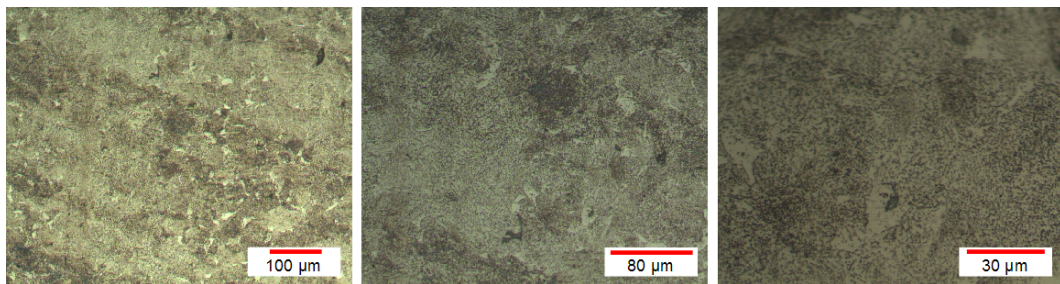
Figure 4.5 Centre microstructure of the LTT C45 (x100, x200, x500).

4.2.3.2 **LTT C38**

The LTT C38 steel presents a normalised microstructure consisting of ferrite - pearlite equiaxial grains in a proportion of ferrite/perlite = 25/75 with banded areas and a pearlitic grain size between 6 and 9 ASTM. Numerous manganese sulphur inclusions are also appreciable.
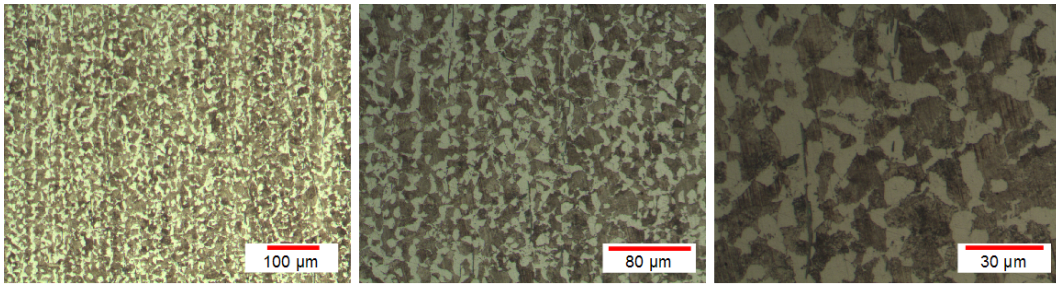
Figure 4.6 Surface microstructure of the LTT C38 (x100, x200, x500).
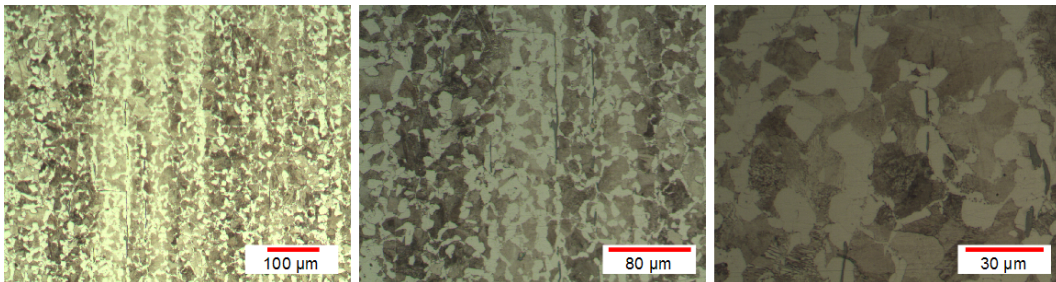
Figure 4.7 Middle radius microstructure of the LTT C38 (x100, x200, x500).
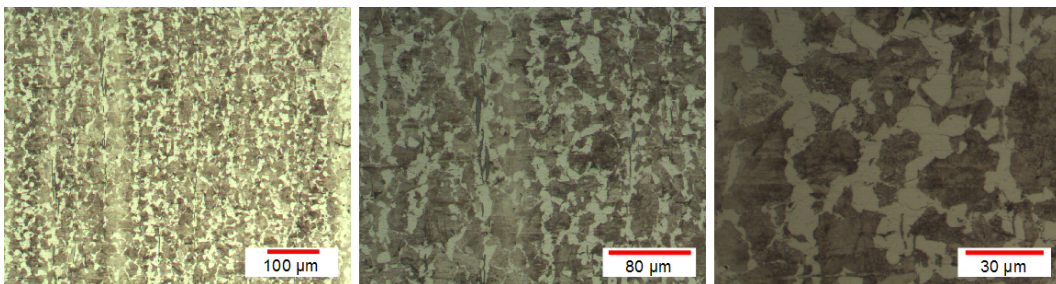
Figure 4.8 Centre microstructure of the LTT C38 (x100, x200, x500).

4.2.3.3   LTT 100Cr6

The last steel grade is a 100Cr6 bearing steel. As mentioned previously in the hardness analysis (4.2.2), it has been submitted to a globulisation annealing process and the microstructure consists of ferrite and globular carbides. Unlike the other LTT steels, there are no banded areas.
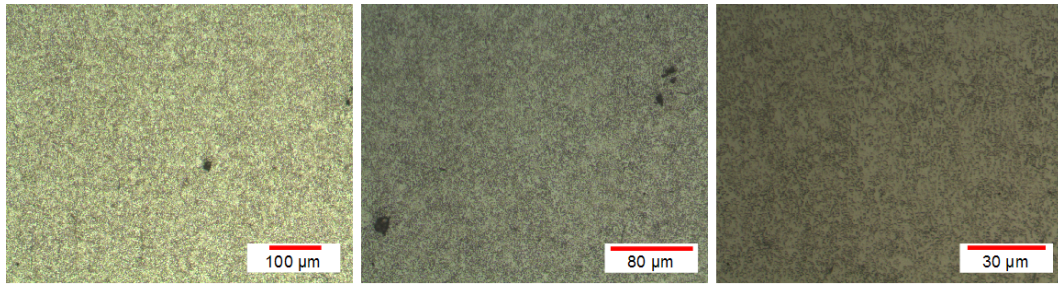
Figure 4.9 Surface microstructure of the LTT 100Cr6 (x100, x200, x500).
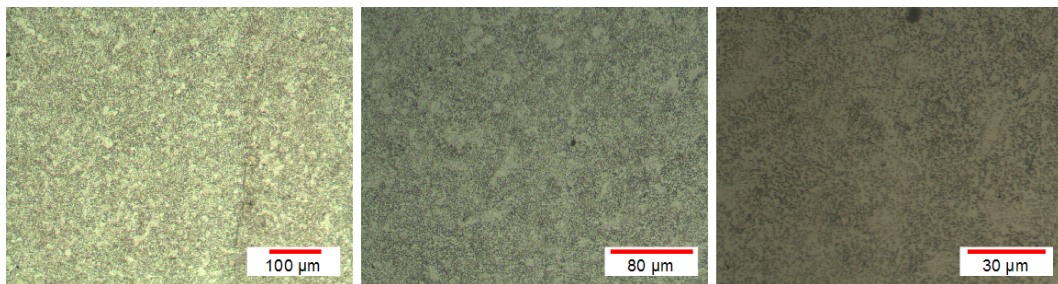
Figure 4.10 Middle radius microstructure of the LTT 100Cr6 (x100, x200, x500).
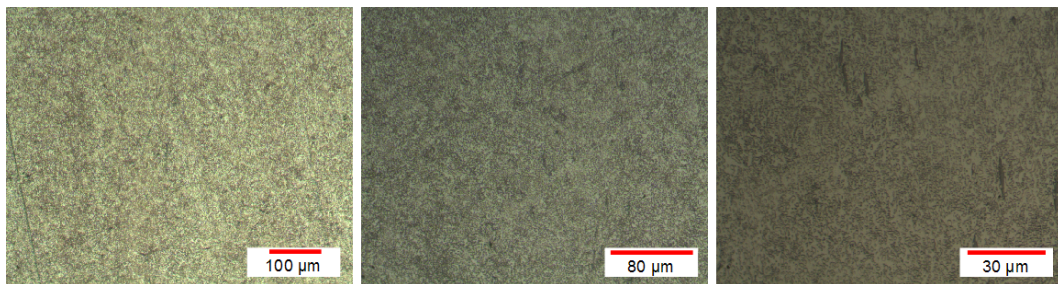
Figure 4.11 Centre microstructure of the LTT 100Cr6 (x100, x200, x500).

4.3 Characterisation of the liquid fraction

The applicability of a material for processing in the semisolid state is defined by the solidus-liquidus interval and the development of liquid phase in the relevant temperature range. The phase fractions for a certain temperature between the solidus and liquidus temperatures under equilibrium conditions can be read off from the appropriate phase diagram. In all other cases, they are dependent on the homogeneity of the material and the previous thermal history. If equilibrium conditions are assumed, the solid phase fraction can be derived

thermodynamically from the lever rule. For non equilibrium conditions, the calculation is possible with various methods. A well known method is the Scheil-Gulliver model, for which it is assumed that no diffusion in the solid phase occurs. This assumption is only valid, however, for short holding times or high cooling rates. For the determination of the solid phase fraction, different processes can be used [13].

1. Thermodynamic data from equilibrium phase diagrams.

2. Thermal processes: Differential Thermal Analysis (DTA) and Differential Scanning Calorimetry (DSC).

3. Quantitative metallography by means of quenched samples from the semisolid interval.

4. Measurement of the propagation rate of ultrasound within the partial liquid medium.

5. Measurement of the electrical resistance of the magnetic permeability.

6. Measurement of mechanical properties; e.g. penetration tests, flow experiments.

In practice, the first three methods are used the most, as the others do not only need extensive calibration, but they also do not exhibit a definite relationship between the measured characteristic parameters and the phase fraction.

In this dissertation, the experimental determination of the volume fraction will be made first, by DSC, second, using thermodynamic calculations with IDS software and third by means of quenching experiments from the partial liquid state. Differential scanning calorimetry (DSC) has an advantage compared over the differential thermal analysis (DTA): it measures the evolution of the heat of melting directly during the solid-liquid phase transformation. Nevertheless, all

methods are approximate and allow for a rough prediction of the phase fraction. The use of thermodynamic data provides information on the maximum width of the semisolid interval. However, consideration of the prior thermal history and of the microstructure is currently not yet possible.

The advantage of the thermal procedures, as mentioned by Uggowitzer and Uhlenhaut [12], is the easy and cost efficient specimen preparation, but a systematic error has to be considered because of the use of peak reference surface integration. In comparison with industrial inductive heating, thermal procedures present a disadvantage concerning the direct transferability of the results for the semisolid technology, the lower heating rate of DSC and DTA devices.

For the metallographic determination of the average phase contents by means of quenching experiments, the random and uniform distribution of the liquid and solid phases in the sample volume has to be ensured. Furthermore, the phase concentrations should not change significantly during quenching. This is generally the case if the liquid phase transforms in such a way that it can be easily distinguished from the already present solid phase components.

4.3.1 **Differential Scanning Calorimetry (DSC)**

Major challenges for semisolid processing include broadening the range of alloys that can be successfully thixoformed and developing alloys specifically for thixoforming. For this to be possible, the alloy must have an appreciable melting range and, before forming, the microstructure must consist of solid metal spheroids in a liquid matrix. Characterisation of thermophysical properties of semisolid steels for thixoforming is useful in two ways: first, to study and optimise the behaviour of alloys to be thixoformed; and second, to obtain parameters to be incorporated in numerical models.

A sufficiently expanded solidus-liquidus interval is required which allows the formation of the desired microstructure under variation of temperature and

holding time. The most preferable structure is a globulitic solid phase in a liquid matrix with decreasing viscosity during forming.

A LabSys Evo DSC from Setaram has been used for the evaluation of the liquid fraction in the semisolid range. The development of the liquid phase with increasing temperature has been calculated based on those DSC measurements. The evaluation of the liquid phase distribution is carried out by the application of a peak partial area integration. The whole area under the enthalpy-area curve is used to determine the melting enthalpy of the material. A typical melting peak obtained during DSC measurement, is shown in Figure 4.12.
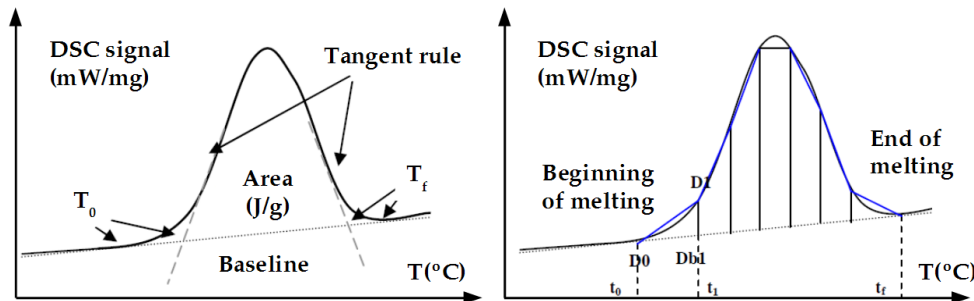
Figure 4.12 Determination of the liquid fraction [37].

The DSC signal is characterised by, the *slope changes*, jumps and peaks showing the thermal events (phase transformations, chemical reactions, etc.); the *peak area*, which is the enthalpy variation of the transformation; the *specific heat*, which is calculated from the baseline; and the *solidus-liquidus interval*, represented in Figure 4.12 by $(T_f - T_0)$.

For the calculations, I assume that the liquid fraction is proportional to the absorbed energy during the transformation even knowing that this will include an error [13, 12]. The sample is heated until total melting. Therefore, the liquid fraction can be calculated considering the peak area of the transformation, as shown in Figure 4.12.

The melting peak is fully defined by the beginning and end of melting and the total area, which is equal to the 100% liquid fraction.

Thus, the liquid fraction at T_i is determined with the following equation [37]:

$$f_l = \frac{Area(T_0 - T_i)}{Total\,Area} \tag{4.1}$$

4.3.1.1 LTT C45

Figure 4.13 shows the f_l for LTT C45. The DSC measurement is made in two different stages, under an argon atmosphere with a flow rate of 20 ml/min.
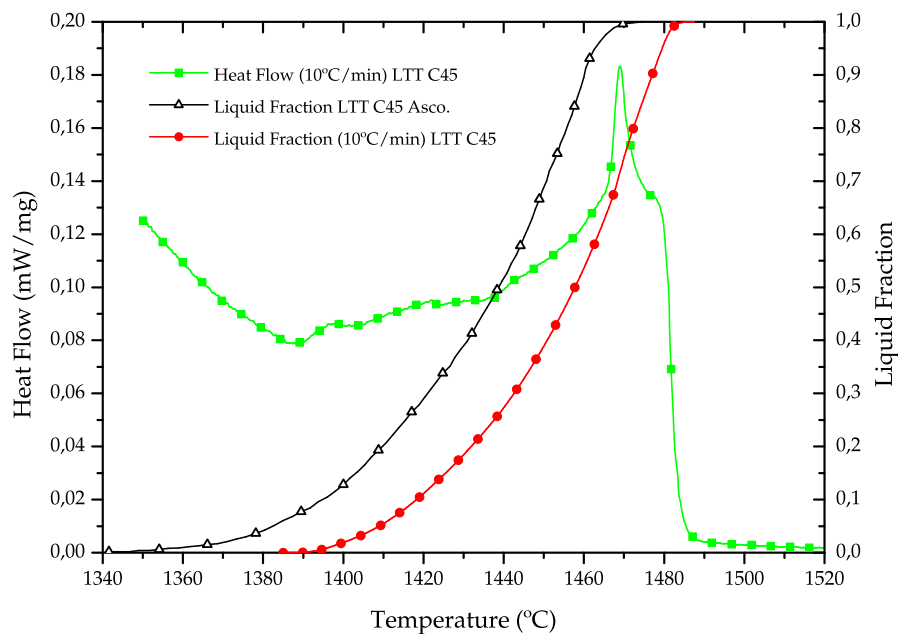
Figure 4.13 DSC signal and liquid fraction of LTT C45.

The first stage occurs before introducing the testing sample, when an empty cycle is carried out in order to condition the alumina crucible. The second stage starts when the sample is introduced. The heating cycle is also divided in two steps: in the first one, the sample is heated up to 1100°C at 50°C/min. At 1100°C the temperature is stabilised during 5 minutes. In the second, the heating continues until 1550°C with a heating rate of 10°C/min. At this point,

the temperature is stabilised again for another 5 minutes and then the cooling starts.

The f_l measured by DSC differs from the one send by Ascometal but is very similar to the 50Mn6 steel described by Lecomte-Beckers *et al.* [37] which is also fabricated by Ascometal.

Nevertheless, the fact of obtaining sound parts under 1360ºC, as described in chapter 6, corroborates that this liquid fraction can be useful only as a guidance and that it is far from straightforward [12].

4.3.1.2 **LTT C38**

The DSC measurement for LTT C38 has been made under the same conditions as those for LTT C45 with the same heating cycle. The results are displayed in Figure 4.14.
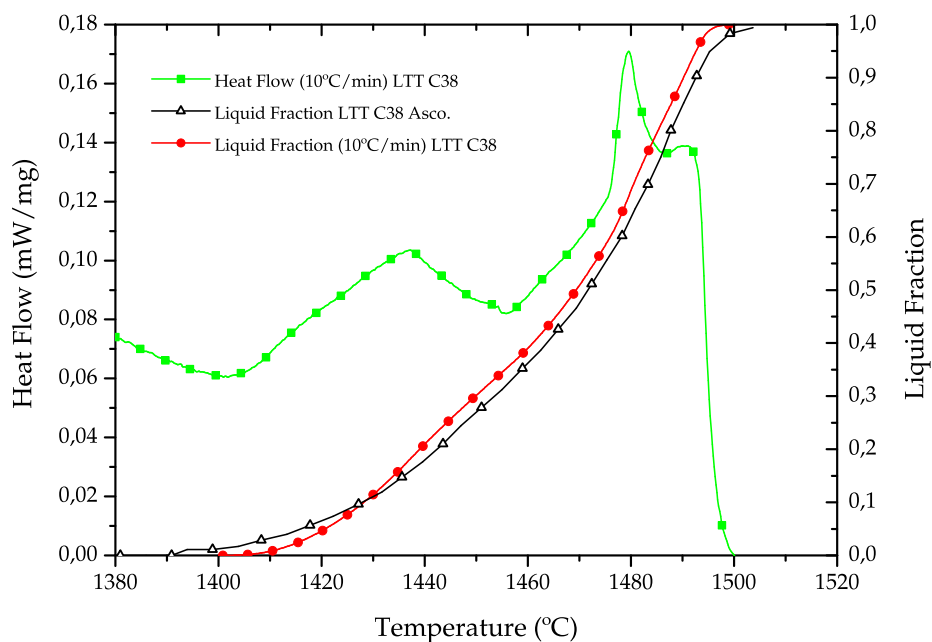
Figure 4.14 DSC signal and liquid fraction of LTT C38.

In this case, the measured DSC signal corresponds to the one send by Ascometal and the C38 Asco Modif 2 measured by Lecomte-Beckers *et al.* in [37].

4.3.1.3 **LTT 100Cr6**

As in the previous cases, the heating cycle of the DSC measurement involves a quick heating until 1100°C, a stabilisation time and a final heating at 10°C/min. Figure 4.15 shows the f_l measured by DSC for LTT 100Cr6.
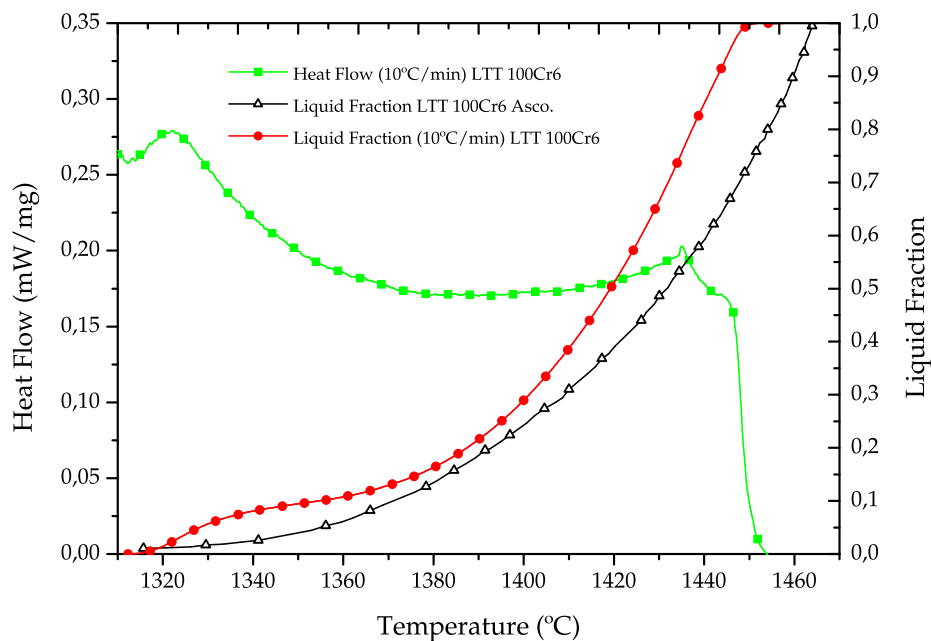
Figure 4.15 DSC signal and liquid fraction of LTT 100Cr6.

In this case, the differences for both curves widen above 0.3 f_l but are still under 20°C. It is important to remark that my working range is below 0.25 of f_l which is precisely the most accurate zone. According to the curves measured by Lecomte-Beckers *et al.* [37], it corresponds to the one for 100Cr6.

4.3.2 **Thermodynamic calculations**

As mentioned in section 4.3, it is possible to determine the fraction of liquid phase experimentally using, for example, DSC, DTA or metallography, but this is far from trivial [5]. The approach presented in this subsection is to calculate the fraction of liquid phase from thermodynamic data.

If the thermodynamic properties of a system are known, then any phase diagram can be calculated. The thermodynamic description actually contains much more information than the phase diagram alone, since the thermodynamic properties of the phases included are defined for the complete composition range, and not only for the range where they are stable. Thus, not only the stable phase diagram, but also any metastable state can be calculated.

Using standard equilibrium calculations is a quick and easy way to obtain an overview of the phases expected to appear in a particular material, their amounts and the temperature range in which they are stable. However, the solidification path, in principle, never follows the equilibrium path, due to the limited diffusion in the solid phase. This results in microsegregation, and possibly in the formation of non-equilibrium phases. The actual fraction of solid phases at a particular temperature is always smaller than the equilibrium fraction. For steels, the equilibrium solidification path is often a reasonable first approximation since C is a fast diffusing element. In thixoforming, where the material is heated from the solid state into the semisolid state, the melting behaviour of the material is also of great importance. However, the melting behaviour of alloys has been far less studied than the solidification behaviour. From the equilibrium point of view, there is no difference between solidification and melting. In order to see a difference, it is necessary to take diffusion into account and in the case of melting, the microstructure of the solid starting material will have a decisive influence on the melting behaviour.

The diffusion in the liquid phase is much faster than in the solid phase and it is often a useful approximation to assume that there is no diffusion at all in the

solid phase, and that there is infinitely fast diffusion in the liquid phase during solidification. However, Scheil solidification in this simple form is not a good approximation for steels, because C diffuses fairly fast also in the solid phase of ferrite and austenite in this case [12]. For steels, it is a better approximation to assume that C diffuses fast enough also in the solid phase to reach global equilibrium.

4.3.2.1 IDS Software

Numerous advanced models applying finite difference and finite element methods have been developed to simulate the solidification process of metallic alloys. Their accuracy, however, depends not only on the mathematical treatments of the models but also on the thermophysical data used as the input data for the calculations. Such data, for example, are the enthalpy-related data, density, and thermal conductivity. Usually, the data of the literature, however, cannot be applied directly due to the phase transformation processes causing discontinuities to the properties, depending on the steel analysis and the cooling of the casting. Hence, a reliable simulation of phase transformations would be necessary to predict these properties [38].

In the IDS software, Miettinen coupled the interdendritic solidification model (IDS) with an austenite decomposition model (ADC) so that the phase transformation calculations could be reached from 1600 °C down to the room temperature. This model package was developed further, to calculate important thermophysical properties as a function of temperature, taking into account the discontinuities of properties caused by the phase transformations. A detailed description of the software calculations is given in [38].

The IDS model was originally developed to simulate the interdendritic solidification of low-alloyed steels and stainless steels containing 16 to 20 pct Cr and 8 to 14 pct Ni. Then, the model that described the thermodynamic properties of solution phases was changed, and due to this, the calculations

could be carried out for a wider composition range of stainless steels. Finally, a semi-empirical phase-transformation model (ADC) was coupled to the IDS model to simulate the decomposition of austenite into various structures containing ferrite and cementite. The model applies the substitutional solution model using a paraequilibrium condition during the cooling process, an analytical diffusion model simulating the carbon diffusion in austenite grains, regression equations based on the German and the British continuous cooling transformation experiments, and it takes into account the effect of solutes C, Si, Mn, Cr, Mo, Ni, cooling rate, and austenite grain size.

4.3.2.2 **LTT C45**

Figure 4.16 shows the comparison between f_l calculated by IDS at different cooling rates an the f_l obtained by DSC measurements for LTT C45.
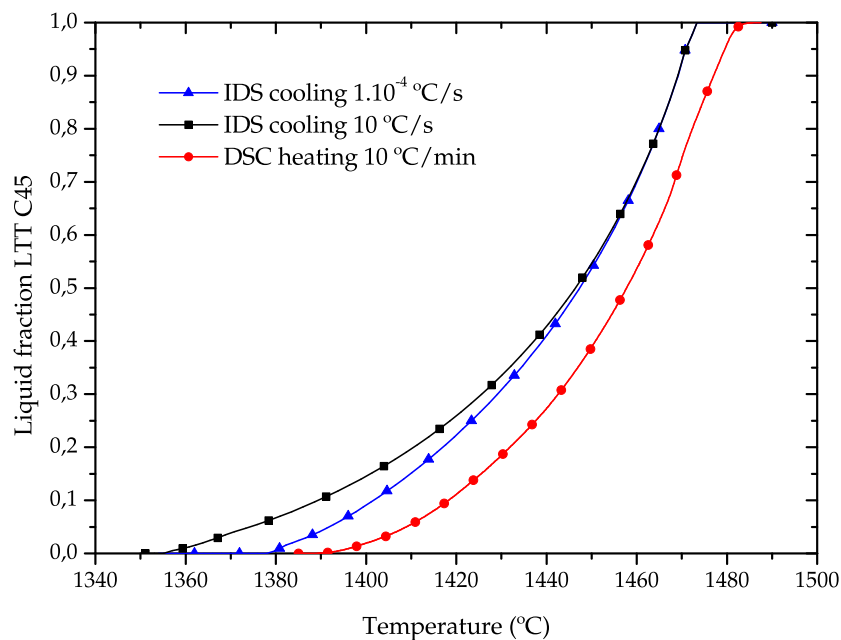
Figure 4.16 Liquid fraction IDS vs DSC of LTT C45.

Differences are significant: the beginning of the melting in DSC corresponds to a 10 % of f_l in the IDS curve with a cooling rate of 10 ºC/s but it has to be taken into account that IDS measurements are calculated during cooling whereas DSC measurements are made during heating.

4.3.2.3 **LTT C38**

Figure 4.17 shows the same tendency as the one for LTT C45 and the shape of the curve obtained by DSC is exactly reproduced by IDS software.
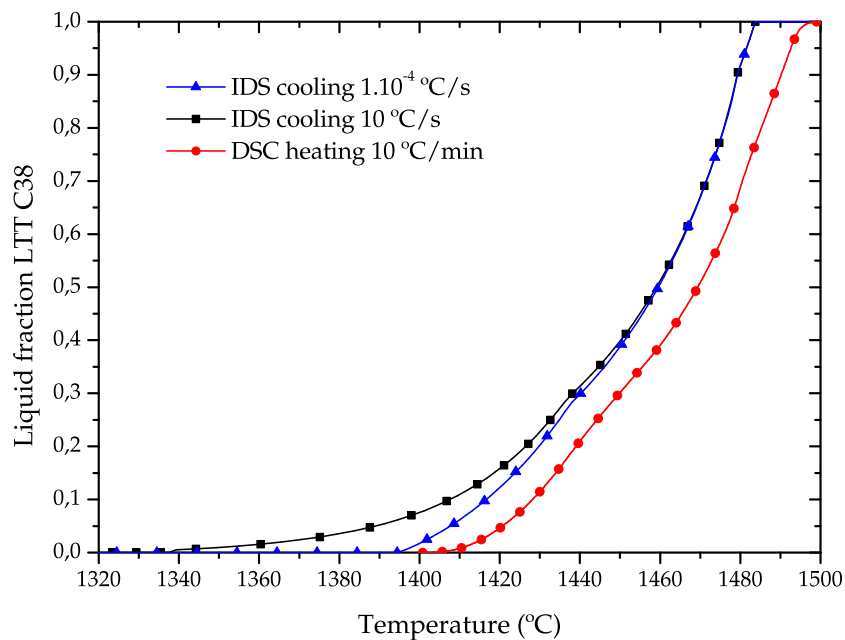
Figure 4.17 Liquid fraction IDS vs DSC of LTT C38.

4.3.2.4 **LTT 100Cr6**

In the case of LTT 100Cr6 the tendency is the same as in the other steel grades, the solidification range is between lower solidus and liquidus temperatures

but in this case the shape of the curves from DSC and IDS software are quite different (Figure 4.18).
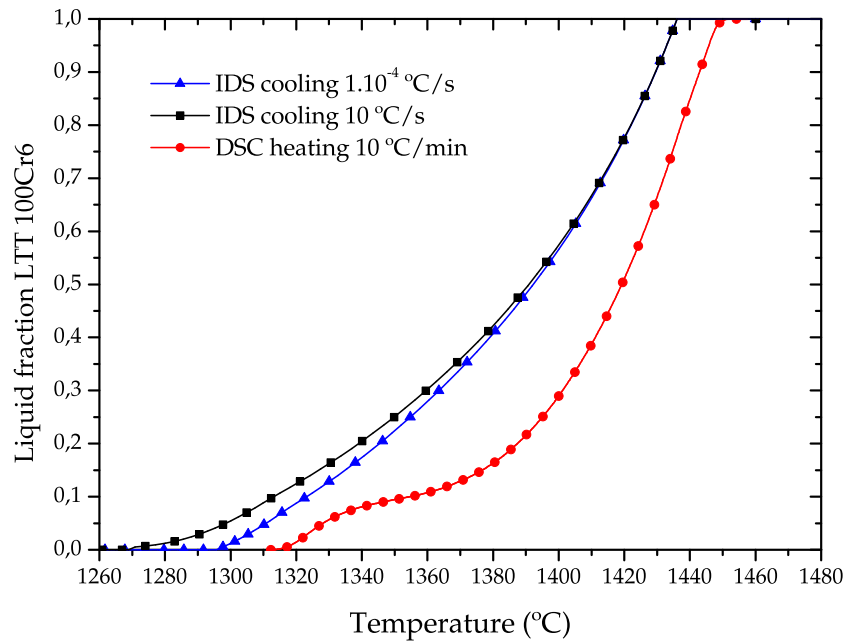
Figure 4.18 Liquid fraction IDS vs DSC of LTT 100Cr6.

At the beginning of section 4.3, it has been mentioned that all the methods for f_l characterisation allow a rough prediction of the phase fraction. In the case of LTT 100Cr6, the prior hot working to which it was submitted and the initial microstructure could have an important influence on the melting behaviour of the alloy as well as the globulisation heat treatment. Thermodynamic calculations do not consider the previous thermal history and microstructure of the alloy promoting the difference between IDS and DSC measurements in this case. One should bear in mind that these hot rolled bars were obtained from square ingots of 540 mm x 540 mm.

4.3.3 **Determination of liquid fraction by quenching**

To determine the liquid fraction in a semisolid sample experimentally is far from straightforward. By quenching the sample quickly, one can hope to be able to retain an image of the original state and, thus, to distinguish the originally liquid and solid phases in metallographic sections. This has worked well for a number of Al alloys, but for steels it is only possible in certain cases. The samples have to be quenched so quickly that the microstructure at room temperature reflects the partial liquid state. Due to diffusion processes and phase transformations, this is often not successful and microstructural changes caused by quenching should be considered. If the structure changes much during quenching, the determined structural parameters must be corrected or can possibly not be determined at all.

Below, the quenched microstructure of the steels that I have tested for thixoforging is presented as well as the calculation of the f_l obtained from micrographs by software where it is possible.

4.3.3.1 **LTT C45**

The LTT C45 has been water quenched from 1360 °C, the same temperature that is reached at the end of the heating cycle during thixoforming tests. Figure 4.19 shows that quenched samples exhibit some light areas, at which the material has already started to melt locally due to the enriched alloying elements at the grain boundaries. The f_l measured goes from 1.3% up to 10.7%.

4.3.3.2 **LTT C38**

As in the previous case, globular solid grains surrounded by light grain boundaries are visible in Figure 4.20. The sample´s temperature has reached around 1390 °C following the designed heating stage and it has been water quenched then. The f_l shown in micrographs is around 1.3%.
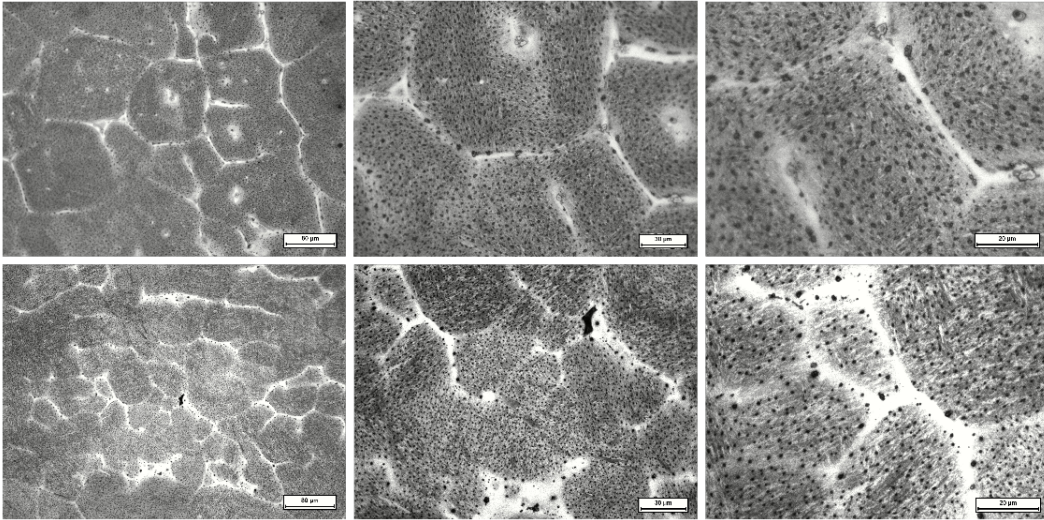
Figure 4.19 Liquid fraction by quenching, micrographs for LTT C45.
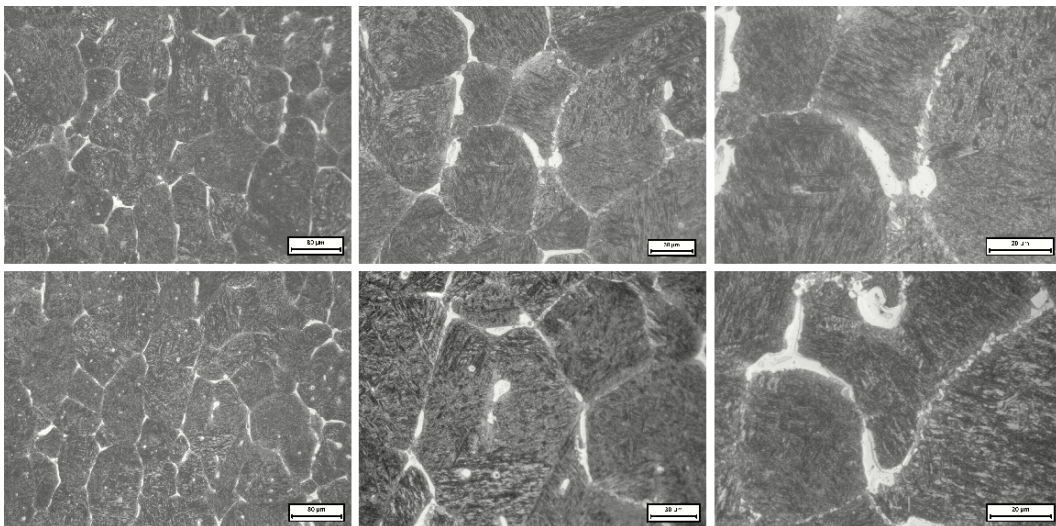
Figure 4.20 Liquid fraction by quenching, micrographs for LTT C38.

Light grain boundary areas suggest the starting of the melting but it is difficult to make a quantitative measurement of the liquid fraction because temperature changes do not involve any significant change in micrographs, as mentioned by Bleck *et al.* [12] for 100Cr6.

4.3.3.3 **LTT 100Cr6**

Analysing Figure 4.21 light grain boundary areas are clearly visible in the specimen that has been water quenched from 1300 °C. In turn, a martensitic formation with retained austenite between the needles is discernible. In contrast to Bleck et al. [12] there has been no holding time at the defined semisolid temperature because the heating step has been the same as in real thixoforming process. Measurement of the f_l in this case is impossible because the software cannot distinguish the grain boundary from the retained austenite.
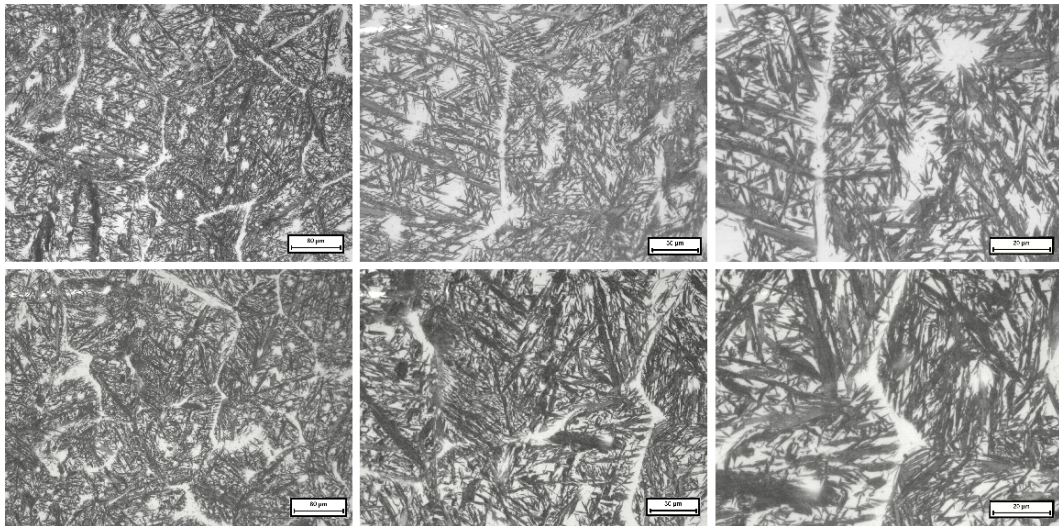
Figure 4.21 Liquid fraction by quenching, micrographs for LTT 100Cr6.

4.4 **Conclusions**

The preconditions for selecting suitable alloys for thixoforming are well understood: it is mainly a low temperature sensitivity and a globular liquid-phase development during heating. Nevertheless, according to the device´s accuracy, (heating furnace, press, etc.) the suitable material range also vary, being wider or narrower.

The fact is that thixoforming requires a deep and thorough understanding of the microsctructure development during all the process. This chapter shows that f_l could not be calculated in a highly accurate manner by any of the proposed methods.

Thermal procedures are easy and have cost efficient specimen preparation, but a systematic error has to be considered because of the use of peak reference surface integration. In addition, the much quicker inductive heating used in the industry disables the direct transferability of the DSC or DTA results for semisolid technologies.

The use of thermodynamic data provides information on the maximum width of the semisolid interval. However, consideration of the prior thermal history and of the microstructure is currently not yet possible. Furthermore, the phase calculation is made during cooling and in thixoforming the desired microstructure is obtained during heating.

For the metallographic determination of the phase contents by means of quenching, a random and uniform distribution of the liquid and solid phases in the sample volume must be ensured and this is hardly possible. Only an average value could be obtained comparing micrographs from different areas of the heated billet. Furthermore, the phase concentrations should not change significantly during quenching. This is generally the case if the liquid phase transforms in such a way that it can be easily distinguished from the already present solid phase components but is really difficult in the case of LTT 100Cr6.

To end up, it is fair to say that these three methods are approximate and allow only a rough prediction of the phase fraction. It is significant that thixoformed parts have been produced with temperatures below the solidus, measured by DSC, and that quenching micrographs and microscope observations demonstrate that melting has occurred at those temperatures. As mentioned in section 4.3, this could be due to the much faster inductive heating but this would theoretically rise the solidus temperature which is not actually

happening. It turns out that a deeper study on the melting behaviour of the alloys is needed.

CHAPTER 5

Industrialisation

In this chapter, I would like to present the current state of thixoforming in its way to industrialisation: the activities carried out to produce complex shape parts in steel, as well as economic comparisons with conventional forming techniques.

5.1 Introduction

Although SSM processing of high melting point alloys offers exciting possibilities and a tremendous potential, it is at the present still in a research and development stage.

In contrast, aluminium and magnesium have become widely accepted materials for industrial manufacturing of near net shape components, especially in automotive industry, where millions of parts are now in everyday use in the cars we drive. For further detail on the evolution of the semisolid technology related to aluminium see Kirkwood et al. [3].

As mentioned in chapter 2, the investigation of the semisolid processing started in the early 70´s at MIT [2] and was followed by Alumax and the University of Sheffield [4]. These investigations showed, by means of
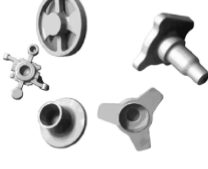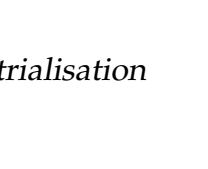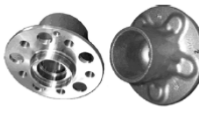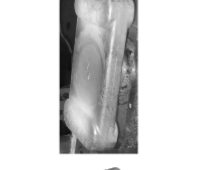
Year	1992	1992	1996	1997	2003	2003	2003
Process	Thixoforging	Thixoforging	Thixoforging	Thixocasting	Thixoforging	Thixoforging	Thixocasting
Part							
Research Group	Alumax, US	University of Sheffield, GB	Tokyo, JP	EFU, RWTH Aachen, DE	RWTH Aachen, DE	University Hannover, DE, ULG Liége, BE	Honda, JP
Forming Material	1.4307, 1.4401	HS 6-5-2, CoCr28MoNi	FC-10/20/30 GCD45	C70S6, 100Cr6, HS 6-5-2	100Cr6, HS 6-5-2	C38, C60, C80, HS 6-5-2	FCD450-10

Year	2004	2004	2004	2005	2008	2008	2009
Process	Thixoforging	Thixocasting	Thixo and Rheoforging	Thixoforging	Thixoforging	Thixoforging	Thixoforging
Part							
Research Group	RWTH Aachen, Daimler AG, University Hannover	RWTH Aachen, DE	RWTH Aachen, DE	University of Sheffield and Leicester, GB	Tubitak, TR	University Stuttgart, DE	RWTH Aachen, DE
Forming Material	49MnVS3, 79MnVS5	X210CrW12	100Cr6, HS 6-5-2, X210CrW12	HP 9-4-30	X210CrW12	TiAl6V4	X210CrW12

Figure 5.1 Results and investigations of different R&D groups [17].

successfully produced parts, that it is possible to apply SSM to the production of steel components. Since then and, due to the expected market potential, several projects have been carried out with the aim of developing the necessary technology for semisolid production of steel components. To give an overview of the past research work, representative parts of the projects are shown in Figure 5.1. Part weights from less than 200 g up to more than 3 kg have been produced using carbon steels, tool steels and cast iron.

From 2007 to 2010, intensive collaboration was taking place between European research groups, with the creation of the collaborative project 'COST 541 - ThixoSteel'. The aim of the project was to demonstrate the economical and industrial feasibility of the thixoforming process for several parts. Figure 5.2 shows the agreed process diagram.
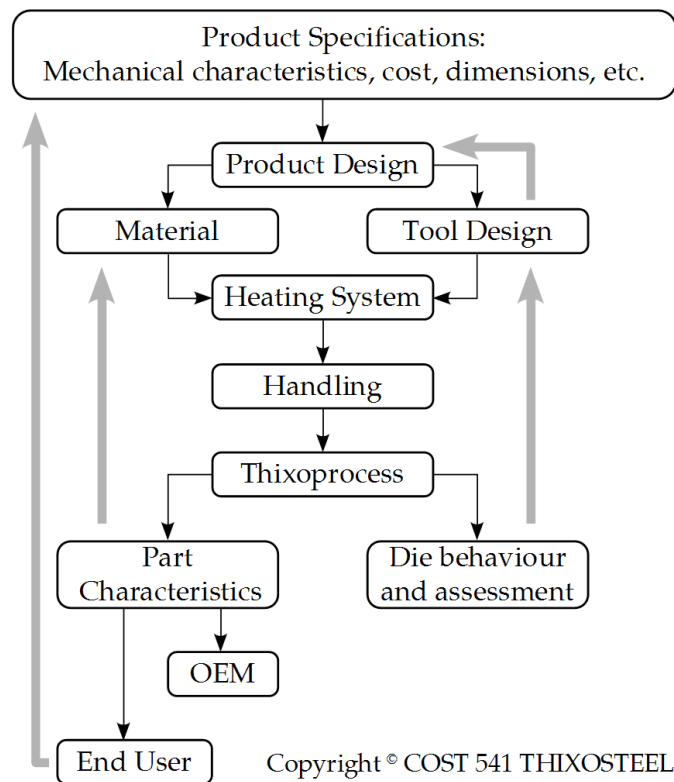

Figure 5.2 Thixoforming of steel, conception and realisation diagram [17].

5.2 Steel Thixoforming Applications

5.2.1 Automotive industry

The automotive industry is one of the world´s most important economic sectors with approximately 1.000 million cars and light trucks on the road around the world in 2012. This large number of vehicles in operation and the expected sales is a reflection of an industry characterised by the production of parts in large series.

The required parts with more or less complex geometries and adapted mechanical characteristics are produced mainly by forging, casting and stamping with materials such as carbon steels, low alloyed steels, cast irons and aluminium alloys.

Over the last 25 years, automakers have faced growing pressure to incorporate environmental objectives into their designs as well. In particular, governments and consumers have pushed for improvements in fuel economy as a way to preserve oil and control pollution.

Now public pressure to improve fuel economy is again rising, partly because of the concern over the prospect of global climate change (automobiles account for about one-quarter of carbon dioxide emissions, and are therefore a major contributor to the greenhouse effect.). The key to improving a vehicle´s fuel economy is weight reduction: the smaller a vehicle is, the less power it requires to accelerate and the less energy to maintain a fixed speed. Traditionally, the automotive industry has reduced weight primarily by downsizing, a strategy that has succeeded in cutting the weight of a typical car from 1500 kg to 1100 kg. Today, the focus of lightweighting has shifted towards vehicle components: chassis, body, suspensions or power train parts (engines, gear boxes and transmisions). These parts are traditionally distributed between: steel forged parts for high mechanical property requirements, cast iron or stamped parts for lower cost parts and aluminium alloy parts for lightweighting.

The place of steel thixoforming in this industrial context requires attention to several part sets and thus related markets. It can be generally positioned somewhere between casting and forging in terms of its characteristics for producing large part series. In any case, it is necessary to point out that it is imperative for every part geometry to be adapted to the thixoforming process by taking into account the properties of the steel used, the flow of the semisolid steel during the deformation and the available means of forming.

5.2.1.1 Cast iron vs. thixoformed steel parts

As mentioned in chapter 2, foundry is used to produce complex shapes, especially thin wall components. Steel thixoforming needs less investment for an installation than foundry and the near net shape capabilities along with a proper design reconception allows to obtain parts with the same cost level as foundry [39]. In addition, steel thixoforming allows an increase of the mechanical properties to be achieved, hence enabling the dimensions to be slimmer than those with cast iron; cast parts are generally over dimensioned.

The brake calliper nose shown in Figure 5.3 is an example of how thixoformed steel can replace a cast iron part. Rassili and Robelet [17] redesigned a calliper nose for automatic braking that requires an increase of the friction surfaces and greater rigidity. These improvements lead to an increase of the part weight if the component is still produced by foundry. To maintain a minimum weight the calliper can be produced in two parts: the part with the piston in cast aluminium and the nose in cast iron.
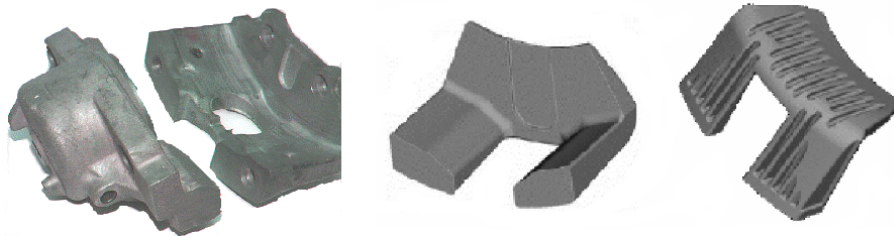

Figure 5.3 Brake calliper nose in thixoformed steel [39].

Another solution is to produce the nose in thixoformed steel, maintaining the weight and increasing the rigidity of the cast iron.

5.2.1.2 **Foundry aluminium parts vs. thixoformed steel parts**

Although the density of aluminium is a third of that of steel, the strength-to-weight ratio is such that, to obtain parts with comparable mechanical characteristics, an aluminium component has to be bigger than a steel one. There is therefore little saving in weight by using aluminium rather than steel. An example of a thixoformed steel part replacing an aluminium alloy part (produced by foundry or forging) can be a diesel automotive piston (Figure 5.4).
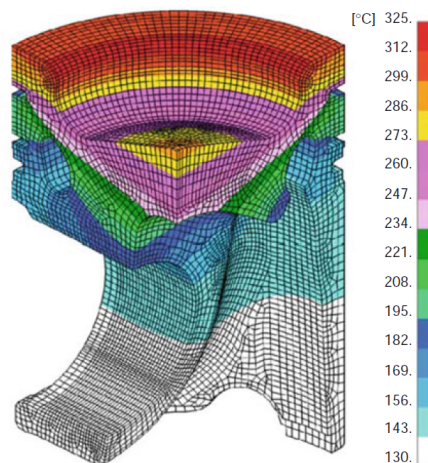
Figure 5.4 Piston FE simulation with the mesh and temperature field in °C [40].

The piston crown is subject to extreme temperature loading with temperatures far above 300°C at which the fatigue strength of the aluminium materials employed already diminishes considerably. Engine operation produces significant thermal cycling at the bowl rim and local heating and the inhibition of deformation by surrounding colder regions can cause piston materials to yield locally and, in the extreme case, to develop thermal cycle fatigue.

The entry into force of the Euro 6 Law related to emissions requires the optimisation of the efficiency in combustion engines. This efficiency

improvement results in a temperature and pressure increase that aluminium pistons cannot support. This problem can be solved by steel thixoformed pistons: without increasing the weight (compared to alumininium ones) and at a lower cost than those produced by KS Kolbenschmidt and Federal-Mogul using traditional forming methods [17].

5.2.1.3 Steel hot forging parts vs. thixoformed steel parts

Usually, hot forging parts require several deformation operations with successive tools to obtain the final geometry. The more complex the part is, the more flash is produced. Steel thixoforming allows to obtain the part in one step without any flash and with a better surface quality than with hot forging. This leads to advantages regarding process costs, mainly based on material savings. Figure 5.5 shows the required forming steps to forge a wheel trunk.

Figure 5.5 Required forming steps for forging a wheel trunk [12].

By thixoforming the process is shortened right from the beginning because pre-forming of the precursor material is not necessary and the forming is carried out in just a single step.

Conversely, in theory, mechanical properties are not as good as in forging. One of the reasons for that might be the impossibility to obtain fibre structure, but a good redesign of the component can help overcome this drawback and achieve good mechanical properties.

Figure 5.6 Fibre structure of a hot forged spindle.

5.2.2 **Mechanical parts**

Rassili and Robelet [17] say that the best suited parts for steel thixoforming
are complex geometry parts with high mechanical characteristics. These
parts are frequently done either in cast iron, with an oversized geometry to
ensure adequate properties, or in machined steel, in which case the machining
costs tend to be significant. The part redesign for thixoforming allows the
optimisation of their geometry which, in turn, reduces the number of machining
operations. The fact that parts can be obtained without flash is also important.
In addition, the surface roughness in the as-thixoformed condition is low, and
provides enhanced fatigue properties compared to other processes.

5.3   **Technology considerations for industrialisation**

As Rassili and Atkinson remark [41], the industrial development of steel
thixoforming must go hand in hand with the knowledge and control of the
various parameters for the process: the identification of the steel grades; the
homogeneous high-temperature heating of the slug before deformation; the
conception or re-conception of the part to adapt it to the process; the parameters

for forming including ram velocity profile, holding time and pressure at the end of the stroke, die temperature and die material. The handling system is also important; it allows the slug to be transferred, in the semi-solid state, between the heating zone and the tooling and to evacuate the thixoformed part so as to ensure the quality of heat treatment of the part. All these aspects contribute to achieving a cost for the finished part which is competitive compared to more conventional processes[39].

Industrial developments include: non-contact temperature measurement during heating [42]; the use of fuzzy logic to control the heating [43]; optimising the induction coil geometry [44]; prediction of thermal losses during transport and after insertion into the die [45]; a device on the hydraulic press to counteract the decrease of the punch speed in the final stages of the stroke [46]; automated handling and industrial vision systems [47, 48].

The next chapter will be devoted to describing the semi-automated thixo-forging cell implemented in the forming lab, as the first step to get the desired industrialization of the process. It consists of an induction unit, six-axes industrial robot for the handling tasks and a servo-mechanical forming press. A special tool has also been designed in order to use all the press capacity during the forming stage.

Issues related to the forming process of the selected part will also be thoroughly described, giving all details of the heating and forming steps for the fabrication of a commercial automotive spindle using steel grades characterised in chapter 4.

Thixoforming Cell: The Component Manufacturing

The present chapter will focus on the thixo-lateral forging of a nearly 3kg commercial automotive spindle. For that purpose, I will fully describe the semi-industrialised thixoforming cell that has been implemented in the forming laboratory, the different stages and devices needed to produce a steel thixoforming component, as well as the first trials carried out.

6.1 Introduction

Thixoforming is an alternative fabrication route for forged steel parts in the automotive sector since it combines the advantages of forging and casting processes. It is related to a decrease in manufacturing costs by means of a reduction of the forming steps and forming loads as well as a reduction of material quantity and final machining operations [49]. Conventionally forged steel components can be geometrically complicated, but the relation between of flow length to the wall thickness is much smaller than in semisolid forming. Compared to casting, semisolid forming results in a reduction of part defects

and in higher mechanical properties [12]. Nevertheless, the high process temperatures entail complex load profiles on dies and nowadays the lack of suitable die material with an economically suitable service life is the major impediment to the commercialisation of this innovative forming technology [50]. As first step towards the desired industrialisation of the process, a semi-industrial thixoforming cell has been implemented in the forming lab. In the following sections, a complete description of the thixo cell is given, as well as the results of the trials carried out.

6.2 The forming part

As mentioned in section 5.2.2, some of the best suited parts for steel thixoforming are complex geometry parts with high mechanical requirements. That is why a nearly 3 kg commercial automotive spindle has been selected as the forming component in this dissertation.
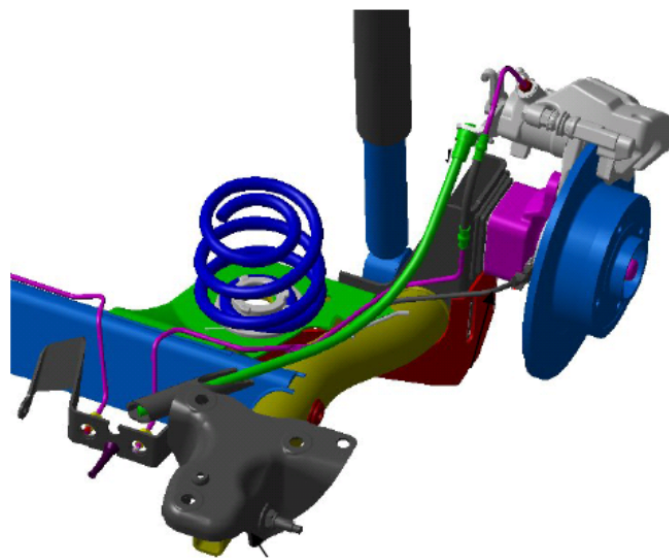
Figure 6.1 CAD drawing of the rear suspension with the spindle in violet.

The spindle is a part of the vehicle´s suspension which ties the wheel and the tire into the steering system. The spindle is in the front of the vehicle in most

cases; however, some front-wheel drive vehicles also have rear spindles. This is the specific case presented in this research work.

The spindle pivots between the upper and lower A-frames or on the strut. Both the inner and outer wheel bearings ride on the spindle and the retaining nut on the end secures the wheel into position. Usually, the brake caliper is also mounted on the spindle as shown in Figure 6.1.

Acting like a short axle, it is used to attach a wheel assembly to the vehicle. Typically manufactured from a forged piece of steel, spindles must be extremely strong and durable to support the weight of the vehicle. While most spindles use a wheel hub to mount the wheel and tire in place, some wheels are mounted directly onto it without the use of a hub. These wheels are known as spindle mount wheels.

Conventionally, the spindle is hot forged in 3 steps, using a mechanical press of 30.000 kN. Then, the flash is removed and after the corresponding thermal treatment and calibration step, it is machined to the final shape. The dimensions of the thixoforged spindle shown in Figure 6.2 are those obtained by conventional hot forging after removing the flash.
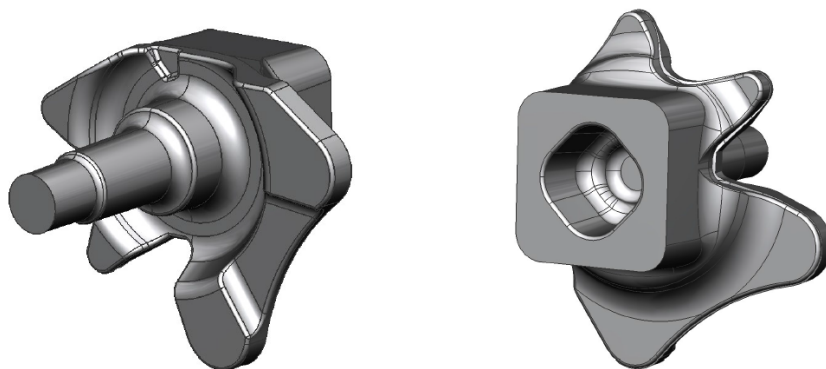

Figure 6.2 CAD drawing of the thixoforged part.

6.3   The starting material

A wide range of steel grades are usable for the thixoforming process as it has been mentioned in Chapter 4. The steel grade choice will depend on the mechanical and physical properties required by the part to function, but also on the semisolid range of the steel. In view of the later, the steel alloy chosen should have as much carbon content as possible. The usual material for this spindle fabrication is a CrMo alloyed steel (W-Nr 1.7225) employed in automotive components with high requirements on toughness. According to this, the steel grades characterised in Chapter 4 have been selected as the most suitable to fulfil the required solicitations.

The bars which are used for obtaining the billet have to present a surface which has been de-scaled, either from precision hot-rolling (a relative economic solution), o peeled (more expensive solution). This last solution does not bring any advantage over the precision hot rolled solution. As-cast steel with globular structure suitable for thixoforming is also an important potential raw material for thixosteel production. The main European steel makers can supply these products in their list of products. Some of them, like Ascometal, have steel bars already adapted for thixoforming. In particular, Ascometal´s peeled steels have been tested here during the forming step.

The steel thixoforming process requires billets with an excellent geometry: flat and perpendicular extremities along with a very good cylindrical surface. The diameter tolerances must be the minimum possible within the batch with the minimum variation among batches.

These parameters are essential to ensure precise and reliable induction heating. From bars, billets must not be cut by shears because it can cause metal deformation, it is better to use sawing in order to ensure the geometrical quality of the slug. This is exactly what has been done in this research work.

6.4 Process stages

To become an industrially applicable process, the steel thixoforming has to face different technical obstacles such as material reheating until semisolid temperature, handling of the semisolid billets from the heating station into the forming tool and the forming process itself.

Due to the high demands involved in semisolid forming and the narrow thixoforming windows of some steels, the use of an automated thixoforming cell is strongly recommendable, since little variations in the process can have a huge influences on the final result.

In order to meet the required reproducibility of the forging process an integrated automation of the production cycle has been introduced. The thixoforging cell consists of an induction unit, an industrial robot for the handling tasks and a servo-mechanical forging press.

6.4.1 The induction heating

The billet re-heating is one of the essential operations of the thixoforming process; the temperature distribution inside the slug must be as homogeneous as possible to enable a uniform distribution of the liquid fraction through the billet volume. In addition, the heating schedule must be such that, whilst achieving the above requirements, the time-temperature curve should be as short as possible since the heating operation regulates the process productivity. Re-heating of billets for thixoforming is normally done by inductive heating which is a convenient method to control. For thixoforming it is mandatory to reach the process temperature as quickly as possible in order to avoid unwanted grain coarsening and to keep the risk of scaling minimal.

6.4.1.1 **Theory of heating by induction**

Compared to other heating methods, contactless induction heating is one of the most effective ways to heat any electrically conducting material. Figure 6.3 shows a conventional induction heating system that consists of a cylindrical load surrounded by a multy-turn induction coil.
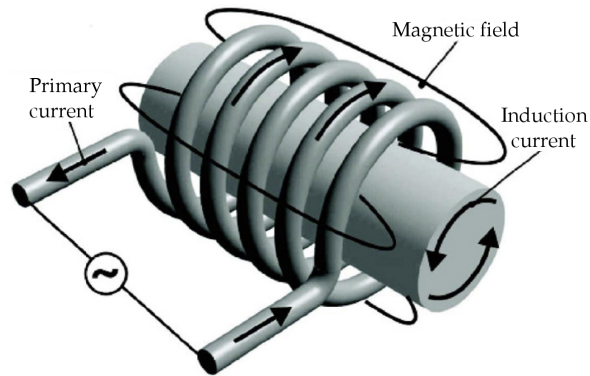

Figure 6.3 Principle of induction heating [51].

An alternating voltage applied to an induction coil will result in an alternating current in the coil circuit. This current will produce in its surroundings a time variable magnetic field, that has the same frequency as the coil current, and which induces eddy currents in the workpiece located inside the coil. Eddy currents will heat the material by the Joule effect ($I^2.R$). Due to the skin effect, a phenomenon produced by eddy currents during induction heating, most of the power density arrives close to the billet´s surface leading to significant higher heating of the surface in comparison with the core. Subsequently radial temperature gradients appear in the billet. Hirt *et al.* [12], characterised the skin effect by the so-called penetration depth, which is the distance from the billet surface within which approximately 86% of the total power is induced into the billet. For a given billet and induction coil geometry, this penetration depth decreases with increasing frequency of the oscillator. This suggests that a low frequency heating should be used if the homogeneity of the temperature distribution is to be considered. On the other hand, low

frequency means high electromagnetic forces, which are in contradiction to heating a soft semisolid billet.

6.4.1.2 **Induction heating for thixoforming**

The reheating of the billet to semisolid state is a critical step, mainly because it defines the microstructure and flow behaviour of the material. To obtain the desired globular structure as well as the correct filling of the dies, the following requirements must be fulfilled [12, 52]:

- Be **fast** to avoid an excessive growth of globules. The heating must be as fast as possible to avoid an excessive growth of globules but ensuring that the material surface does not start melting too early, so as to promote liquid pooling and the so called run off [3]. Furthermore, since it has to be as economical as possible, a fast heating is crucial.

- Be **precise** in order to be able to reproduce the desired liquid fraction. It has to be a very accurate process due to the narrow thixoforming window of some alloys.

- Be **homogeneous** throughout the billet. The temperature distribution throughout the material has to be as homogeneous as possible to obtain an acceptable liquid phase in every section of the billet. It can be monitored with direct measurements obtained from thermocouples during trials, but it is not possible to monitor under production.This means that the heating has to be made in an unsupervised way by application of previously proven heating cycles [43].

In hot forging industry, the most used heating devices to reheat steel feedstock are induction furnaces due to the shorter heating time and flexible process control. As it has been mentioned at the beginning of this section, induction heating is also the most preferable heating technology for steel

thixoforming. Keeping the heating requirements in mind, (fast, precise, homogeneous), it is easy to imagine how the heating curve should be.

Induction reheating should start with a quick heating while the material remains solid, followed by a power decrease when it starts melting. The objective of this power decrease is to achieve a homogeneous temperature throughout the billet reducing the skin effect. During this stage, radiation losses must be compensated while the heat is transferred into the billet by conduction. If enough power is not supplied to compensate radiation losses, the surface can start to solidify. When this happens, a solid skin of various millimetres is created on the surface. In any case, the control of the process and the heating parameters depend on the means at our disposal.

Lecomte-Beckers *et al.*[37] propose an optimisation of the heating cycle by numerical simulation. This technique involves the use of adequate software based on the finite element method for field calculations. Thanks to the simulations, optimising the coil geometry leads to an adapted magnetic field, assuring a homogeneous temperature distribution in the billet considering the expected energy losses caused by radiation and convection. Generally, it can be said that these approaches work quite well but obtaining valid material data such as thermo-physical properties for the simulation tasks is a problem. The reason for this is that the usually available laboratory equipment is not suitable to reproduce the same conditions found in industrial relevant heating cycles. Consequently, the recorded material data has to be adjusted experimentally to suit the real process. This procedure is quite time-consuming and its effectiveness relies on the experience of the user.

Behrens *et al.* [43] introduced an approach to conduct an unsupervised heating process by application of heating curves that were optimised with a fuzzy-logic controller. The main advantages of the fuzzy logic based approach are that no specific material data is required, system specific properties such as the efficiency have not be explicitly determined, and that the practical

implementation can be done with a minimum of experimental work. This can be a good way to control the heating cycle in an industrial environment, where due to technical restrictions, temperature measurements, especially inside the billet, are difficult to conduct.

Another contact-less way to at least measure the billet´s surface temperature is the one proposed by Schönbohn *et al.* [42] who suggest using a radiation pyrometer. The accuracy of the pyrometer mainly depends on the exact knowledge of the radiation coefficient. Usually, it is roughly known and changes from billet to billet and during the course of heating owing to scale formation, for example, lead to wrong measured values. As the measured temperature is not necessarily close to the real value, the control scheme cannot rely on the pyrometer directly.

In my case, since the tests presented in this dissertation are laboratory scale experiments, I have decided to control the heating step using two S type thermocouples as Becker *et al.* [53, 54] made before (see Figure 6.4).
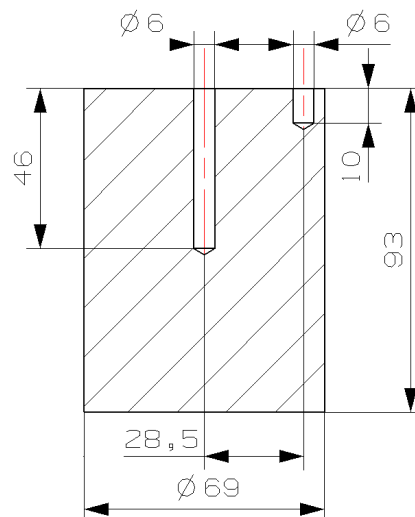
Figure 6.4 Thermocouple´s location into the billet during heating.

6.4.1.3 **The heating step**

In order to carry out the first stage of the process, a vertical induction heating equipment has been acquired from EFD Induction with a maximum power of 150 kW and a frequency range of 1,7-3 kHz.
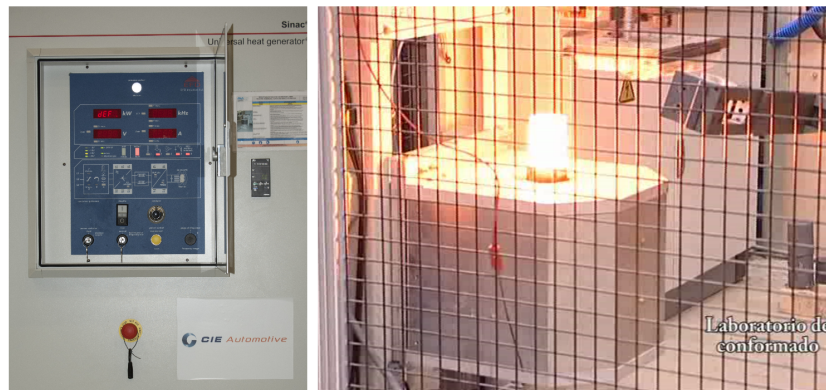

Figure 6.5 Induction heating equipment.

Figure 6.5 shows the control panel of the furnace on the left and, a vertically heated billet on the right side. For further detail of different thixoforming heating devices, see Kirkwood *et al.* [3] and Hirt *et al.* [12].

As mentioned previously in this chapter, during induction heating most of the power density arrives close to the billet´s surface leading to a significant radial temperature gradient. In order to get a homogeneous temperature throughout the billet, different steps have been programmed for temperature equalising through heat conduction. A programmable logic controller (PLC) has been implemented in the heating control system to manage the signal transferred from the two S type thermocouples displayed in Figure 6.4. When the outer surface reaches a predetermined temperature, the heating stops and the heat is transferred by conduction to the centre of the billet. When both temperatures equalise, the heating restarts until the next programmed temperature. Step by step the temperature increases until the target temperature is reached. In any case, and due to the cost of this kind of thermocouples once the cycle is defined,

the control is taken over time. This obviously this introduces some error, but it is not significant.

The automatic control of the furnace power has turned out to be of great difficulty. First we realised that the 0 percentage of power corresponded to 24 kW, and thus, the billet continued heating until the surface melting by just turning the power to 0. Second, we tried to use a PID heating control but due to the high power of the heating device the generated axial gradient was so big that the surface was completely melted in the first step. Due to this, the heating has been carried out with a constant power of 24 kW and, after each heating step, the furnace has been switched off (0 kW). This is precisely the homogenisation time. Then, the heating restarts.

To protect the steel billets from surface oxidation and possible defects arising from it, the heating has been made within an inert argon atmosphere with an argon flow rate between 14 to 20 l/min, thus, avoiding oxide inclusions inside the final component. At the same time, and due to the lower heat radiation capacity of a blank surface compared to an oxidised one, radiation heat losses have been reduced.

Nevertheless, even if the radial temperature gradient is not too big, around 7ºC or less at the end of the heating, there is also an axial temperature gradient that has not been quantified.
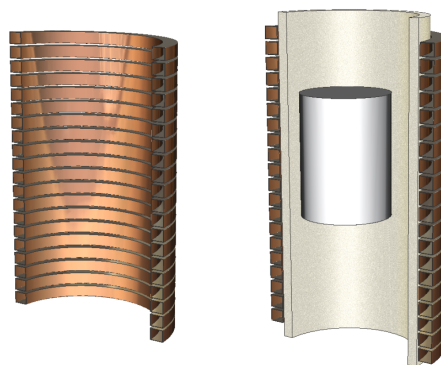
Figure 6.6 CAD drawing of the induction coil.

It is possible to assume that this temperature difference is due to the coil geometry and the billet location into it on the one hand (see Figure 6.6), and due to the insulating pedestal on the other. According to the supplier´s explanations, the coil geometry has been designed for a wide range of billet diameters and lengths, what means that it has not been optimised for the tested billet dimensions. Furthermore, the insulating pedestal causes the thermal conditions to be different between the top and the bottom side of the billet, increasing the axial temperature gradient.

Down below the heating steps corresponding to LTT C45, LTT C38 and LTT 100Cr6 are presented. These are the materials that have been used for the subsequent forming step.

6.4.1.4 **LTT C45 heating**

Figure 6.7 shows the heating cycle used for LTT C45 steel, with four different steps, for a total duration of 231 seconds.
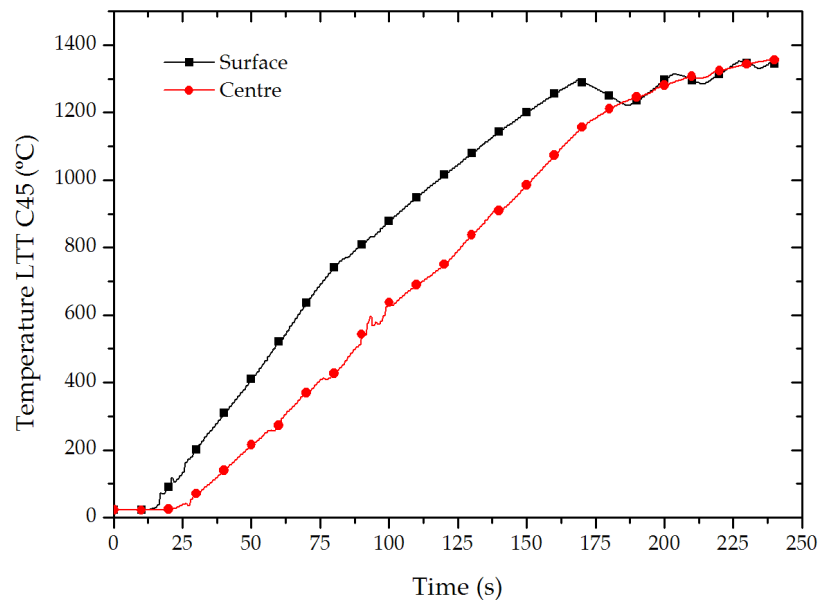
Figure 6.7 Heating cycle of LTT C45 steel before forming.

The measured temperature gradient at the end of the heating between the surface and the centre is of 7ºC. In this case the centre is hotter, with a temperature of 1356ºC, due to the shortness of the last heating step. It is important to have in mind that this is not the forming temperature. Due to the transport time and the contact with different tools, we know that the forming temperature is lower but it has not been quantified.

6.4.1.5 **LTT C38 heating**

The heating cycle of LTT C38 is represented in Figure 6.8. As its semisolid temperature is higher than the one for LTT C45, another step has been added and some times changed. The heating is made in 256 seconds and the billets´ temperature reaches 1394ºC. The surface - interior temperature difference is shortened to 4ºC in this case. In any case, the axial temperature gradient is also evident but it could not be measured.
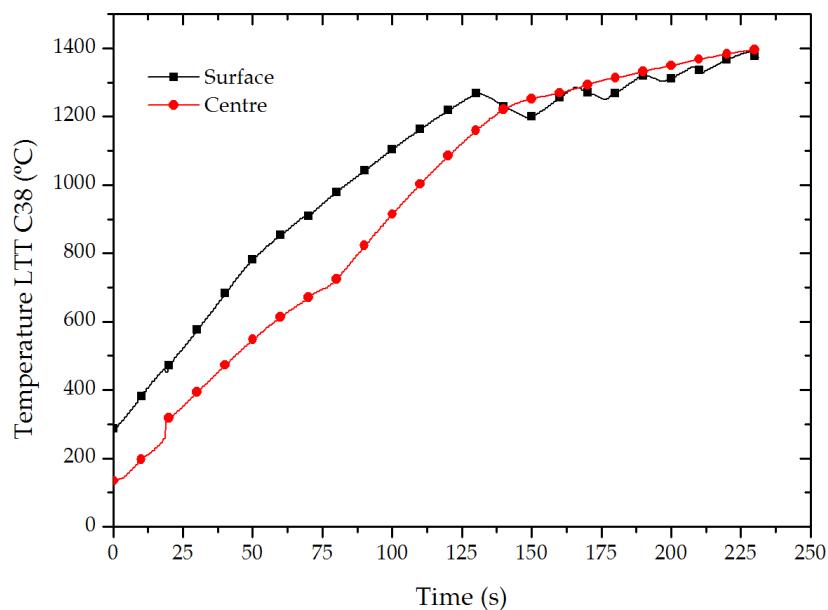
Figure 6.8 Heating cycle of LTT C38 steel before forming.

6.4.1.6 **LTT 100Cr6 heating**

As it is displayed in Figure 6.9, the heating cycle of LTT 100Cr6 is the same as for LTT C45. However, the working steel is different and so is the achieved temperature. In this case, the billet leaves the furnace at 1297ºC and a temperature gradient of 6ºC.
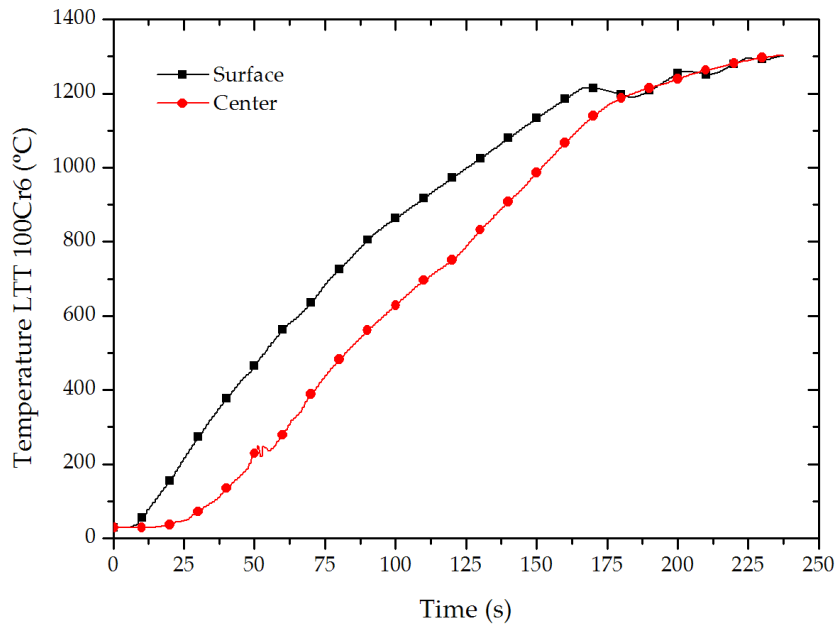

Figure 6.9 Heating cycle of LTT 100Cr6 steel before forming.

6.4.1.7 **Final remarks concerning heating**

To sum up, I would like to make a series of considerations about heating. It has been demonstrated that the heating cycle is highly reproducible and is not affected by the environmental conditions, at least at our forming laboratory. All the heatings have been made within a cold furnace, which means that the refractory concrete surrounding the coil was cold. I have noticed that it gets hotter cycle by cycle until it reaches a steady state. This temperature increase affects the defined heating cycles leading the billet to a partial melting after five consecutive heatings. Beside this, the possibility to heat so different

billet dimensions leads to an unoptimised coil geometry and therefore to radial and axial temperature gradients that can be minimised with a proper coil design. The isolating pedestal also contributes to the axial temperature gradient changing the thermal conditions of the top and the bottom of the billet.

Furthermore, as mentioned in chapter 4, temperatures with which sound parts are obtained are lower than the expected by DSC or IDS measurements. Two main variables could be responsible for this: the thermocouples´ measurement or the different heating rate between the DSC, and the induction furnace. In my opinion, the later is the key factor, which suggests that further study on the melting behaviour of the alloys is needed.

Finally, it is necessary to keep in mind that to ensure a productivity comparable to other forming processes, billets must be heated on a carrousel. In any case, these are quite affordable issues for the industry to cope with, due to their extensive experience in this area.

6.4.2 **The transfer of the billet**

The transport from the induction furnace to the forming tool is another important step. During this transfer, heat losses in the material are unavoidable and have to be minimised because they rise the solid fraction, specially on the billet surface, and consequently the forming loads. To compensate these heat losses, which can be big enough [17] depending on the billet size, temperature in the reheating step can be raised a little bit more.

As in the heating stage, the minimisation of oxides is also important, since the increase of the friction coefficient [18] affects the material flow during forming, spoiling the properties of the final product.

Due to this, in order to achieve the required reproducibility of transfer and handling operations, robots are necessary. In this research work, as dies are closed before the transfer of the billet, a robot is important to ensure a reproducible placing of the billet into the hole of the upper die holder. With that

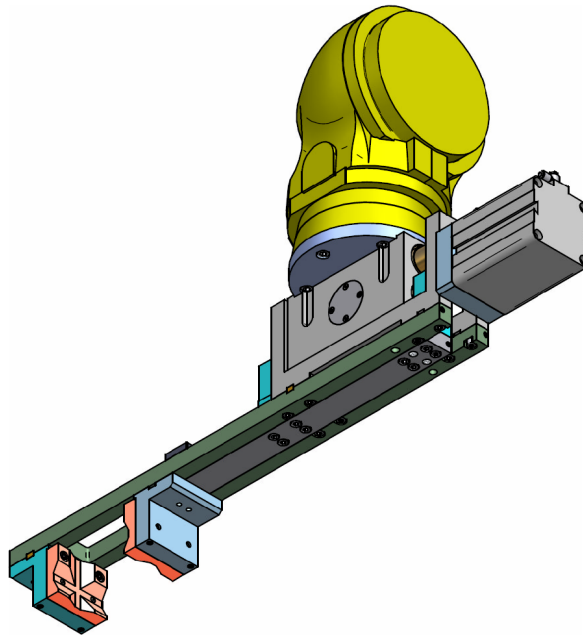aim, a specifically designed gripper shown in (Figure 6.10) has been designed.

Figure 6.10 CAD design of the gripper.

This special gripper allows to handle billets in a diameter range between 50 to 100 mm with the objective of minimising temperature losses and, if needed, sustaining the billet in an inert gas atmosphere to avoid scaling. Although it is not visible in Figure 6.10, the steel billet could be covered for a better protection. Nevertheless, argon has not been used in these tests during billet´s transport.

Depending on the cell´s automation degree, more than one robot could be required. In any case, in hot forging industries billet cutting and introduction into the continuous heating device is made by different handling systems. Once the billet has reached the forging temperature, a robot is used to make the transfer to the forming zone. A second robot located in the forging area could transfer the part from one step to the other and, finally, to the evacuation or heat treatments zones. However, this is usually made by a person because the forged part is not always ejected in the same place and the robot is not able to pick the part and put it in the next step.

6.4.3 **The forming step**

The semisolid forming stage, which requires a special movement of the ram, is made by high-speed presses that can be hydraulic or mechanical [55]. The approximation to the billet must be as fast as possible in order to avoid premature cooling and to minimise the cycle time. Once the forming tool gets in contact with the semisolid material, the speed should decrease significantly to prevent liquid ejections. An arrangement between high and low speed has to be always maintained since a high speed entails high shear rates and low forming loads, but also, possible liquid ejections and turbulent die filling that can generate defects on the finished component. On the other hand, low ram speed avoids those defects and makes a better flow of the material during die filling possible; but it promotes unexpected cooling during forming with its subsequent problems and larger cycle times.

When the die is filled, the solidification of the liquid phase starts, and pressure should be increased and maintained until it finishes completely in order to avoid shrinkage problems.

6.4.3.1 **The servomechanical press**

Although the servo-motors were used in metal cutting machine tools as early as in the 1950s, they were not mounted on metal forming presses for a long time because their power was not strong enough. High powered AC servo-motors were made in the 1980s with the development of the strong magnets. Together with the development of transistor controllers, they were applied to injection moulding machines in the late 1980s.

Since some metal forming processes, such as enclosed die forging, necessitated complicated motions of multiple slides, hydraulic servo-presses were built in the 1970s. A general purpose servo press was not built until 1997 when Komatsu HCP3000 appeared. Since then, several types of mechanical servo presses have been developed, according to the transmission of movement from

the motor to the ram [56]: by means of a pulley and a screw; by means of a direct screw; by means of a pulley, a gear, a crank and a link; by means of a pulley, a screw and a link; by means of a gear and crank; and by means of a gear, a crank and a link.

The mechanical servo-drive press offers the flexibility of a hydraulic press (infinite ram speed and position control, availability of press force at any ram position) with the speed, accuracy and reliability of a mechanical press [57].

Because all the press motions such as starting, velocity change and stopping are done only by the servo-motor, the mechanical servo press has a simple driving chain without any flywheel, clutch and brake which are essential for a conventional mechanical press, and thus, the maintenance of the servo press is simplified.

Compared with the hydraulic servo press which has been used for many years, the mechanical servo press has higher productivity, better product accuracy and better machine reliability without the noise of the hydraulic pump nor the complicated piping [57]. In any case, the servo motor driven mechanical press employed in this research work has a disadvantage compared with a hydraulic press. It has a reduction by means of a gear and transmits the movement from the motor to the crank. Due to this, the nominal press capacity is not available at any ram position (it depends on the crank angle). However, this can be easily compensated by the stroke adjustment which allows to locate the upper ram in the right position to work with the nominal press force.

The most important feature of the servo press is the flexible ram movement. In fact, the flexibility to perform a wide range of working cycles is what makes it suitable for semisolid forging. The main characteristics of the press used in this dissertation are summarised in Table 6.1.

Taking into account the geometry of the forming parts as well as the press´ limitations, it has been decided to carry out the forming stage by thixo-lateral (or transverse) forging (Figure 2.7). It is an alternative forging process with

Table 6.1 4000 kN servo motor driven mechanical press.

Servo motor driven mechanical press $SDM2 - 400 - 2400 - 1200$	
Press capacity (kN)	4000 at 20 mm from the BDC
Number of points	2
Working torque Max / Nominal (N.m)	5500 / 3000
Max stroke (mm)	400
Max ram speed (mm/s)	800
Die height (mm)	1000 to 1200 (str 400mm)
Stroke adjustment (mm)	200
Table size (mm x mm)	2400 x 1200
Max cadence (spm)	100
Die cushion capacity (kN)	400
Die cushion stroke (mm)	100
Motor power Maximum / Nominal (kW)	450 / 250

important advantages over the conventional thixoforging. The forming velocity is of the same order of magnitude and it is characterised by squeezing the semisolid material into an already closed die, thus eliminating any possible material ejection. Furthermore, in terms of diversity of parts, it allows an increased degree of geometric freedom [12].

To make this possible and in order to use all the force capacity of the press during forming, I have designed a special tool (Figure 6.11).

6.4.3.2 **The forming tool**

As it has been mentioned just before, forming by thixo-lateral forging involves die closing prior to the slug transfer. Four hydraulic cylinders, located at the upper die holder give the closing force by clamping the wedges of their rods in the holes of the columns opposite them. Thus, the columns will be tensioned with the desired force, which is in turn the die´s closing force. This system is able to provide a maximum die closing force of 1200 tons. Once the component

is formed and the ram is up, two lateral cylinders open the die and the expulsion system ejects the part.
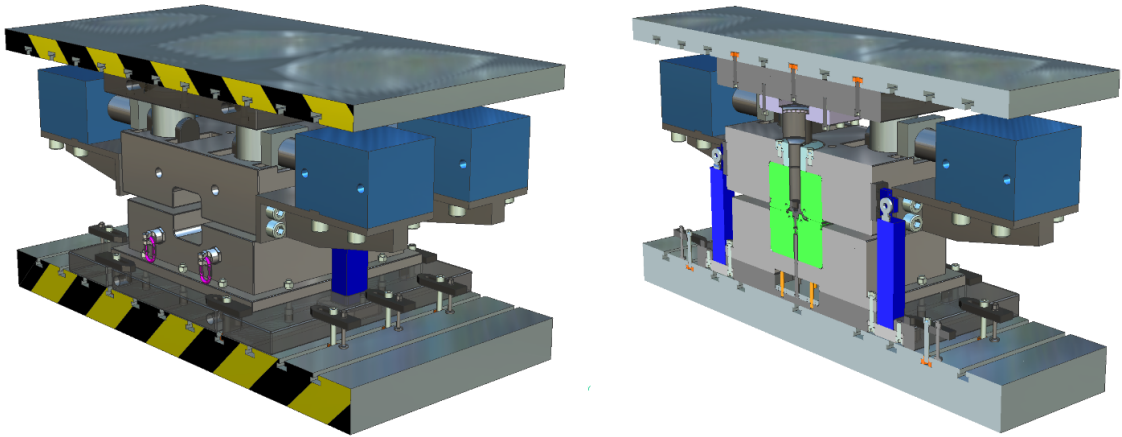
Figure 6.11 CAD design of the forming tool.

An integrated automation of the production cycle has been introduced in order to meet the required reproducibility of the forging process.

6.4.3.3 **The the overall coordination of the forming cell**

As mentioned in section 6.4 and displayed in Figure 6.12, the thixoforging cell comprises an induction unit, a six-axes industrial robot for the handling tasks and the servo-mechanical forging press.

The overall coordination and sequence control depends on the robot controller but the heating and forming processes are performed independently on dedicated hardware, so that changes conducted at these components do not affect the sequence control of the production cycle.

Communication with the individual automation components is done by means of direct wiring and digital I/O lines. In areas where the gripper could collide with moving components such as induction coil, furnace lid, opened die tool or closed press, sensor signals reflect components´ actual status. Based on

this sensor signals robot movement will be inhibited if a collision is predicted to result from the movement.

Figure 6.12 Overview of the implemented thixoforging cell.

The production cell is sealed with railings and equipped with a door which must be locked to keep the cell working. Once it is opened everything stops, and for security reasons, clearance has to be given manually to all working devices. A person is needed to place the steel slug on the furnace pedestal and to remove the final part from the die. The operator thus opens the door in every cycle, making manual clearance compulsory before each forming cycle. Finally, it is worth mentioning that the production cycle can be controlled with a panel located outside the cell.

6.4.3.4 The forming cycle

The complete die filling was reached with a force of approximately 3.500 kN. The Brankamp, a press force control device, was programmed to stop the punch at 3.800 kN. In some exceptional cases that limit was exceeded and the press

overload system triggered. Ceraspray[©], a long lasting ceramic varnish with lubricant effect that acts also as a thermal shock barrier between the billet and dies was used in the forging step [58]. The plunger position against punch load and speed can be seen in Figure 6.13. Surface defects are not appreciated on finished parts, only little areas where Ceraspray has accumulated are not completely full filled.

The measured thixoforming parameters during trials are listed in Table 6.2. The dies were heated up to 270°C by circulating oil and the clamping force given by the tool is 1.200 t. No liquid phase was squeezed between the dies. The transportation time was 17 seconds, measured since the coil of the heating furnace is down until the punch gets in contact with the semisolid billet. Five seconds of solidification time was applied to avoid shrinkage problems.

Table 6.2 Thixo-Lateral forging parameters.

Parameter	Value
Argon gas volume rate (l/min)	14 - 20
Transportation time (s)	17
Clamping load (MN)	12
Punch load (kN)	3.300 - 3.800
Ram speed (mm/s)	410
Die temperature, thermocouple (°C)	270

Figure 6.13 shows how the approximation to the billet is fast at the beginning and when the ram reaches 150 mm above the BDC (Bottom Dead Centre) the speed is decreased until it stops completely at the established position. While the billet is deformed the press force rises and it is maintained during 5 seconds for the solidification of the liquid phase. After this, the ram returns to the TDC (Top Dead Centre).
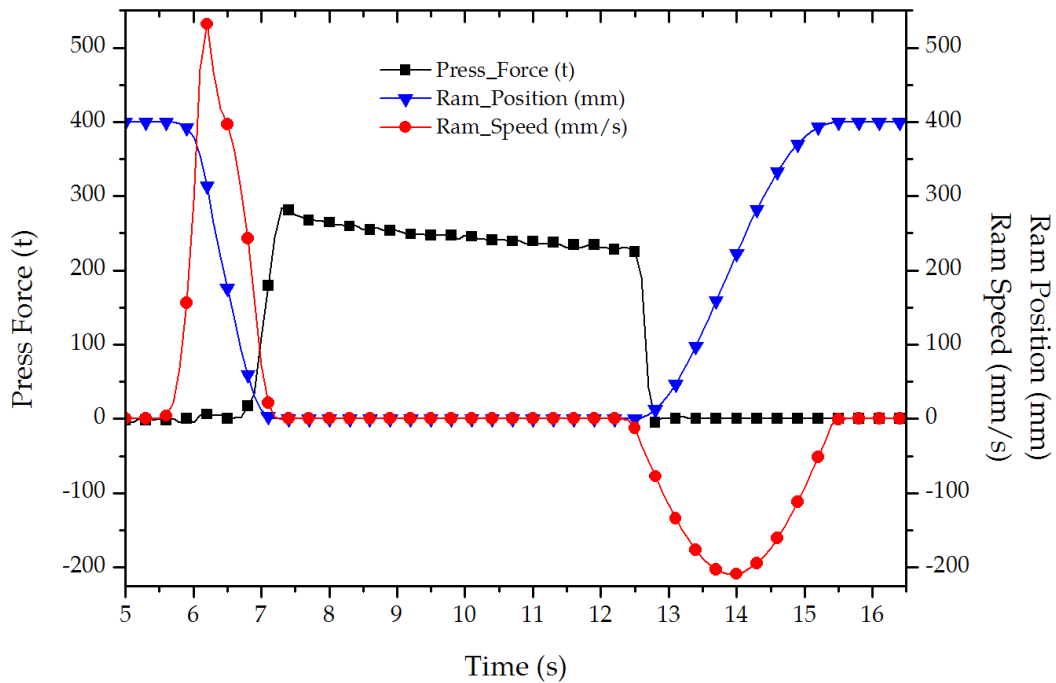
Figure 6.13 Press force, ram position and speed during forming.

6.4.4 **Dies**

In principle, it seems that the major drawback for industrial implementation of semisolid steel forming technology is the lack of suitable tools and dies that meet the demands and exhibit an economically satisfactory service life within the range of tolerated degradation. The reason for this severe attack on forming dies has to be found in the complex load profile acting on them during semisolid processing. Four main categories may be distinguished [59]: (1) mechanical, (2) thermal, (3) chemical and (4) tribological impacts.

The load profiles acting on steel thixoforming dies are displayed in Figure 6.14. Whereas chemical and tribological loads are of secondary importance regarding applicability since they are leading to slow surface degradation (long term effects), the thermal and mechanical loads are decisive for instant failure (short term effects) of the parts due to the induced stresses [59].

Short term effects		Long term effects
Mechanical loads • ~ 20 MPa axial compression required for form filling. • ~ 100 MPa axial compression for final densification.		**Chemical loads** • Corrosive attack by the fraction liquid of the semi-solid steel. • Corrosive attack by scale, mould release agents and lubricants.
	Demands on tool materials • Excellent mechanical strength up to high temperatures (>500°C). • Outstanding thermal shock resistance (ΔT800-1000°C). • Low wettability by semi-solid steel (Θ>90°, better >120°). • High hardness (HV10 >5).	
Thermal loads • Die preheating temperature 200-400°C. • Primary material temperature 1200-1500°C.		**Tribological loads** • Abrasion by solid particles during form filling. • Adhesion during the solidification of the parts.

Figure 6.14 Press force, ram position and speed during forming [12].

6.4.4.1 Mechanical loads

The mechanical loads comprise the forming pressure for the die filling and also, the final densification pressure to avoid possible porosity in the work piece. While the forming pressure is about 25 Mpa, according to experiments carried out by Hirt and Kopp [7,27], the densification pressure data found in the literature ranges from 50 MPa to more than 1500 MPa. However, 100 MPa, is a widely accepted densification pressure to obtain fully dense steel parts.

Mechanical loads result in stress states that can initiate cracks, if material strength is exceeded, and can promote die failure.

6.4.4.2   **Thermal loads**

During the forming stage, the semisolid material keeps in contact with die surface and thus, the heat is transferred from the semisolid slug to the die during form filling and solidification. The severe thermal shocks in each forming cycle are unavoidable since the temperature of the semisolid billet is in the range of 1200-1500ºC and the maximum tool temperatures in conventional forming processes restricted to the annealing temperature of metallic tool frames, usually around 500-550ºC.

As mechanical loads, thermal loads also result in stress states that promote die failure.

6.4.4.3   **Chemical and tribological loads**

During die filling, the liquid fraction of the semisolid steel can cause chemical attack on the die surface. Moreover, scale coming from the reheated slug has also a strong influence on the chemical interaction between the die and the steel during forming.

On the other side, tribological loads involve the abrasive attack of solid particles from the semisolid steel during material flow and those coming from the solidified components during ejection.

This kinds of loads lead to slow surface degradation and are considered long term effects.

6.4.4.4   **Possible alternatives**

High process temperatures, above 1250ºC, involve high temperature gradient between the dies´ surface and interior, and the thermal stress exposed to, require tool materials with very specific features.

Conventionally used hot working steels deteriorate quickly under severe thixoforming conditions and subsequently, it is crucial to find different alterna-

tives. These alternatives can include refractory metals, superalloys, bulk ceramics or different kinds of coatings [20]. TZM (Titanium-Zirconium-Molibtenum) alloy has demonstrated encouraging results but it suffers oxidation. Some ceramic alloys, like silicon nitride (Si_3N_4), show excellent fracture toughness and thermal fatigue resistance, besides good mechanical stress endurance, however, around 1000°C they are sensitive to corrosion and oxidation. Other feasible options are cooper alloys, nickel alloys and superalloys, as well as titanium, molybdenum and tungsten alloys which have superior resistance to thermal fatigue.

In general, ceramic materials have many of the desired properties for the semisolid processing: hardness, thermochemical stability and corrosion resistance against molten metal above thixoforming temperatures. On the other hand, when compared with metallic materials, they present little fracture toughness and thermal fatigue resistance. A feasible strategy to solve these inconveniences can be to combine properties of metallic materials with those of ceramic ones, through deposition of ceramic coatings over metallic substrates by Physical Vapour Deposition (PVD) or Chemical Vapour Deposition (CVD) processes. This way, mechanical stresses will be supported by the metallic base and the ceramic coating will be the responsible to deal with thermal, corrosive and tribological attacks. The temperature and thermal fatigue are usually not critical for vapour deposited thin films since they are designed for that, but they force the substrate to support part of those efforts. To avoid this, thermal sprayed (TS) coatings can be used. They have bigger thickness and more porosity which allows a better thermal protection of the base material. Nevertheless, the porosity presented reduces their loading capacity.

The fabrication of ceramic materials is limited by means of size and geometrical complexity, but furthermore, it is crucial to know the stresses and limitations of different coatings and ceramic materials in order to select the appropriate technology, since not all technologies are able to coat every cavity.

6.4.4.5 **Working dies and possible coatings**

The first thixoforming dies where used without any coating. They were made from 1.2344 hot working steel, very usual in hot forging industry, with a hardness of 48-50 Rocwell C. The punch and the ejector, in turn, where made in 1.2365 steel and hardened to 50-52 Rocwell C. The lower die failed after 72 forming cycles. Everything suggests that the failure occurred due to the proximity between the die´s tempering circuit and its surface. Apart from the load profile it is important to take another issue into account: the number of times that the die has been heated to the working temperature and cooled. Specifically, in the industrial fabrication of this component, each die, is heated only twice during its service life and I have heated it more than twenty times due to tooling modifications and short testing series. That is why it is reasonable to point to the heating-cooling cycles as responsible for the cracking.

Figure 6.15 Lower die crack.

Besides the crack, wearing and adhesion phenomena are also visible in areas where the semisolid material flow is greater. To analyse those areas the

die has been cut by electric wire erosion and examined in a scanning electron microscope (SEM).
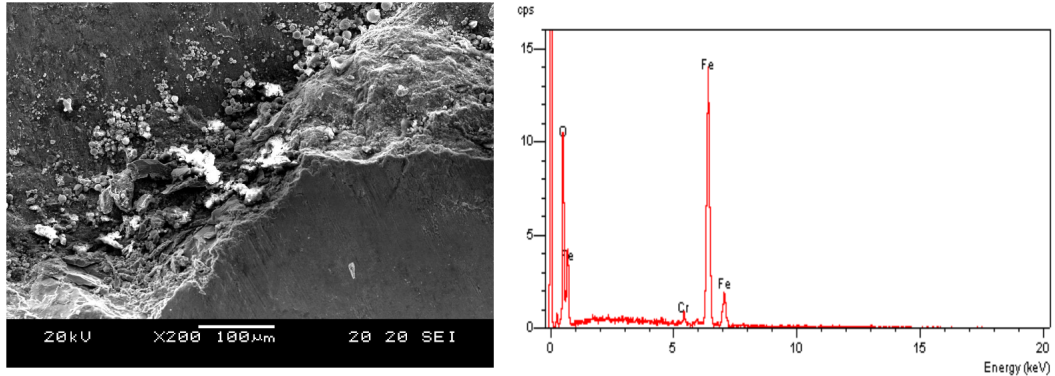
Figure 6.16 Adhesion area and layer spectrum.

Figure 6.16 shows the transition area from the die surface to the iron oxide layer together with its composition spectrum. The upper left side of the SEI image corresponds to the die surface, while the bottom right side is the iron oxide layer.

In order to continue with the programed test series, two new dies were machined from the same steel grade (1.2344). This time, after the corresponding quenching and tempering to get a hardness of 53 Rocwell C, they were gas nitrided and oxidised in the furnace. To finish the process, dies were cooled in the oven under a nitrogen atmosphere.

Several trials have been made with these new dies and there is still no significant damage.

Together with the thixoforming trials, other base materials, coatings and deposition methods have also been studied and proposed for testing. In any case, due to premature failure in some cases, or lack of time in others, these are issues to deal with in the future work.

Regarding the base materials tree electrically conductive composites were proposed: $ZrO_2 - WC$, $ZrO_2 - TiN$, $ZrB_2 - SiC$. In principle, they have

good mechanical properties to support the process requirements: hardness, thermochemical stability and molten metal corrosion resistance. Besides, compared with conventional ceramic materials, they are easily machinable by sinker EDM.
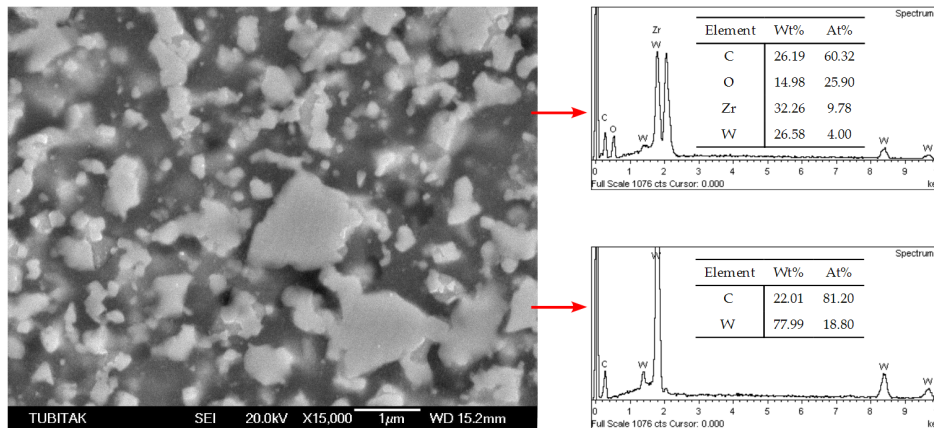
Figure 6.17 $ZrO_2 - WC$ (60/40) composite identification.

Figure 6.17 displays a micrograph obtained by Birol for the characterisation of the $ZrO_2 - WC$ (60/40) along with the composition of the different compounds. The density of the material was around 9.8 g/cc and its hardness of 80 Rocwell C. Thermal fatigue testings were also carried out at Tubitac research centre.

Birol has been testing different possible die alloys and superalloys [60, 61, 50, 62, 63] and has designed a laboratory scale test simulating the thermal fatigue to which dies are exposed during thixoforming [64, 65]. The test consists of a cyclical heating and cooling of prismatic samples of 25x25x20 mm. The heating is made by oxyacetylene flame during 30s until the sample surface reaches the maximum die surface temperature measured during trials with commercial hot rolled X120CrW12 steel (730ºC)[64]. Consecutively, die cooling by forced air starts for another 30s, down to 450ºC, dies´ initial temperature. The maximum temperature is below the one mentioned by Hirt et al. [66] for the same steel thixoforming and the same die material. By computer simulation with Forge®,

they measured that the temperature on the die surface reached 950°C while material was flowing, decreasing to 750°C a few seconds after removing the component.

The performance of $ZrO_2 - WC$ (60/40) to thermal fatigue was unexpectedly poor. The tested samples failed after only two cycles. The conductive ceramic material broke into many pieces as soon as thermal cycling started (Figure 6.18 left). A couple of pieces were heated in a resistance furnace to find out if thermal shock was the problem. However, these samples disintegrated into pieces shortly after placing them in the furnace at 750 °C (Figure 6.18 right). The change in the colour of the sample implies some sort of transformation.
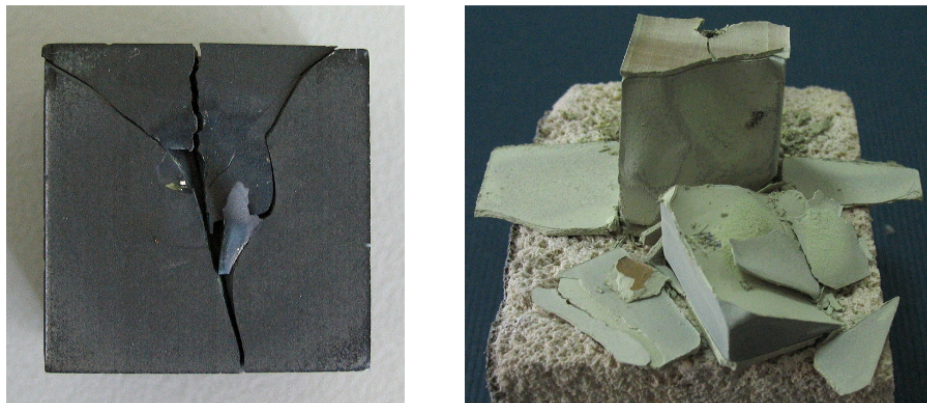
Figure 6.18 Thermal fatigue (left) and isothermally heated (right) samples.

Due to these bad results I decided not to continue testing electrically conductive ceramic materials and to focus all the effort on increasing the die´s service life by means of coatings. High Velocity Oxigen Fuel (HVOF) and PVD methods were selected for coating deposition, with, WC-Co cermets and MEX6000 respectively. WC-Co cermets can be a viable alternative in tool live extension applications due to their attractive combination of properties [67]: strong adhesion, high cohesive strength, high residual stresses, wear and silt erosion resistance capabilities, comparable with those of $ZrO_2 - WC$. These properties can be enhanced using nanostructured powders that,

under proper spraying conditions, could present improvements of 21% in microhardness, 100% in wear and 350% in corrosion compared to conventional and bimodal HVOF sprayed coatings [68]. On the other side, MEX6000 is a nanostructured multilayer coating with high hardness, high thickness and low friction coefficient that is able to work properly at 1100°C which can be a challenging PVD coating for semisolid forming.

6.5   Final remarks about the process

Based on the results, it is possible to say that the thixo-lateral forging is a robust process, highly repeatable but still with much more optimisation margin. As mentioned in section 6.4.1.7 radial and axial temperature gradients can be minimised with a proper coil design and a carrousel or continuous heating. Components must be redesigned in order to obtain all the process´ advantages and the forming step must be overhauled to ensure that the compaction force is well distributed through the forming part.

Regarding the material, it turns out that a deeper study on the melting behaviour of the alloys is needed and also a wider study of the suitable steels for thixoforming.

With respect of dies, it seems that the major drawback for industrial implementation of semisolid forming is the lack of suitable tools. In any case, this is a contentious issue if we take into account the results from Thixofranc where the reported die damage after 3500 cycles is similar to the wear found in conventional hot forging.

Keeping all this in mind, the aim of chapter 7 is to show the final results of the thixoforged automotive spindle and demonstrate that semisolid forming of steels could become an industrially applicable technology that will open new prospects to forging companies.

Properties of the Semisolid Forged Components

This chapter will be devoted to analysing the properties of the semisolid forged spindle. As it is an automotive component, the analysis has been focused on the mechanical properties and soundness of the part, with the aim of validating the semisolid forging as a possible manufacturing process for the automotive sector.

7.1   Introduction

All the components were manufactured in the forming cell of Mondragon Unibertsitatea using the designed tool shown in section 6.4.3. More than two hundred parts were obtained. At the beginning, the objective was to ensure that the selected steel alloys could be formed in the semisolid state; due to this, the first components were used to validate the geometry of the parts and to adjust all the process´ parameters.

The components analysed below were manufactured using the press forming cycle displayed in Figure 6.13 with each corresponding heating cycle

defined in section 6.4.1. Geometrically the component is fine as Figure 7.1 demonstrates.

Figure 7.1 Semisolid forged part (left) and hot forged part (right).

Other heating cycles were also tested but the components presented high porosity and cracks thus making them completely useless, as can be seen in Figure 7.2.

Figure 7.2 Semisolid forged part with defects along the axle.

These defects show up due to the excessive temperature during forming.

Shrinkage porosity was clearly visible in parts formed around 1400°C using LTT C45. By lowering the forming temperature to around 1350°C, the porosity disappeared. Another way to overcome this problem could be to increase the compaction force, impossible in our case due to the force of the servo mechanical press at our disposal.

7.2 Microstructural analysis of components

In this section components fabricated with different steel alloys (LTT C45, LTT C38 and LTT 100Cr6) will be analysed. Their microstructures and mechanical properties will be presented after semisolid forming and after the corresponding heat treatment. The microstructures have been analysed in two different areas of the spindle, on the axle and on the base. Different microstrucures are easily distinguishable.

7.2.1 Microstructure after semisolid forging

As it is described in section 7.4. the component´s geometry is all right. Then, the microstructure after semisolid forming is analysed.

7.2.1.1 LTT C45

Axle area. Microstructures obtained from the axle area are shown in Figure 7.3. The picture to the left corresponds to an upper bainite structure, formed between 550-400°C. It is made up of ferrite and cementite parallel needles with more or less tree structured contour. Ferrite needles that act as crystallisation centres are developed in parallel, separated by a cementite edge.

Furthermore, in the right-hand picture lower bainite is visible, formed between 400-200°C and thinner than upper bainite, with a more acicular striking appearance. When temperature decreases, bainite evolves from a tree structure towards an acicular one. The structure is then refined, becoming
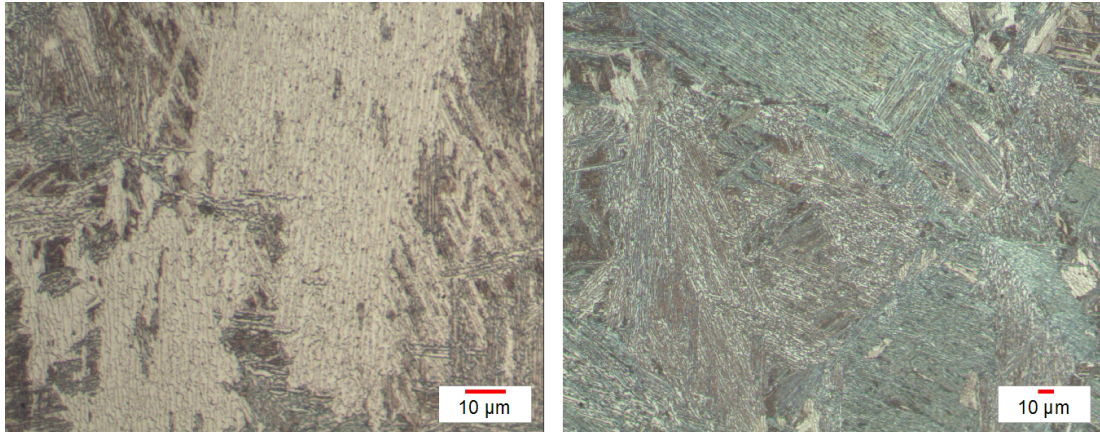
Figure 7.3 Different areas of the axle microstructures from LTT C45.

observable only under large magnifications. At those magnifications thin parallel carbide plates could be observable within the long ferrite needles, forming a 60 degree angle with their axle.

Other microstructures are also visible in the same area as displayed in Figure 7.4. Here the picture to the left shows a dense martensitic microstructure with some retained austenite and some bainite areas. On the right hand side, martensite needles over a white background are clearly displayed.
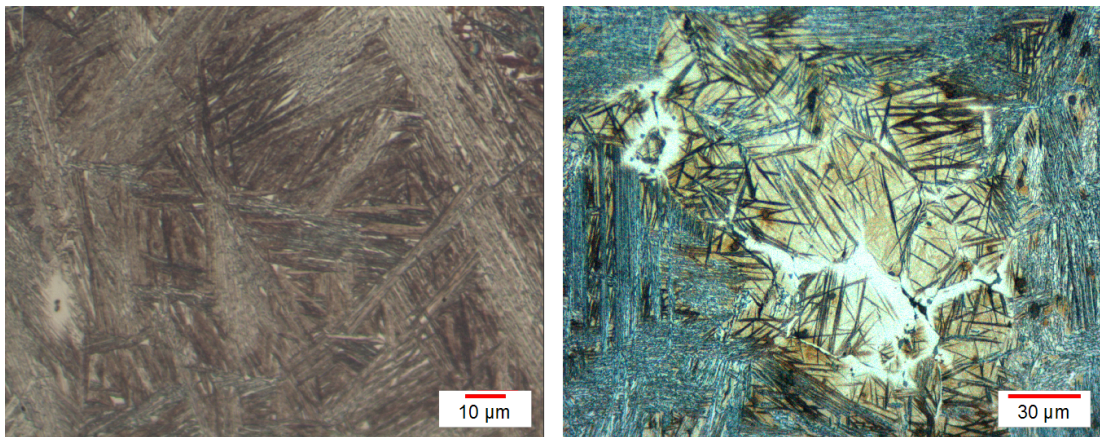
Figure 7.4 Different areas of the axle microstructures from LTT C45.

The martensite presents a marked acicular aspect with needles in zigzag

forming angles of 60 degrees. This is an easy observation if, as in this case, martensite needles are highlighted over the retained austenite. When the transformation is complete and there is no retained austenite, the observation is more difficult.

Base area. In the base area (Figure 7.5) the microstructure is more homogeneous. It consists basically of bainite and martensite areas with retained austenite, as it is shown in the picture on the left, or bainite areas with some small and dispersed martensite and retained austenite areas visible on the picture on the right.
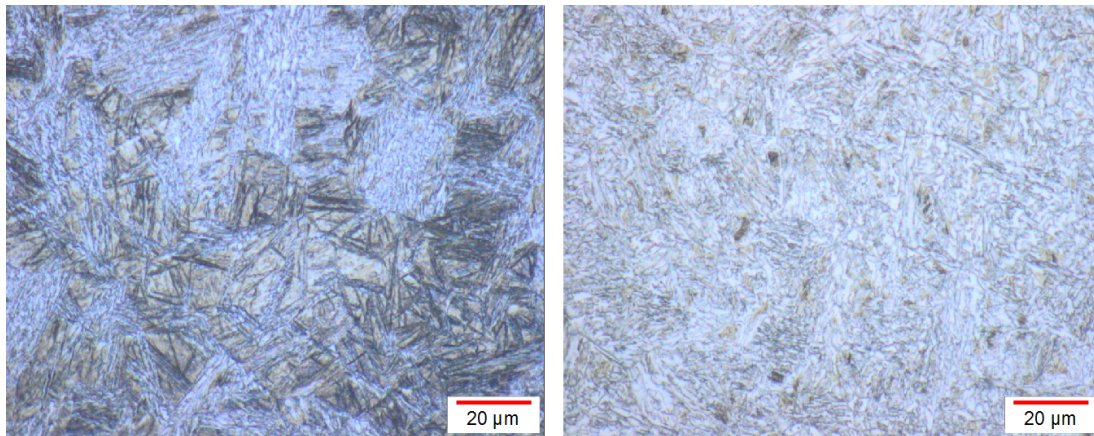
Figure 7.5 Different areas of the spindle base microstructures from LTT C45.

7.2.1.2 **LTT C38**

Axle area. The visible microstructure consists of ferrite (white) perlite (black) with different grain size areas, as shown in Figure 7.5. The picture on the left presents a coarser grain size than the one on the right. In the latter, some rounded and light grey coloured manganese sulphides can also be seen.

Base area. The microstructure present in the base is similar to that from the axle, consisting of ferrite perlite grains as it is shown in Figure 7.7.
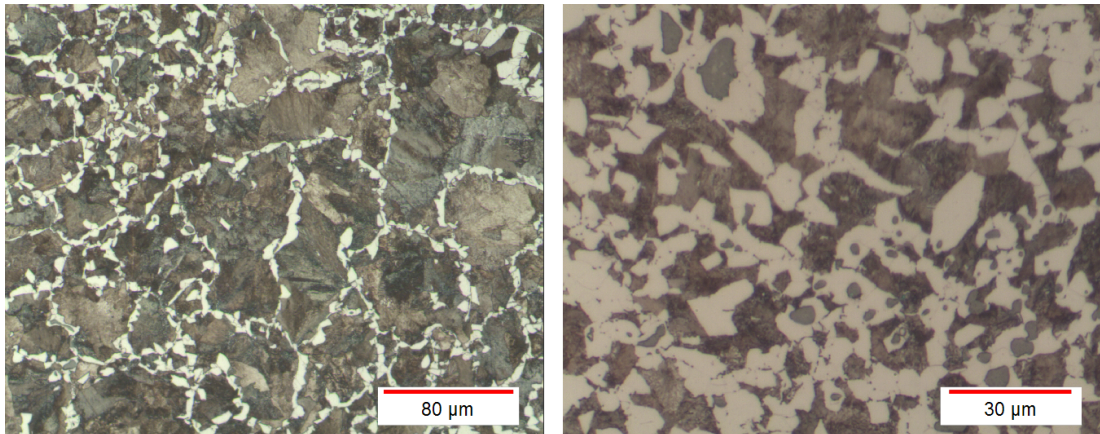
Figure 7.6 Different areas of the spindle axle microstructures from LTT C38.
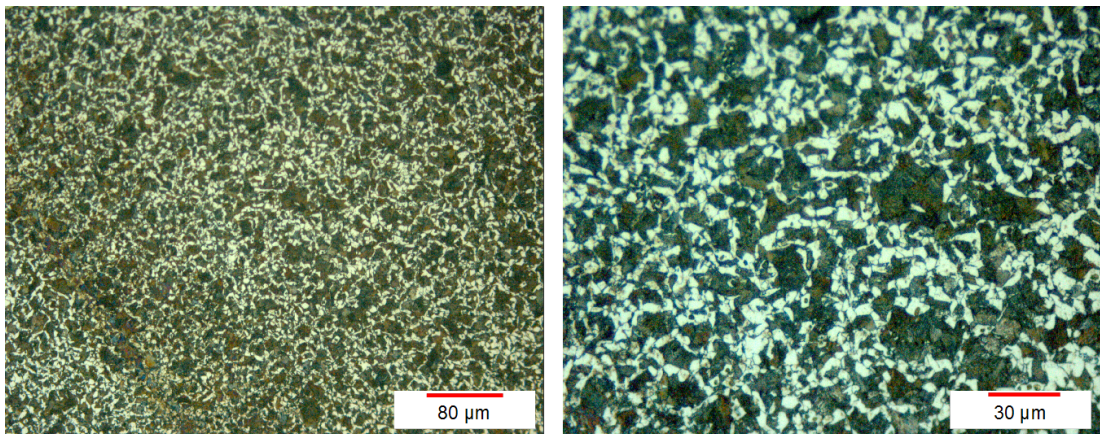
Figure 7.7 Different areas of the spindle base microstructures from LTT C38.

7.2.1.3 **LTT 100Cr6**

Axle area. The material presents a quenched microstructure consisting principally of bainite and martensite, as Figure 7.8 shows in pictures on the left and on the right respectively.

However, areas with retained austenite are also visible in the semisolid forged part as the picture on the left of Figure 7.8 demonstrates. The white phase surrounded by martensite needles corresponds to that retained austenite.

Furthermore, the fine black lines almost present in all 100Cr6 microstruc-
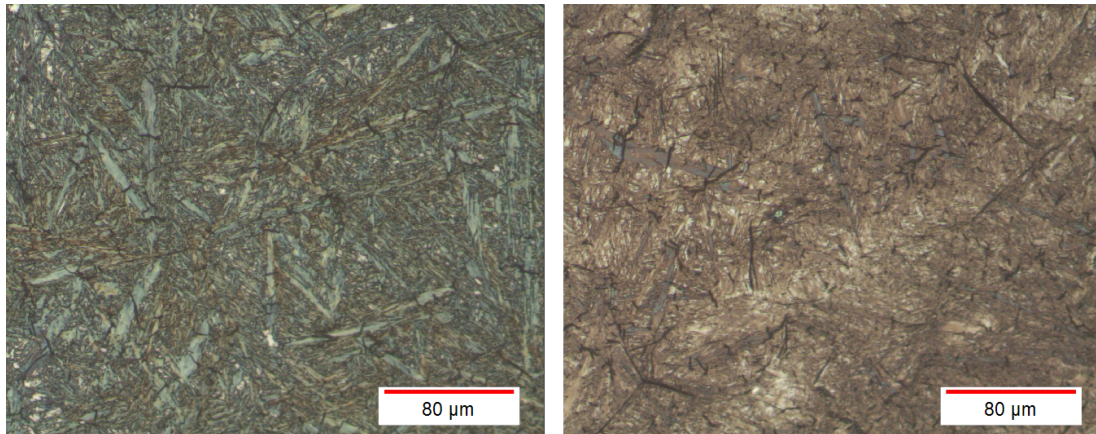
Figure 7.8 Different areas of the spindle base microstructures from LTT 100Cr6.
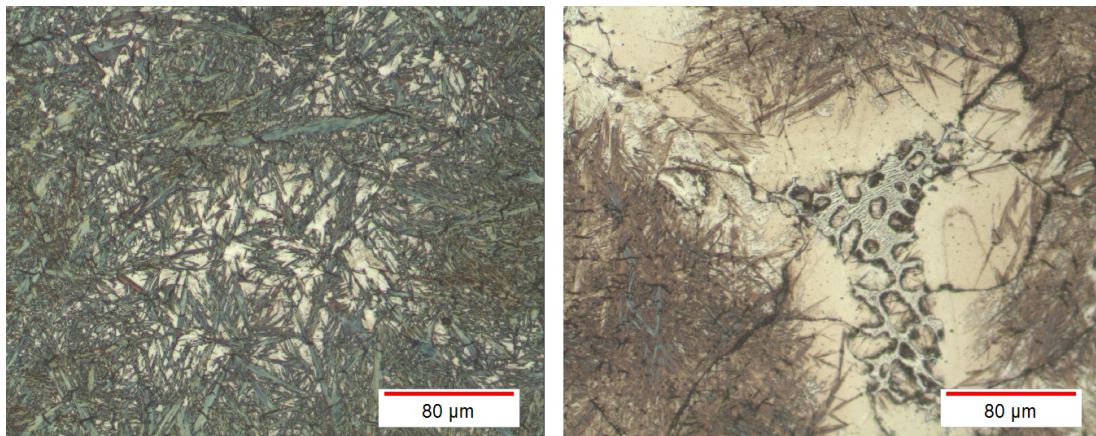
Figure 7.9 Different areas of the spindle base microstructures from LTT 100Cr6.

tures are micro cracks formed by the low process temperature used during the trials. By increasingthe heating cycle time a little bit more, they will disappear completely. The picture on the right of Figure 7.9 shows a different microstructure that is also present in the studied sample. In this case, the white phase is not retained austenite, it could correspond to a carbon segregation area surrounding a chromium carbide.

Base area. The microstructure visible in Figure 7.10 is completely different from that present in the axle area. The cooling is slower in the massive

zone and, due to this, a pearlitic microstructure including some proeutectoid cementite at the prior austenite grain boundaries is shown in Figure 7.10. This microstructure is usual for 100Cr6 steel grade when it is supplied in a hot rolled condition.
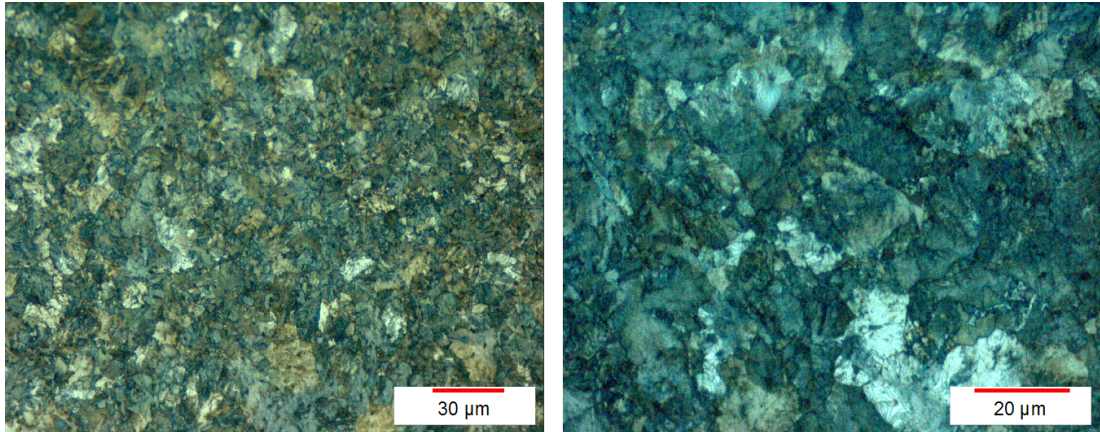
Figure 7.10 Different areas of the spindle base microstructures from LTT 100Cr6.

As expected, the microstructure of the component directly after semisolid forging is quite heterogeneous, except in the case of LTT C38, where the only change is the grain size. In order to get similar mechanical properties along all the part, a subsequent heat treatment is needed. The microstructure obtained after the heat treatment is analysed precisely in the following section.

7.2.2 Microstructure after heat treatment (Q + T)

The aim of giving a quenching and tempering heat treatment to the manufactured components was to ensure that they reach the desired mechanical properties. The used austenisation temperature was of 860ºC and then, all of them were quenched in oil at 100ºC. The tempering temperatures were 180ºC for LTT C38 and LTT C45 and 540ºC for LTT 100Cr6. It should be kept in mind that these steel grades are not the best suited to obtain the final mechanical requirements and that the thermal treatment to which they were submitted were not the most appropriate ones.

7.2.2.1 **LTT C45**

Axle area. In principle it is well quenched and tempered. During the tempering, the martensite needles are slightly deformed, and due to this, they are not so clearly defined. It is possible to have some residual bainite areas but is hardly appreciable at these magnifications. The pictures of Figure 7.11 present a banded microstructure which suggests that there is some segregation.
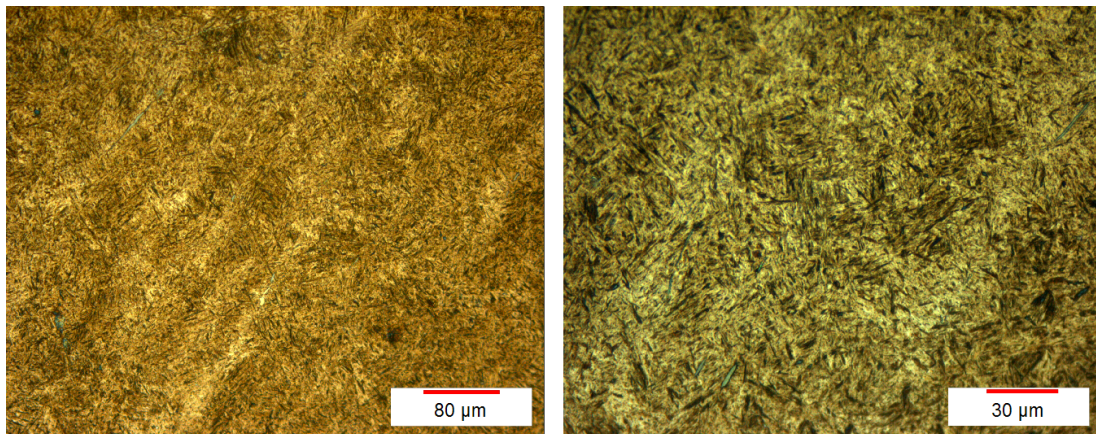
Figure 7.11 Quenched and tempered micrographs from LTT C45 axle.

Base area. Microstructures from the base area are shown in Figure 7.12.
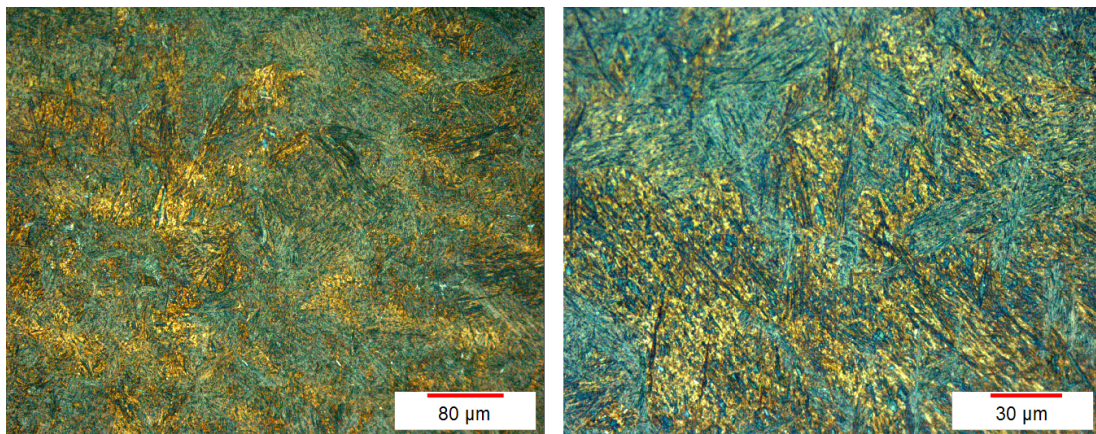
Figure 7.12 Quenched and tempered micrographs from LTT C45 base area.

Differing from the axle, at least two clearly distinguishable microstructures can be identified. The bright brown areas correspond to tempered martensite as in the previous picture (Figure 7.11) but now wide bainite areas coloured in grey-blue are also visible.

7.2.2.2 LTT C38

Axle area. It is not a steel grade to work with in the quenched and tempered state. The white phase visible in Figure 7.13 corresponds to untransformed ferrite and the dark phase is perlite. The bright brown phase is constituted by martensite and bainite although the latter is hidden. Sulphides are also visible in the pictures which is in concordance with the high sulphur content in its chemical composition.
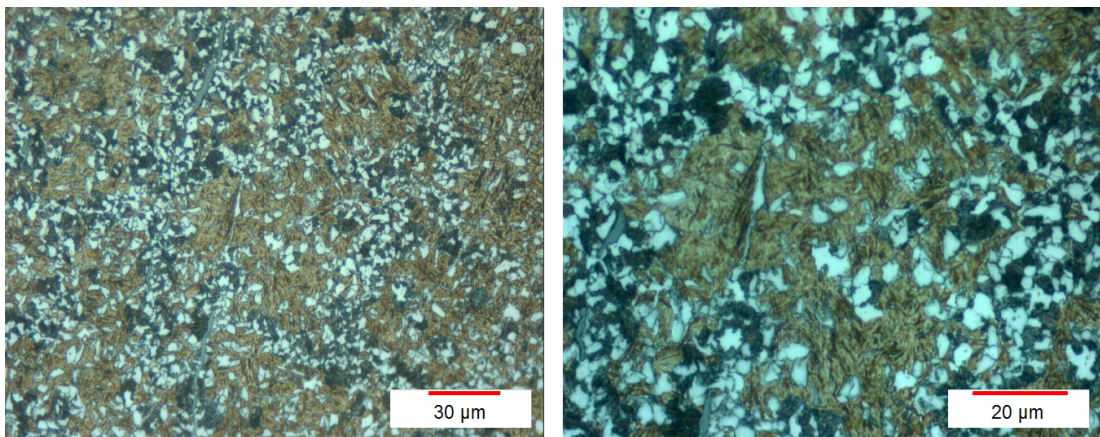
Figure 7.13 Quenched and tempered micrographs from LTT C38 axle.

Base area. Visible microstructural phases are the same as in the axle area (Figure 7.12) but the presence of bright brown areas of martensite and bainite is reduced. This suggests that the quenching process does not affect both areas in the same way and has a much lower effect in the massive base of the component.

This steel grade is commonly used in bulk state or submitted to some annealing processes. The quenching and tempering process used here with the
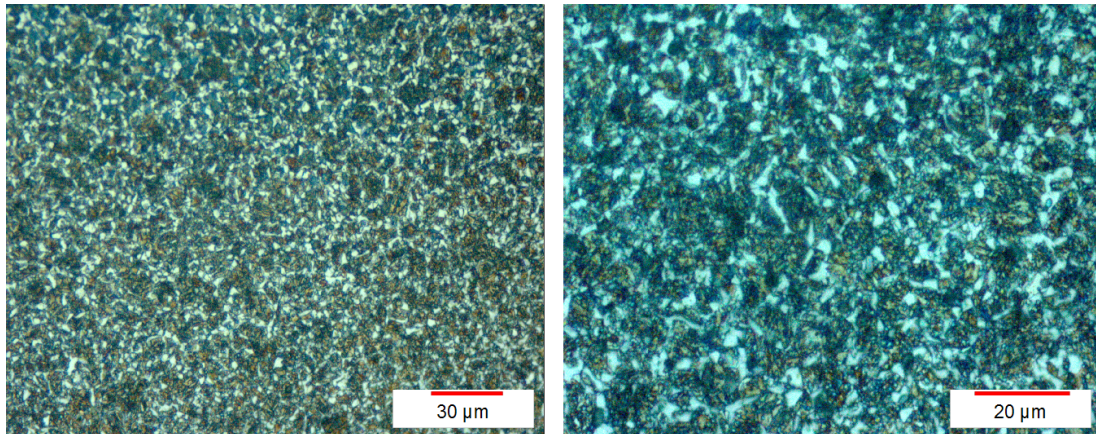
Figure 7.14 Quenched and tempered micrographs from LTT C38 base area.

aim to improve its mechanical behaviour has as consequence the presence of a martensite-bainite phase. This phase makes the microstructure to be mixed which entails a poor machinability.

7.2.2.3 LTT 100Cr6

Axle area. Figure 7.15 shows heat treated microstructure of LTT 100Cr6.
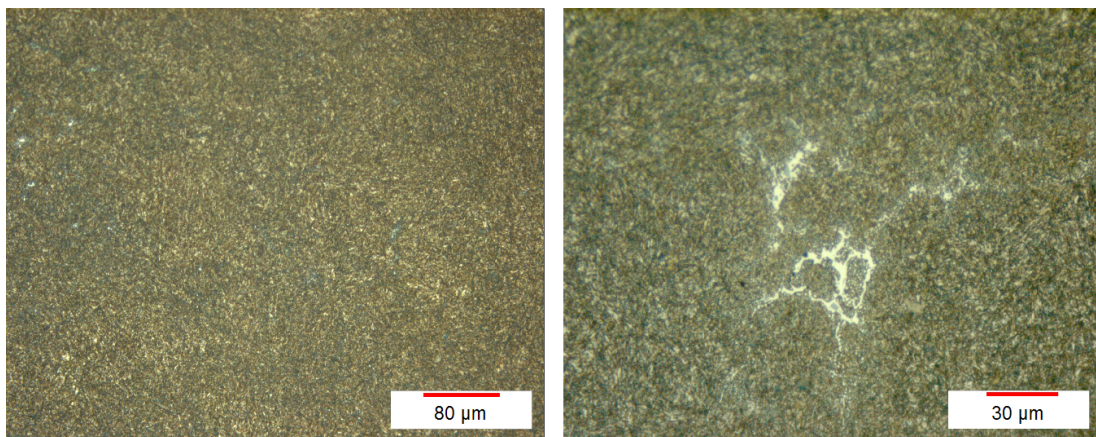
Figure 7.15 Quenched and tempered micrographs from LTT 100Cr6 axle.

As can be seen, almost everything is tempered martensite with some white areas that can be cementite, already present in the steel before the heat

treatment.

In this case, having used the same forming cycle as in the component analysed just after the semisolid forging, the microcracks present in Figure 7.8 and Figure 7.9 have completely disappeared.

Base area. The micrographs present in Figure 7.16 show the same tempered martensite microstructure as the axle area.
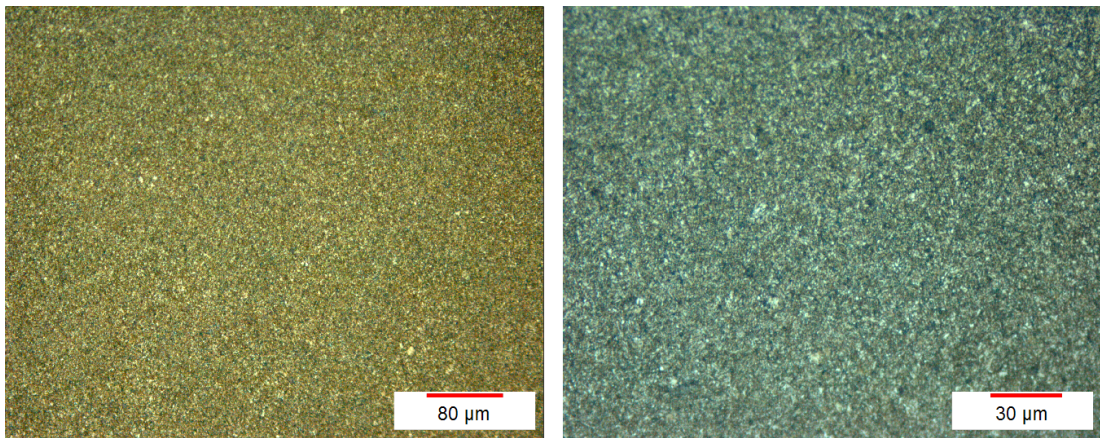
Figure 7.16 Quenched and tempered micrographs from LTT 100Cr6 base area.

7.3 Mechanical analysis of components

In order to measure the mechanical properties after the semisolid forging and after the heat treatment, round tension test specimens were used. The specimens were obtained from the axle of the manufactured spindle as shown in Figure 7.17.

The spindle´s axle was not long enough to get standard specimens and because of that proportional small-size specimens with $\varnothing = 6mm$ were used following ASTM E 8M - 04 standard (Standard Test Methods for Tension Testing of Metallic Materials). As it can be seen in Figure 7.17, only one specimen was
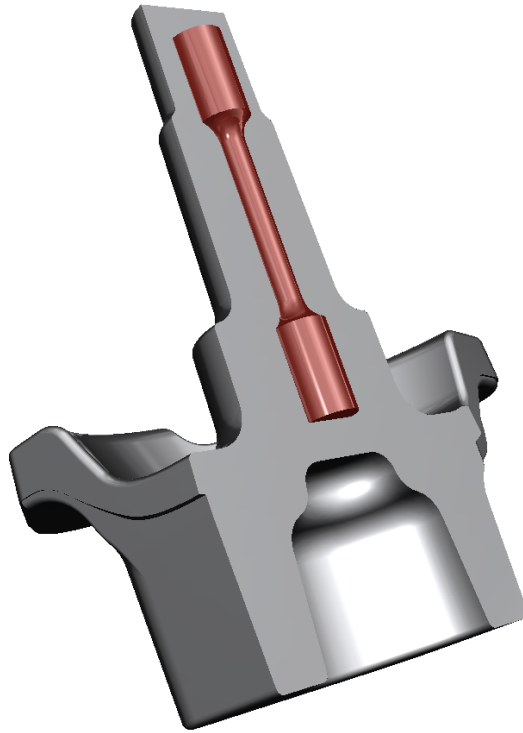
Figure 7.17 Figure from where the tension test specimens were obtained.

obtained from each component. Tests were carried out according to UNE-EN ISO 6892 - 1 : 2010 B and P - 51 at 20 mm/min.

The mechanical properties of the hot forged spindle required by the OEM after the quenching and tempering heat treatment are shown in Table 7.1.

Table 7.1 Mechanical properties required to the hot forged spindle.

Y.S.$_{0.2\% \, Offset}$ (MPa)	**T.S.** (MPa)	**Elong.** $(L_0 = 5d)(\%)$
1000	1100	11

7.3.1 **Mechanical properties after semisolid forging**

The mechanical properties measured after the semisolid forging of LTT C45, LTT C38 and LTT 100Cr6 are displayed in Table 7.2, Table 7.3 and Table 7.4

respectively.

Table 7.2 Mechanical properties of LTT C45 after SS forging.

Tensile test LTT C45					
Reference test piece	**Ø** (mm)	**Y.S.**$_{0.2\% \, Offset}$ (MPa)	**T.S.** (MPa)	**Elong.** $(L_0 = 5d)(\%)$	**Z** $(\%)$
Asco. Mat.	6	553	794	22.5	63
SS Forged 1	6	826	1143	14.9	29
SS Forged 2	6	588	919	2.7	16
SS Forged 3	6	586	982	6.9	16

Looking at the results of LTT C45, it is possible to see that compared with the starting material (Asco. Mat.) the yield strength and the tensile strength have increased slightly but the elongation is considerably reduced. Specially in the case of SS Forged 2.

Table 7.3 Mechanical properties of LTT C38 after SS forging.

Tensile test LTT C38					
Reference test piece	**Ø** (mm)	**Y.S.**$_{0.2\% \, Offset}$ (MPa)	**T.S.** (MPa)	**Elong.** $(L_0 = 5d)(\%)$	**Z** $(\%)$
Asco. Mat.	6	647	900	18.3	54
SS Forged 1	6	707	957	9.5	28
SS Forged 2	6	710	836	1.4	16
SS Forged 3	6	722	996	10.5	37

The case of LTT C38 is similar to the previous one, the yield strength and the tensile strength increase a little bit but the elongation decreased significantly compared to the starting material. The SS Forged 2 specimen presents an elongation of only 1.4 %.

In both steel grades (LTT C38 and LTT C45), the presence of a specimen with so low elongation suggests that the process is not robust enough yet. A priory, the presence of oxides is ruled out due to the reached strengths.

Table 7.4 Mechanical properties of LTT 100Cr6 after SS forging.

Tensile test LTT 100*Cr*6					
Reference test piece	**Ø** *(mm)*	**Y.S.**$_{0.2\% \: Offset}$ *(MPa)*	**T.S.** *(MPa)*	**Elong.** $(L_0 = 5d)(\%)$	**Z** *(%)*
Asco. Mat.	6	476	786	24	60
SS Forged 1	6	–	660	–	–
SS Forged 2	6	–	533	–	–
SS Forged 3	6	–	601	–	–

For LTT 100Cr6 it was impossible to determine the yield strength and the elongation due to the dramatic failure of the specimens. The reason for this brittle fracture can be found in the microcracks of Figure 7.8.

7.3.2 **Mechanical properties after heat treatment**

The mechanical properties measured after the heat treatment of LTT C45, LTT C38 and LTT 100Cr6 are displayed in Table 7.5, Table 7.6 and Table 7.7 respectively.

Table 7.5 Mechanical properties of LTT C45 after heat treatment.

Tensile test LTT C45				
Reference test piece	**Ø** *(mm)*	**Y.S.**$_{0.2\% \: Offset}$ *(MPa)*	**T.S.** *(MPa)*	**Elong.** $(L_0 = 5d)(\%)$
Asco. Mat.	6	553	794	22.5
SS Forged 1	6	1493	1647	0.6
SS Forged 2	6	–	1397	–
SS Forged 3	6	1430	1445	0.6

After the quenching and tempering heat treatment described in section 7.2.2, the yield strength and the tensile strength are well above that required by the OEM. In any case the elongation is almost null. As demonstrated in the tomography inspection (section 7.4) there are no defects in the axle area so the lack of elongation could be related to the unsuitable heat treatment parameters.

Table 7.6 Mechanical properties of LTT C38 after heat treatment.

Tensile test LTT C38				
Reference test piece	Ø (*mm*)	**Y.S.**$_{0.2\% \ Offset}$ (*MPa*)	**T.S.** (*MPa*)	**Elong.** $(L_0 = 5d)(\%)$
Asco. Mat.	6	667	900	18.3
SS Forged 1	6	1092	1176	0.6
SS Forged 2	6	886	1004	0.5
SS Forged 3	6	–	783	–

In the case of LTT C38 the specimens hardly reaches the required mechanical specifications and the elongation is negligible. As in the case of LTT C45, the parameters of the heat treatment could have a big influence. First of all, a water quenching could be better for both steel grades instead of the implemented oil quenching. The latter promotes a great hardness heterogeneity that can also influence the mechanical behaviour.

Table 7.7 Mechanical properties of LTT 100Cr6 after heat treatment.

Tensile test LTT 100Cr6				
Reference test piece	Ø (*mm*)	**Y.S.**$_{0.2\% \ Offset}$ (*MPa*)	**T.S.** (*MPa*)	**Elong.** $(L_0 = 5d)(\%)$
Asco. Mat.	6	476	786	24
SS Forged 1	6	–	1096	–
SS Forged 2	6	–	1167	–
SS Forged 3	6	–	1280	–

The correct measuring of the tensile strength has been impossible in the case of LTT 100Cr6. Due to the high hardness of this steel grade after the quenching and tempering process, the grippers of the tensile test machine were not able to hold and fix the round specimens and they started to slip off during the tensile test. Because of that, these results are completely useless.

7.3.3 **Fracture analysis**

Looking at the tables of the mechanical properties, it is possible to see that all quenched and tempered specimens broke down under fragile fracture. A first quick visual analysis of the broken specimens, with brilliant textured surfaces and perpendicular fracture plains respecting to the maximum tension stresses clearly denotes a fragile fracture.

Reviewing the results obtained directly after semisolid forging, there are at least a couple of cases (one in LTT C45 and one in LTT C38) where the fracture was also fragile. Down below, Figure 7.18 and Figure 7.19 show different fragile rupture mechanisms found in different specimens.
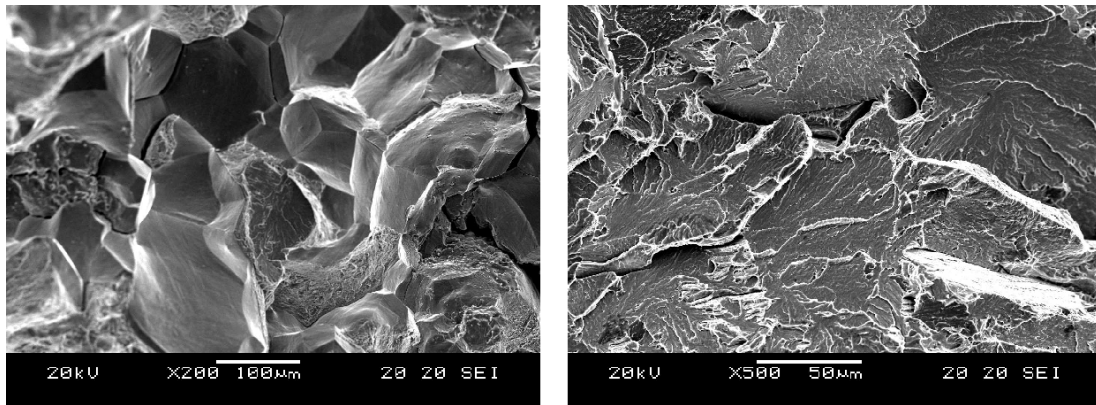
Figure 7.18 SEM inspection for fracture of LTT C45 semisolid forged part.

Figure 7.18 presents two pictures obtained from semisolid forged specimens. An intergranular fragile rupture can be seen in the picture to the left of Figure 7.18. The grain shapes can be observed and no plastic deformation can be noticed. A transgranular fragile fracture produced by cleavage of crystallographic planes is presented in the picture to the right. Neither here is appreciated any plastic deformation.

In Figure 7.19, rupture surfaces of a quenched and tempered specimens can be seen. An intergranular crack is clearly visible and no deformation is noticed.
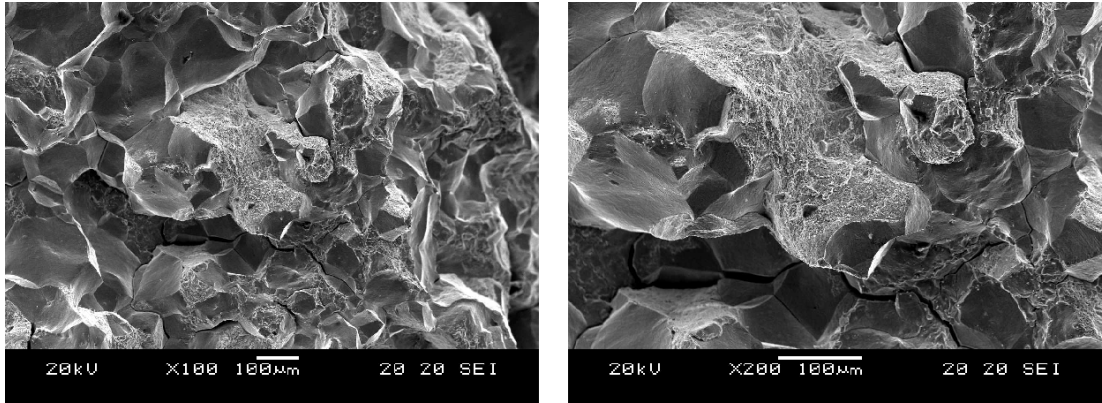
Figure 7.19 SEM inspection for fracture of LTT C45 after heat treatment.

7.4   Tomography inspection

To ensure that semisolid forged components were sound, a complete tomography inspection was also made, obtaining axial planes each 1 mm and each 0.25 mm as specified in Figure 7.20.
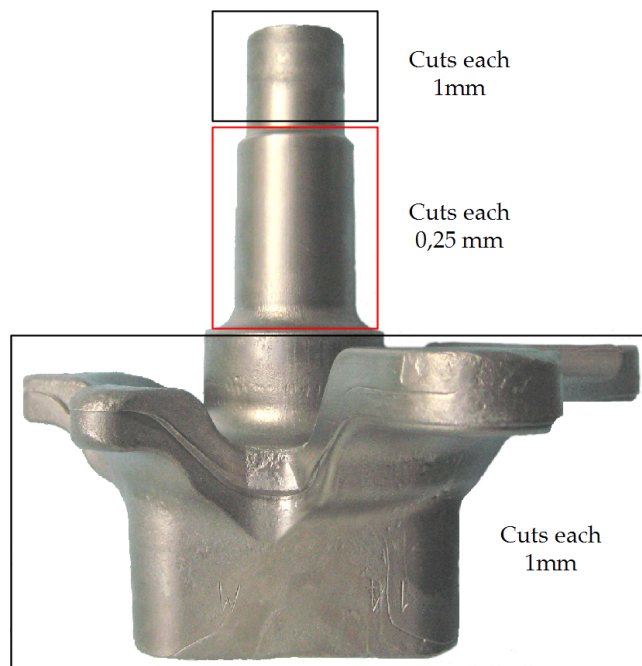
Figure 7.20 Tomography inspection for LTT C45 semisolid forged part.

The tension of the beam was 450 kV. The analysis of the middle axle was done more accurately because it is the most critical area, the one that ensures the wheel rolling; where the induction surface treatment is given and the disk brake is located.

Figure 7.21 shows the most representative images obtained during the tomography inspection of a quenched and tempered LTT C45 semisolid forged component.
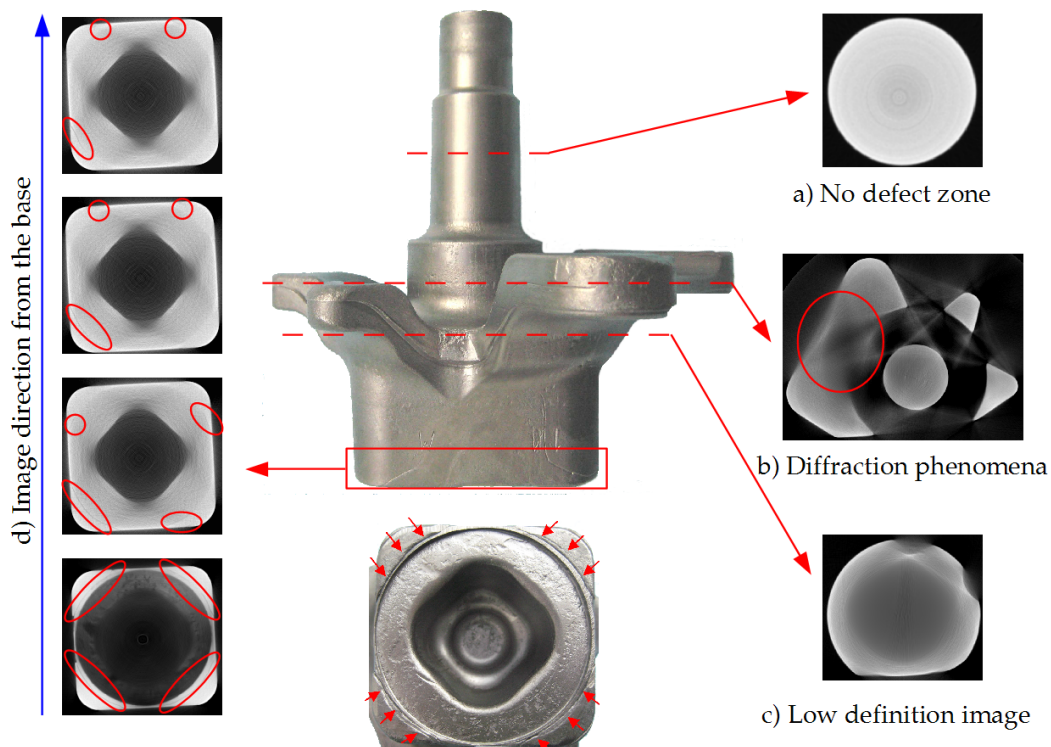
Figure 7.21 Tomography images of the LTT C45 semisolid forged part.

The images on the left side (d) show some discontinuities on the base along 11 mm. These discontinuities are formed by the punch during the forming operation, they do not affect the integrity of the component and are only superficial. The starting points of those discontinuities are visible on the base image, highlighted by red arrows. Looking carefully at Figure 7.20, it is possible to see that the material flowing during form filling generates folds that go

upwards starting at the rounded base corners of the component. In any case, they have been analysed and more than defects they can be considered surface irregularities because they do not continue inside the part. In the remaining areas, apparently, the component is sound.

When the beam passes trough massive areas, images with low definition are obtained, as can be seen in picture c). Diffraction phenomena are also visible in other zones. One of those areas is presented in picture b).

7.5   Concluding remarks

The tomography inspection show that it is possible to manufacture sound steel components by semisolid forging. In any case, the mechanical properties presented in section 7.3 leave a bitter taste. Indeed, better results were expected from the steel grades recommended by Ascometal.

Mechanical properties obtained just after thixoforming are promising although the low elongation of one of the specimens tested brings uncertainty about the robustness of the forming cell. What is quite clear is that the applied heat treatments are not appropriate enough to get the desired mechanical behaviour for each steel grade, and must be adapted and optimised. For example, in the case of LTT C45 and LTT C38, a water quenching should work better in minimising the hardness heterogeneity along the component.

Taking the results after quenching and tempering into account, the question that arises is whether the lack of sufficient elongation is only due to the given heat treatment or also due to the material used, due to the forming process itself or a combination of all that. In my opinion the determining factor is the material, the steel grade used for manufacturing the component, together with a suitable heat treatment. Whatever the case may be, this question will be treated in detail in the next chapter entitled *Research Conclusions and Future Work*.

Research Conclusions and Future Work

8.1 Conclusions

8.1.1 Material selection for semisolid forming

The preconditions for selecting suitable alloys for semisolid forming are well understood: mainly, a low temperature sensitivity and a globular liquid-phase development during heating. So far everything seems correct, with the sole nuance of how globular is defined.

The fact is that semisolid forging requires a deep and thorough understanding of the microstructure development during all the process. As described in Chapter 4, f_l could not be calculated in a highly accurate manner by any of the proposed methods.

Thermal procedures are easy and have cost efficient specimen preparation, but the use of peak reference integration involves an error. Besides, the much quicker inductive heating used to heat the material disables the direct

transferability of the results obtained by these methods.

Thermodynamic software such as IDS can provide information about the maximum width of the semisolid interval, but consideration of the prior thermal history and of the microstructure is currently not yet possible. Furthermore, the phase calculation is made during cooling and in thixoforming the desired microstructure is obtained during heating.

The metallographic determination of the phase contents by means of quenching is not accurate. For that, a random and uniform distribution of the liquid and solid phases in the sample volume must be ensured and this is hardly possible. Figure 4.19 on page 55 displays two different areas of quenched LTT C45 and the difference in f_l is considerable. Depending on the area, liquid fractions from 1% up to more than 10% have been measured in the same billet using an image analysis software. Furthermore, as in the case of LTT 100Cr6, the differentiation of the liquid phase is really difficult.

To end up, it is fair to say that these three methods are approximate and allow only a rough prediction of the phase fraction. It is significant that semisolid forged parts have been produced with temperatures below the solidus, measured by DSC, and that quenching micrographs and microscope observations demonstrate that melting has occurred at those temperatures. It turns out that a deeper study on the melting behaviour of the alloys is needed. One of the methods to determine the semisolid forging temperature more precisely could be the Nil Strength Temperature test. The nil strength temperature (NST) is the temperature level at which material strength drops to zero while the steel is being heated above the solidus temperature.

Another question to keep in mind is the steel grade needed to obtain the final mechanical properties. It was demonstrated along the research work that hot rolled material is adequate for semisolid forging and that its chemical composition plays a fundamental role in its mechanical behaviour, as it happens in all the other classic manufacturing processes.

8.1.2 **The heating**

The heating stage has been considered one of the key factors for the semisolid material processing, and it is indeed. Moreover, the narrow semisolid window of steels has been the Achilles heel for the process development according to a widely held view. During this research work, different heating cycles at a constant power of 24 kW have been tested and geometrically filled parts have been obtained using different heating times that goes from 231 seconds up to 260 second. This time range demonstrates that the semisolid window is not too narrow and that it could be controlled in a feasible way.

The reason to obtain sound parts below temperatures expected by DSC or IDS could be related to this: the thermocouples´ measurement error or the different heating rate between the DSC, and the induction furnace. In my opinion, the later is the key factor, which makes it necessary to carry out a further study on the melting behaviour of the steel alloys.

In any case, as described in Chapter 6, it is important for the heating to be fast, precise and homogeneous, thus encouraging soundness of the components and process productivity.

8.1.3 **The forming step**

The forming step differences between traditionally hot forged spindle and semisolid forged spindle are summarised in Table 8.1.

Table 8.1 Differences between hot forging and SS forging.

	Steps	Press Load (t)	Material (kg)
Hot Forging	4	2500	3.5
SS Forging	1	400	2.8

The required forming forces are substantially reduced and material savings of 20% have been reported due to the near net shape capabilities of the process. A redesign of the component will increase the material saving, taking

advantage of the increased material´s fluidity. The latter allows to fill thin walls and reinforcement ribs, as well as a greater definition of the part´s details.

The selection of the thixo-lateral (or transverse) forming process has also its importance because it avoids liquid ejections and allows an increased degree of geometric freedom.

Based on the results achieved, it is possible to say that the thixo-lateral forging is a robust process, highly repeatable but still with much more optimisation margin. The productivity of the forming cell can be increased using a carrousel or a continuous heating system and the forming step must be overhauled to ensure that the compaction force is well distributed through the forming part.

Another issue that must be overhauled is the lack of suitable tools and dies that meet the demands and exhibit an economically satisfactory service life within the range of tolerated degradation. So far, there was a need to find bulk materials or coatings able to withstand temperatures 200ºC or more above the hot forging temperature. This research work has demonstrated that it is possible to obtain semisolid forged components at temperatures slightly above those used in classical hot forging, making it possible to test the innovative coatings, already present in forging industry, for SS forging.

8.1.4 **Mechanical results**

The thixo-lateral forging of spindles is a robust process as the tomography inspection to which some components were submitted demonstrates. In any case, the mechanical properties presented in section 7.3 leave a bitter taste. Indeed, better results were expected from the steel grades recommended by Ascometal and the low elongation of the tested specimens brings some uncertainty. In my opinion, neither were the selected steel grades suitable to achieve the final mechanical requirements nor were the applied thermal treatments appropriate. They should be adapted and optimised.

This opinion relies on some other tests carried out using other steel grades from a different steel supplier. These steel grades were optimised to fulfil the components mechanical requirements after quenching and tempering and the obtained results are very encouraging. Table 8.2 shows the final average mechanical properties.

Table 8.2 Average mechanical properties of the SS forged new steel grade after quenching and tempering heat treatment.

Tensile test of the New SS forged material					
Reference test piece	Ø (*mm*)	**Y.S.**$_{0.2\% \; Offset}$ (*MPa*)	**T.S.** (*MPa*)	**Elong.** $(L_0 = 5d)(\%)$	**Z** (%)
New. Mat.	6	945	1073	13.3	59

These new steel grades are not fully analysed yet and, because of that, they were not included in this dissertation. What is clear is that doubts casted over the process robustness disappear once we look through these results, thus reflecting the idea of the unsuitability of applied heat treatments and the steel grades used.

8.2 Future work

Even if this dissertation demonstrates the viability of semisolid forging of steel, there is almost everything to do yet in the way for industrialisation.

First of all, from the material point of view, much more steel grades must be analysed and validated. With that purpose, it will be necessary to establish a testing method to determine the suitability of each steel grade, as well as the exact working window, because the methods used up to now have demonstrated a high grade of inaccuracy. At the same time, these efforts should focus on study the microstructure development during the whole process in depth.

Continuing with the material but from another point of view, it is really important to be able to determine the semisolid metal behaviour in order to develop helpful simulation software. There have been some attempts for this, but the high temperatures involved and the difficulty of working with two phases together makes it currently impossible. And going a step further a complete simulation of the process from the heating to the forming would be really interesting.

Regarding the process itself, it is in the pre-industrial phase and ready to take the definitive step towards the desired industrialisation. That will be the litmus test where problems with dies and long term effects will arise. It is time to fight with industrialisation and productivity issues. In any case, at laboratory scale, it would be interesting to be able to validate some more components coming from sectors interested in the advantages that SS forging presents.

Thinking ahead, future goals must be focused on the semisolid forging of higher melting point alloys as titanium or nickel base alloys.

List of Figures

List of Tables

Bibliography

[1] EUROFORGE. Production of forgings, 2012, http://www.euroforge .org/statistics/production-figures.html.

[2] B. Spencer, R. Mehrabian, and M. C. Flemings. Rehological behaviour of sn-15 pct pb in the cristalisation range. *Metallurgical transactions*, 3:1925 – 32, 1972.

[3] D.H. Kirkwood, M. Suéry, P. Kapranos, H.V. Atkinson, and K.P. Young. *Semi - solid Processing of Alloys*. Springer, 2010.

[4] P. Kapranos, D.H. Kirkwood, and C.M. Sellars. Semi-solid processing of tool steel. *Journal de Physique IV*, 3, 1993.

[5] P. Kapranos, D.H. Kirkwood, and C.M. Sellars. Thixoforming high melting point alloys into non - metallic dies. In *Proc. of the 4th Int. Conf. on Semi-Solid Processing of Alloys and Composites*, 1996.

[6] D.H. Kirkwood. Semisolid processing of high melting point alloys. In *Proc. of the 4th Int. Conf. on Semi-Solid Processing of Alloys and Composites*, 1996.

[7] W. Bleck, G. Hirt, and W. Püttgen. Thixoforming of steels - a status report. *Material Science Forum*, 539-543:4297–4302, 2007.

[8] H.V. Atkinson and A. Rassili. A review of the semi-solid processing of steel. *Int J Mater Form*, 3:791–795, 2010.

[9] P.A. Joly and R. Mehrabian. The rheology of a partially solid alloy. *J. Mater. Sci.*, 1:1393–1418, 1976.

[10] H.K. Moon. PhD thesis, Massachusetts Institute of Technology, 1971.

[11] M.C. Flemings. Behaviour of metall alloys in the semisolid state. *Metallurgical and Materials Transactions A*, 22A:957–981, 1991.

[12] G. Hirt and R. Koop. *Thixoforming, Semi - solid Metal Processing*. WILEY - VCH Verlag GmbH & Co. KGaA, 2009.

[13] E. Tzimas and A. Zabaliangos. Evaluation of volume fraction of solid in alloys formed by semisolid processing. *Journal of Materials Science*, 35:5319–5329, 2000.

[14] W. Loué and M. Suéry. Microstructural evolution during partial remelting of al-si7mg alloys. *Materials Science and Engineering*, A203:1–13, 1995.

[15] J. Gurland. *Trans. Met. Soc. AIME*, 212:452, 1958.

[16] A. Fiqueredo. *Science and technology of Semi-solid metal processing*. Worcester Polytechnic Institute, 2001.

[17] H.V. Atkinson and Ahmed Rassili. *Thixoforming Steel*. Shaker Verlag, 2010.

[18] M. Suéry. *Mise en forme des alliages métalliques à l´état semi-solide*. Lavoisier, 2002.

[19] D.H. Kirkwood. Semisolid metal processing. *International Materials Reviews*, 39:173–189, 1994.

[20] A. Vogel, R.D. Doherty, and B. Cantor. Solidification and casting of metals. *The Metals Society*, pages 518–525, 1979.

[21] R.D. Doherty, H.I. Lee, and E.A. Feest. Microstructure of stir-cast metals. *Mater. Sci. Eng.*, 65:181–189, 1984.

[22] Z. Fan. Semisolid metal processing. *International Materials Reviews*, 47, 2002.

[23] D.H. Kirkwood and C. Sellars. Rap process, 1987.

[24] P. Kapranos, D.H. Kirkwood, and P.H. Mani. Semi-solid metal processing of ductile iron. *Proc. of the 5th Int. Conf. on Semi-Solid Proc. of Alloys and Composites*, pages 431–438, 1998.

[25] R. Bulte and W. Bleck. Effects of pre-processing on thixoformability of steel grades 100cr6. *Steel Res. Int.*, 75:588–592, 2004.

[26] M.Z. Omar, H.V. Atkinson, E.J. Palmiere, A.A. Howe, and P. Kapranos. Viscosity - shear rate relationship during the thixoforming of hp9/4/30 steel. *Solid State Phenomena*, 116-117:677–680, 2006.

[27] K. B. Kim, H. I. Lee, and H. K. Moon. Microstructures and formability of electromagnetically stirred billet of high melting point alloys. *Proc. of the 5th Int. Conf. on Semi-Solid Proc. of Alloys and Composites*, pages 415–422, 1998.

[28] R. Song, Y. Kang, and A. Zhao. Semi-solid rolling process of steel strips. *Jounal of materials processing technology*, 198:291–299, 2008.

[29] G. Walmag, P. Naveau, A. Rassili, and M. Sinnaeve. A new processing route for as-cast thixotropic steel. *Solid State Phenomena*, 141-143:415–420, 2008.

[30] I. Seidl and R. Kopp. Semi-solid rheoforging of steel. *Steel Research International*, 75:545–551, 2004.

[31] G. Hirt, H. Shimahara, I. Seidl, F. Kuthe, D. Abel, A. Schonbohm, and R. Kopp. F15 - semi-solid forging of 100cr6 and x210crw12 steel. *ANNALS-CIRP*, 54:257–260, 2005.

[32] M. Ramadan, M. Takita, H. Nomura, and N. El-Bagoury. Semi-solid processing of ultrahigh-carbon steel castings. *Material Science and Engineering A*, 430:285–291, 2006.

[33] F. Pahlevani and M. Nili-Ahmadabadi. Development of semi-solid ductile cast iron. *International Journal of Cast Metals Research*, 17:157–161, 2004.

[34] T. Haga, M. Kouda, H. Motoyama, N. Inoue, and S. Suzuki. High speed roll caster for aluminum alloy strip. *Proceedings of ICAA7 Aluminium Alloys: Their Physical and Mechanical Properties*, 1:327–332, 1998.

[35] D.C. Milostean and I. Ioan. Laboratory stage experiments on the semisolid state steel die forging. *Metalurgia International*, 13:49–54, 2008.

[36] M. Robelet. Acier pur construction mécaniqui, procédé de mise en forme à chaud d´une pièce de cet acier, et pièce ainsi obtenue, 2004.

[37] J. Lecomte-Beckers, A. Rassili, M. Carton, M. Robelet, and R. Koeune. Study of the liquid fraction and thermophysical properties of semi-solid steels and application to teh simulation of inductive heating for thixoforming. *Advanced Methods in Material Forming*, 8:321–347, 2007.

[38] J. Miettinen. Calculation of solidification-related thermophysical properties for steels. *Metallurgical and Materials Transactions B*, 28B:281–297, 1997.

[39] A. Rassili, M. Robelet, and R. Bigot. Thixoforming of steel: Parameters and means for industrialization. *Solid State Phenomena*, 141-143:213–218, 2008.

[40] K. Mollenhauer and H. Tschoeke. *Handbook of diesel engines*. Springer, 2010.

[41] A. Rassili and H.V. Atkinson. A review on steel thixoforming. *Trans. Nonferrous Met. Soc. China*, pages 1048–1054, 2010.

[42] A. Schönbohm, R. Gasper, and D. Abel. Inductive reheating of steel billets into the semi-solid state based on pyrometer measurements. *Solid State Phenomena*, 116-117:734–737, 2006.

[43] B.A. Behrens, D. Fischer, and A. Rassili. Strategies for re-heating steel billets for thixoforming. *Solid State Phenomena*, 141-143:121–126, 2008.

[44] A. Rassili, M. Robelet, and D. Fischer. Thixoforming of carbon steels: Inductive heating and process control. *Solid State Phenomena*, 116-117:717–720, 2006.

[45] R. Baadjou, F. Knauf, and G. Hirt. Investigations on thermal influences for thixoforging and thixojoining of steel components. *Solid State Phenomena*, 141-143:37–42, 2008.

[46] P. Cezard, R. Bigot, E. Becker, J. C. Mathieu, S. nad Pierret, and A. Rassili. Thixoforming of steel: New tools conception to analyse thermal exchanges and strain rate effects. *AIP Conference Proceedings*, 907:1155–1160, 2007.

[47] M. Robelet, A. Rassili, and D. Fischer. Steel grades adapted to the thixoforming process: metallurgical structures and mechanical properties. *Solid State Phenomena*, 116-117:712–716, 2006.

[48] F. Kuthe, A. Schombohn, D. Abel, and R. Kopp. An automated thixo-formin plant for steel parts. *Steel Research International*, (75):593, 2004.

[49] P. Kapranos. Past, present and future of semi-solid forminng of high temperature alloys. *The 2nd JSME/ASME International Conference on Materials and Processing 2005*, 2005.

[50] Y. Birol. The use of crnico-based superalloy as die material in semi-solid processing of steels. *Solid State Phenomena*, 141-143:289–294, 2008.

[51] R. Pfeifer, M. Hustedta, V. Weslinga, C. Hurschlerb, G. Olenderb, M. Machc, T. Göslingd, and C.W. Müllerd. Noninvasive induction implant heating: An approach for contactless altering of mechanical properties of shape memory implants. *Medical Engineering & Physics*, 35:54–62, 2013.

[52] G. Hirt, A. Bleck, W.and Bührig-Polaczek, H. Shinamara, W. Püttgen, and C. Afrath. Semi solid casting and forging of steel. *Solid State Phenomena*, 116-117:34–43, 2006.

[53] E. Becker, R. Bigot, and L. Langlois. Thermal exchange effects on steel thixoforming processes. *Int J Adv Manuf Technol*, 2009.

[54] E. Becker, G. Gu, L. Langlois, R. Pesci, and R. Bigot. Effects of thermal exchange on material flow during steel thixoextrusion process. *AIP Conference Proceedings*, 1315:751–756, 2010.

[55] Z. Azpilgain, R. Ortubay, A. Blanco, and I. Hurtado. Servomechanical press: A new press concept for semisolid forging. *Solid State Phenomena*, 141-143:261–266, 2008.

[56] C. García, R. Ortubay, L. Galdos, and T. Azpiazu. Accuracy in a 400t fagor servo-motor driven mechanical press. In *International Conference on Accuracy on Forming Technology, ICAFT*, 2006.

[57] K. Osakada, K. Mori, T. Altan, and P. Groche. Mechanical servo press technology for metal forming. *CIRP Annals Manufacturing Technology*, 60/2, 2011.

[58] J.C. Pierret, A. Rassili, G. Vaneetveld, R. Bigot, and J. Lecomte-Beckers. Friction coefficients evaluation for steel thixoforming. In *ESAFORM*, 2010.

[59] S. Müenstermann, T. V. Tonnesen, and R. Telle. Functional ceramic and refractory parts in advanced metal formal processes. *Proc. Unified Int Technical Conf on Refractories*, page 367, 2007.

[60] Y. Birol. Testing of a novel crnico alloy for tooling applications in semi-solid processing of steels. *Int J Mater Form*, 3:65–70, 2010.

[61] Y. Birol. Thermal fatigue testing of cucrzr alloy for high temperature tooling applications. *J Mater Sci*, 2010.

[62] Y. Birol. Ni - based superalloy as potential tool material for thixoforming of steels. *Ironmaking and Steelmaking*, 36:555–560, 2009.

[63] Y. Birol. Ni- and co- based superalloys as potential tool materials for thixoforming of steels. In *ESAFORM*, 2010.

[64] Y. Birol. Effect of bulk die temperature on die cavity surface strains in thixoforming of steels. *Ironmaking and Steelmaking*, 36:397–400, 2009.

[65] Y. Birol. Response to thermal cycling of tool materials under steel thixoforming conditions. *Ironmaking and Steelmaking*, 37:41–46, 2010.

[66] G. Hirt, K. Bobzin, L. Khizhnyakova, M. Ewering, and N. Bagcivan. Semi-solid forming of non axis-symmeric parts from steel grade x210crw12 with pvd coated tools. In *ESAFORM*, 2010.

[67] E. Chicaracara, S.N. Aqida, D. Brabazon, S. Naher, J.A. Picas, M. Punset, and A. Forn. Surface modification of hvof thermal sprayed wc - cocr coatings by laser treatment. In *ESAFORM*, 2010.

[68] S. Dosta, J.R. Miguel, and J.M. Guilemany. Nanostructured cermet coatings with enhanced properties produced by hvof thermal spray. *Materials Science Forum*, 587-588:1024–1028, 2008.